Reducing the Effects of Spectral Interferences in Inductively Coupled Plasma Mass Spectrometry

By

Abdulaziz Saleh Bashammakh

A Doctoral Thesis

Submitted in partial fulfillment of the requirements for the award of

Doctor of Philosophy of Loughborough University

January 2003

Abstract

This thesis reports studies aimed at reducing the effects of spectral interferences in inductively coupled plasma mass spectrometry (ICP-MS). Two approaches are described and evaluated: the use of chemometric deconvolution of the spectra and the use of a collision/reaction cell for reactive transformation of interfering or analyte species.

Bayesian analysis, in particular the Massive Inference (MI) algorithm was used for the deconvolution of ICP-MS spectra, covering the mass range from 46 to 88 Daltons, derived from multielement standards and biological reference materials. This approach provides information on both the nature of the species that comprise the observed spectrum and the magnitude of their individual contributions. Various tests are applied to determine the goodness of fit between the actual and predicted spectra including the statistical Evidence, the deviation at each mass and the predicted value for the isotopic abundances, the latter proving to be particularly difficult to rationalise for all elements in the data set. Bayesian deconvolution is not a calibration technique, but the data derived from it are used to produce calibrations and subsequently to carry out quantitative analyses of reference materials. The algorithm uses the known isotopic distribution patterns in synthesising spectra, but these are corrupted by mass bias introduced by the instrument. Estimates of isotopic mass bias are used to model the instrument response function in order to remove this distortion from the data before it is subjected to processing.

ICP-MS instruments have recently been introduced that incorporate collision/reaction cells which can dissociate or reactively transform interfering species. An ICP-MS instrument equipped with a hexapole collision/reaction cell was used for the multielement determination of trace elements in biological samples. The use of a reaction or collision gas reduces serious spectral interferences such as those from ArO^+ or Ar_2^+. On introducing H_2 as a reaction gas and He as a buffer gas to the cell, the analytical performances for several elements were improved.

Sample preparation methods were investigated with the aim of finding those involving the minimum of chemical intervention commensurate with providing accurate data. A method was developed for the determination of iodine in milk samples using ICP-MS. The method was applied to determine iodine levels in whole, semi-skimmed and skimmed milk samples. Milk samples were digested using tetramethyl ammonium hydroxide, Triton X-100 and hydrogen peroxide with the addition of Sb as internal standard. Two reference materials were analysed for validation of the proposed method. The iodine levels found in the milk samples were in a good agreement with the certified values. The results obtained showed differences in the iodine levels in different kinds of the milk sample.

Acknowledgements

Described in this thesis is work that could not have possibly been undertaken without the kind help, excellent supervision and guidance of my supervisor, Dr Barry Sharp. I have learnt many things from his approach to the subject and I wish to express my sincere appreciation.

I am also indebted to King Abdulaziz University (Jeddah - Saudi Arabia) for the financial support and for giving me the opportunity to continue my higher education.

I would like to show my sincere gratitude to Dr H. Reid for her assistance and helpful suggestions. I am grateful to Mr. Malcolm Baxter for providing the data used in the Bayesian spectral deconvolution. Thanks also go to Dr John Lewis and Miss Nicola Langford for providing the reference materials used in the collision/reaction cell analysis and their sample preparation method for iodine determination. Thanks to Dr David Worrall for allowing me to carry out the UV digestion for milk samples in his lab.

I would like to thank Dave, Jill, Sonia and Linda for their help in the laboratory. For helpful discussions, comments and friendship I am indebted to my colleagues in the lab Fabienne, Christopher, Matthew, Mark, Earny, Simiso, Maggi, Shikha, Jo, Hussain, Ruziyati and Dongfang who made of those years an enjoyable time.

Most important of all is the support I have received from my family. I would like to express my sincere thanks and love to my wife and sons for their understanding and all the sacrifices that they made, without which this thesis could not have been prepared. I wish also to thank my brothers, sisters and friends for their encouragement and moral support. I would like to thanks Prof. Hawkey, Mr. Bourke and their team at the Queen's Medical Centre (Nottingham, UK) for the great care I found.

The above was a list of the people who have helped with this project. If I left you out, I am sorry, it was not intentional. Thank you, one and all!

Dedication

To my father and mother who have given me inspiration and guidance. I am indebted to their care and affection that gave me much and took very little. To their soul I dedicate this thesis.

Presentations and Publications

1. Bayesian deconvolution of quadrupole ICP-MS elemental spectra.
   10th Biennial National Atomic Spectroscopy Symposium, 17-20 July 2000, Sheffield, UK.

2. Using Bayesian deconvolution in quadrupole ICP-MS to reduce spectral interferences in the analysis of biological samples.
   Analytical Research Forum (Incorporating Research and Development Topics), 16-18 July 2001, Norwich, UK.

3. Reducing spectral interferences in quadrupole ICP-MS using Bayesian deconvolution.
   28th Annual Meeting of the Federation of Analytical Chemistry and Spectroscopy Societies, 7-12 October 2001, Detroit, USA.

4. Alkaline oxidation procedure for the digestion of milk for iodine and multi-element determinations by ICP-MS.
   11th Biennial National Atomic Spectroscopy Symposium, 8-10 July 2002, Loughborough, UK.

5. Bayesian analysis of inductively coupled plasma mass spectra in the range 46-88 Daltons derived from biological materials.
   Journal of Analytical Atomic Spectrometry, 2002, **17**, 459.

6. A sample preparation procedure for the determination of total iodine in milk samples using ICP-MS. (*In preparation*)

Table of Contents

List of Figures

List of Tables

Chapter 1:

Inductively Coupled Plasma Mass Spectrometry

1.1. Introduction

Inductively coupled plasma mass spectrometry (ICP-MS) is a fast, precise and accurate multielement analytical technique for the determination of trace and ultra-trace elements in liquid and solid samples. ICP-MS was first developed in the early 1980's and has become increasingly popular for the analysis of chemical, biological, environmental, industrial, geological and petrochemical materials[1-3].

In ICP-MS, elemental abundances or isotopic ratios are determined by the mass spectrometry (MS) of ions generated in the inductively coupled plasma (ICP). Using a stream of Ar carrier gas, liquid or solid sample is introduced into the ICP, which serves as an efficient source of charged analyte ions. The ions are extracted from the high temperature, atmospheric pressure environment of the plasma into a high vacuum enclosure via an interface region. The ions are focussed by an ion lens system then the analyte ions are separated according to their mass-to-charge (m/z) ratio by a mass spectrometer and these ions are detected and measured by a detector.

1.2. Instrumentation

An ICP-MS instrument consists of several integrated components and these parts are the:

1. Sample introduction system
2. Ion source
3. Ion transport system
4. Mass separation device
5. Detector

The layout of a typical ICP-MS instrument is shown in Figure 1.1.[4]

1.2.1. Sample introduction system

The sample introduction system facilitates the transport of liquid or solid sample material into the centre of the ICP. The majority of ICP-MS applications involve the analysis of liquid samples. There are many ways of introducing a liquid into an ICP-MS instrument; however, they almost achieve the same result. They generate a fine aerosol of the sample so that it can be efficiently ionised in the plasma. Normally only 1-2% of the sample finding its way into the plasma (for standard nebulisers operating at 1-2 ml min^{-1} uptake rate). Although there has been much improvement in this area, the fundamental design of an ICP-MS liquid sample introduction system has not dramatically changed since the technique was first introduced[5].

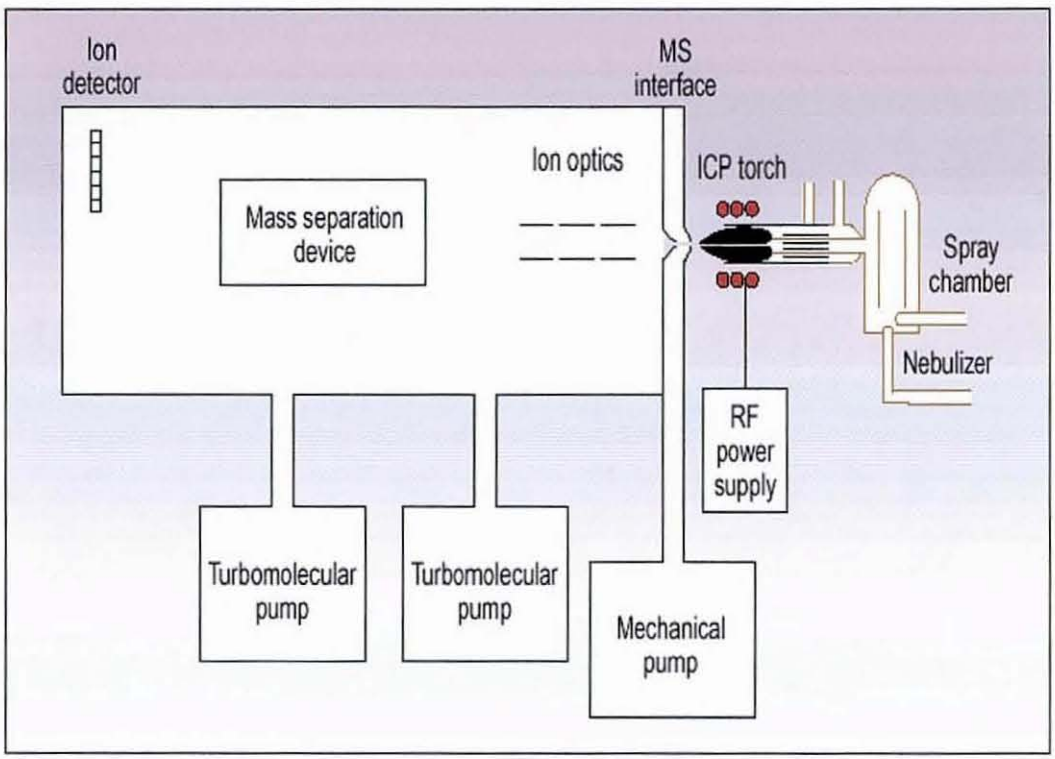

Figure 1.1. Layout of a typical ICP-MS instrument. Reproduced from R. Thomas, Spectroscopy, 2001, 16 (10), 44.

The mechanism of introducing a liquid sample into the plasma involves two separate events. The first step is aerosol generation using a nebuliser

and the second step is droplet selection by way of a spray chamber. Sharp[6, 7] carried out a thorough investigation of both processes.

A liquid sample is normally pumped via a peristaltic pump into the nebuliser. The benefit of a peristaltic pump is that it ensures a constant flow of liquid, irrespective of differences in viscosity between samples, standards, and blanks. An autosampler may be used for the automated, sequential analysis of several samples. After the sample enters the nebuliser, the liquid is broken up into a fine aerosol by the pneumatic action of gas flow (~1 l min^{-1}) smashing the liquid into tiny droplets[5].

Because the plasma is inefficient at processing large droplets, the spray chamber's function is primarily to allow only the small droplets to enter the plasma. It also smoothes out pulses that occur during the nebulisation process. Several ways exist to ensure only the small droplets get through, but the most common way is to use a double pass spray chamber where the aerosol emerges from the nebuliser and is directed into a central tube running the whole length of the chamber. The droplets travel the length of this tube, where the large droplets (i.e. >10 μm in diameter) fall out by gravity and turbulent deposition and exit through the drain tube at the end of the spray chamber. The fine droplets (i.e. <10 μm in diameter) then pass between the outer wall and the central tube, where they eventually emerge from the spray chamber and are transported into the sample injector of the plasma torch[1].

Vapour generation as a mode of sample introduction system for ICP-MS has been reported. The volatile compounds of many elements (mainly as hydrides) are generated and may be separated from the matrix and swept to the plasma without the need for conventional nebuliser/spray chamber assembly. Electrothermal vaporisation (ETV) was used to introduce liquid or solid samples into the ICP. The advantages of these methods are that the transport efficiency is improved and the ability to separate the analyte from the matrix is achieved and these results in lowering the detection limit[3, 8].

Solid materials may be introduced into the plasma and the common method is to employ laser ablation to produce an aerosol of sample particles[9]. Arcs and sparks have also been used[9]. In all types of sample introduction systems, Ar is mainly used as a carrier gas.

1.2.2. Ion source

The ion source used in ICP-MS is mainly the Ar inductively-coupled plasma. The plasma comprises a highly ionised gas at very high temperature (Ar plasma temperature: ~ 6000 - 10000 K). The Ar plasma is generated and maintained at the end of a quartz glass torch located inside the loops of a cooled copper load coil[1].

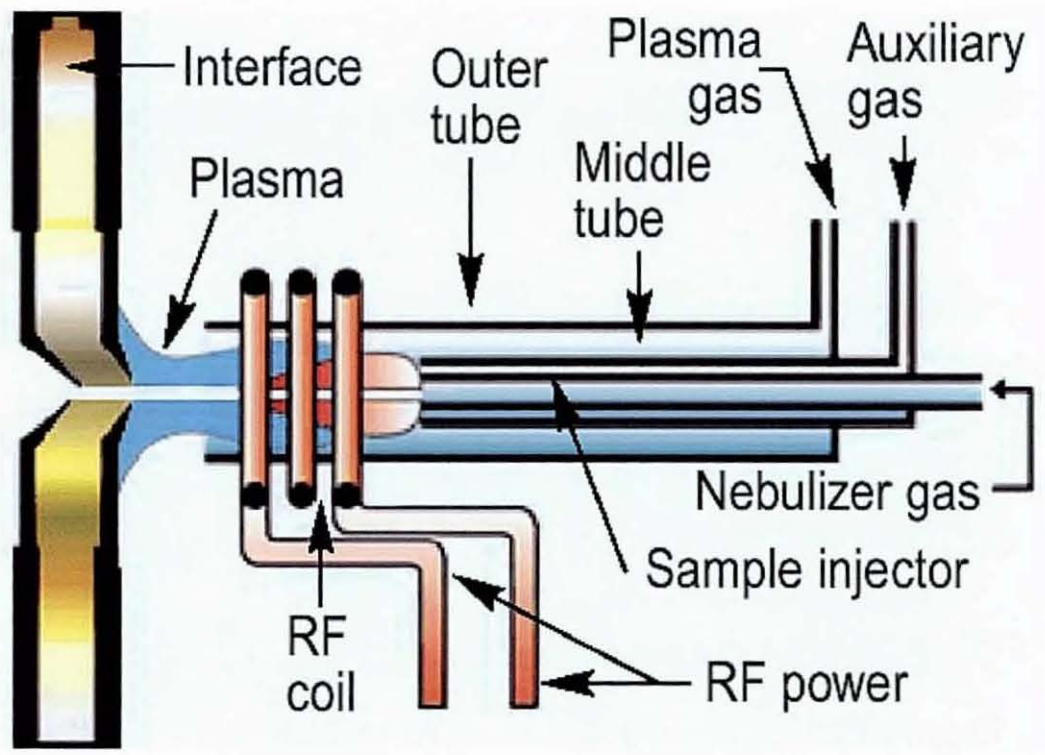

Figure 1.2. Detailed view of a plasma torch and RF coil relative to the MS interface. Reproduced from R. Thomas, Spectroscopy, 2001, 16 (6), 26.

The basic components that are used to generate the plasma are a torch, radio frequency (RF) coil and RF power supply. Figure 1.2 is a view of the

plasma torch and RF coil relative to the MS interface. The plasma torch consists of three concentric tubes, which are usually made from quartz. In Figure 1.2, these are shown as the outer tube, middle tube, and sample injector. The plasma torch is mounted horizontally and positioned centrally in the RF coil, approximately 10–20 mm from the MS interface region. The most common type of torch used is the Fassel torch, which is designed to produce a stable plasma[10].

Argon gas is usually used to form the plasma (plasma gas) and is passed between the outer and middle tubes at a flow rate of 12-15 l min^{-1}. This gas flow is responsible for the main supply of Ar to the plasma. It helps also to stabilise the plasma and finally cool the outer glass jacket of the torch. A second gas flow, the auxiliary gas, passes between the middle tube and the sample injector at ~ 1 l min^{-1}. This is used to change the position of the base of the plasma relative to the tube and the injector and once again avoid torch melting problems. A third gas flow, the nebuliser gas, also flowing at ~ 1 l min^{-1} carries the sample, in the form of a fine droplet aerosol from the sample introduction system, and physically punches a channel through the centre of the plasma[10].

The coil is made usually of 2-3 turns of copper tube through which water is circulated for cooling. The coil is wrapped around the end of the torch and is connected to a radio frequency power generator. This creates an oscillating RF magnetic field within the Ar flowing through the torch[10].

The components of RF generators have become significantly smaller. Most of today's generators use solid state electronic components. This makes modern instruments significantly smaller and more suitable for routine operation. Two frequencies have typically been used for ICP RF generators: 27 and 40 MHz. The early RF generators used 27 MHz while the more recent designs prefer 40 MHz. There appears to be no significant analytical advantage of one type over the other for ICP-MS. However, it is worth mentioning that the 40 MHz design typically runs at lower power

levels, which produces lower signal intensity and reduced background levels[10].

The mechanism of formation of the plasma is started when a spiral flow of argon gas is directed between the outer and middle tube of a quartz torch. A load coil, usually copper, surrounds the top end of the torch and is connected to a RF generator. When RF power (typically 750–1500 W) is applied to the load coil, an alternating current oscillates within the coil at a rate corresponding to the frequency of the generator. This RF oscillation of the current in the coil causes an intense electromagnetic field to be created in the area at the top of the torch. With argon gas flowing through the torch, a high voltage spark is applied to the gas, which causes some electrons to be stripped from their argon atoms. These electrons, which are caught up and accelerated in the magnetic field, then collide with other argon atoms, stripping off still more electrons. This collision induced ionisation of the argon continues in a chain reaction, breaking down the gas into argon atoms, argon ions, and electrons, forming what are known as an inductively coupled plasma discharge. The ICP discharge is then sustained within the torch and load coil as RF energy is continually transferred to it through the inductive coupling process. The sample aerosol is then introduced into the plasma through the sample injector[10].

Due to the high temperature inside the plasma, the sample is vaporised, atomised and ionised. The efficiency of ionisation of the analyte in the plasma can be estimated from Saha equation[2]:

$$\frac{[M^+]}{[M]} = \frac{2}{n_e}\left(\frac{2\pi m_e kT_e}{h^2}\right)^{3/2}\frac{Q^+}{Q^0}\exp\left(-\frac{IP}{kT_{ion}}\right) \qquad (1\text{-}1)$$

where

$[M^+] / [M]$ is the ratio of partition functions of the ion and atom respectively.

n_e is the electron number density in the plasma.

m_e is the mass of the electron.

k is Boltzmann's constant.

T_e is the free electron temperature.

h is Planck's constant.

Q^+ and Q^0 are the electronic partition function of the ion and atom respectively.

IP is the ionisation potential.

T_{ion} is the ionisation temperature.

Most elements in the periodic table are about 90% ionised in the high temperature environment of the Ar plasma. Exceptions are elements with first ionisation potentials close to or greater than that of Ar (15.76 eV), such as As (9.81 eV) and Se (9.75 eV). Since the first ionisation potential of Ar is greater than that of most other elements, but smaller than the second ionisation potential of most elements, the majority of sample ions in Ar plasma are singly charged positive ions. Only small amounts of doubly charged ions occur but these ions such as Ba^{++} still cause a measurable interference[2] (See Section 1.4.).

1.2.3. Ion transport system

The ion transport system of an ICP-MS instrument consists of the interface region and the ion lenses system and facilitates the transfer of ions produced in the ICP to the mass spectrometer. It can be said that the detection capability of ICP-MS is generally recognised as being superior to any of the other atomic spectroscopic techniques; it is probably most susceptible to the sample's matrix components. The inherent problem lies in the fact that ICP-MS is relatively inefficient; out of every million ions generated in the plasma, only one actually reaches the detector. One of the main contributing factors to the low efficiency is the higher concentration of matrix elements compared with the analyte, which has the effect of defocusing the ions and altering the transmission characteristics of the ion beam. This is referred to as the space charge

effect, and it can be particularly severe when the matrix ions have a heavier mass than the analyte ions[11].

The role of the interface is to transport the ions efficiently, consistently, and with electrical integrity from the plasma, which is at high temperature and atmospheric pressure (760 Torr), to the mass spectrometer analyser region, which is operating at room temperature and under vacuum (~ 10^{-6} Torr). The interface consists of two metallic cones with small orifices, which are maintained at a vacuum of 2-3 Torr with a mechanical pump. After the ions are generated in the plasma, they pass through the first cone, known as the sampler cone, which has an orifice diameter of 0.8 – 1.2 mm. The ions are then further extracted through the orifice of the skimmer cone, which generally has a more pointed shape than the sampler cone and has a smaller orifice (0.4–0.8 mm), into the front section of the mass spectrometer chamber that is maintained at a pressure of about 10^{-6} Torr by a turbo vacuum pump. Both cones are usually made of nickel, but they can be made of other materials such as platinum. To reduce the effects of the high temperature plasma on the cones, the interface housing is water cooled and made from a material that dissipates heat easily[12].

The ion focusing system of an ICP-MS instrument is situated in the front part of the evacuated mass spectrometer housing and may consist of one or several ion lenses. The role of the ion lens is to transport the maximum number of analyte ions from the interface region to the mass separation device while rejecting as many of the matrix components and non-analyte based species as possible. These species cause signal instability and contribute to background levels, which ultimately affect the analytical performance of the instrument. In addition, if particles from the matrix penetrate farther into the mass spectrometer region, they have the potential to deposit on lens components and, in an extreme case, get into the mass analyser. Basically two approaches will reduce the chances of these undesirable species making it into the mass spectrometer. The first method is to place a grounded metal stop (disk) behind the skimmer cone.

This stop allows the ion beam to move around it but physically blocks the particles, photons, and neutral species from travelling downstream. The other approach is to set the ion lens or mass analyser slightly off axis. The positively charged ions are then steered by the lens system into the mass analyser, while the photons and neutral and non-ionic species are rejected out of the ion beam[12].

Most lens systems incorporate an extraction lens after the skimmer cone to electrostatically pull the ions from the interface region. This has the benefit of improving the transmission and detection limits of the low mass elements (which tend to be pushed out of the ion beam by the heavier elements), resulting in a more uniform response across the mass range. The optimum lens voltage is mass dependent and varies with the mass of the analyte being measured. The heavier the mass of the analyte is the higher the optimum lens voltage[12].

1.2.4. Mass separation device

The mass analyser is positioned between the ion optics and the detector and is maintained at a vacuum of approximately 10^{-6} Torr. The most commonly used mass separation device used in ICP-MS is a quadrupole mass filter. A quadrupole acts as a mass filter that separates ions according to their mass-to-charge (m/z) ratio. There are other kinds of mass analysers available, but they are less common and expensive compared with the quadrupole mass analyser. These include the double focusing magnetic sector and time of flight mass spectrometers.

A quadrupole consists of four cylindrical or hyperbolic rods of the same length and diameter. By placing a direct current (dc) and RF field of opposite polarity on opposing pairs of rods, a complex electromagnetic field is generated in the space between the rods that controls the ions that can pass through the mass spectrometer. For a given combination of RF and DC potentials, only ions of a specific (m/z) ratio can pass through the mass spectrometer to the detector. Ions with lower and higher (m/z) ratios

are filtered and Figure 1.3 shows this in greater detail. This scanning process is then repeated for another analyte at a completely different (m/z) ratio until all the analytes in a multielement analysis have been detected[4].

The quadrupole mass analyser can only separate masses that are approximately 1 amu apart. It is important to understand that the quadrupole mass spectrometer cannot distinguish between charged particles of different species (e.g. isotopes of different elements, molecular ions and doubly charged ions) that have the same (m/z) ratio and as a result, the quadrupole mass analyser is not sufficient to resolve the spectral interferences away. A recent successful development in ICP-MS is the use of a collision/reaction cell that is positioned in front of a conventional quadrupole mass spectrometer in order to eliminate/reduce certain molecular ion interferences from the ion beam before they enter the mass analyser (See Chapter 4).

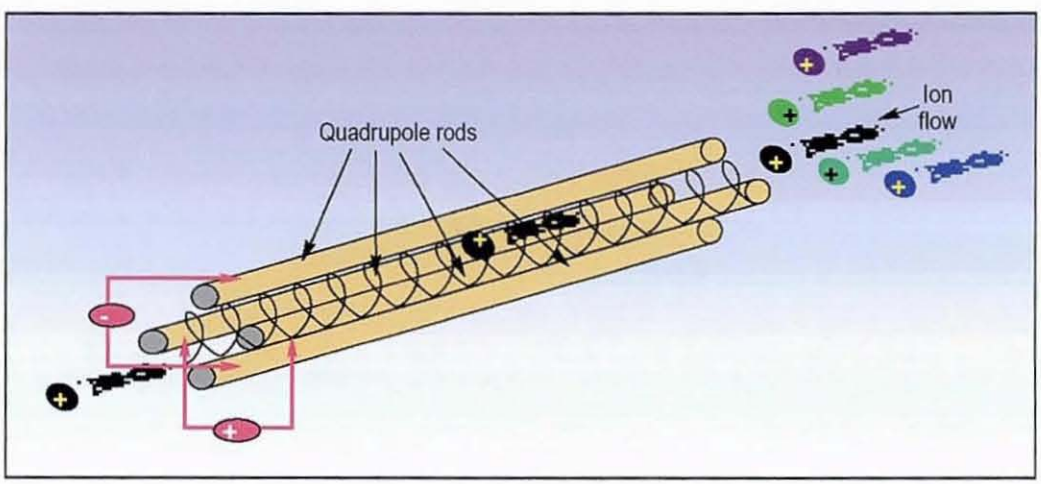

Figure 1.3. Schematic diagram showing principles of a quadrupole mass filter. Reproduced from R. Thomas, Spectroscopy, 2001, 16 (10), 44.

Two important performance specifications of a mass analyser govern its ability to separate an analyte peak from a spectral interference. The first is resolving power (R), which in traditional mass spectrometry is represented by the following equation[13]:

$$R = m / \Delta m \qquad (1\text{-}2)$$

Where m is the nominal mass at which the peak occurs and Δm is the mass difference between two resolved peaks. The second specification is abundance sensitivity, which is the signal contribution of the tail of an adjacent peak at one mass lower and one mass higher than the analyte peak[2]. The abundance sensitivity is probably the most critical. If a quadrupole has good resolution but poor abundance sensitivity, it will often prohibit the measurement of an ultra-trace analyte peak next to a major interfering mass[4].

The ability to separate different masses with a quadrupole is determined by a combination of factors including shape, diameter, and length of the rods, frequency of quadrupole power supply, operating vacuum, applied rf-dc voltages and the motion and kinetic energy of the ions entering and exiting the quadrupole analyser. All these factors might have a direct impact on the stability of the ions as they travel down the middle of the rods and thus affect the ability to separate ions of different m/z ratios. This is represented in Figure 1.4, which shows a simplified version of the Mathieu mass stability plot of two separate masses (A and B) entering the quadrupole at the same time[4].

In Figure 1.4, any of the rf-dc conditions shown under the light blue plot will allow only mass A to pass through the quadrupole, while any combination of rf-dc voltages under the yellow plot will allow only mass B to pass through the quadrupole. If the slope of the rf-dc scan rate is steep, represented by the light blue line (high resolution), the spectral peaks will be narrow, and masses A and B will be well-separated (equivalent to the distance between the two blue arrows). However, if the slope of the scan is shallow, represented by the red line (low resolution), the spectral peaks will be wide, and masses A and B will not be so well separated (equivalent

to the distance between the two red arrows). On the other hand, if the slope of the scan is too shallow, represented by the grey line (inadequate resolution), the peaks will overlap each other (shown by the green area of the plot) and the masses will pass through the quadrupole without being separated.

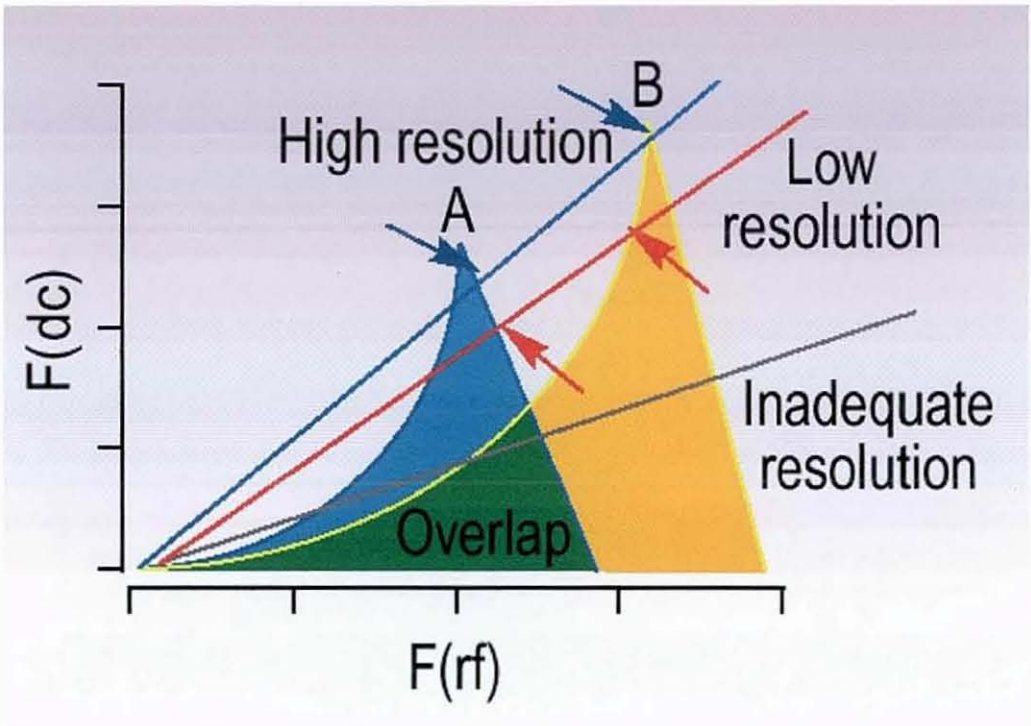

Figure 1.4. Simplified Mathieu stability diagram of a quadrupole mass filter, showing separation of two different masses, A (light blue plot) and B (yellow plot). Reproduced from R. Thomas, Spectroscopy, 2001, 16 (10), 44.

In theory, the resolution of a quadrupole mass filter can be varied between 0.3 and 3.0 amu. However, improved resolution is always accompanied by a sacrifice in sensitivity, as seen in Figure 1.5, which shows a comparison of the same mass at a resolution of 3.0, 1.0, and 0.3 amu. It can be seen that the peak height at 3.0 amu is much larger than the peak height at 0.3 amu but, as expected, it is also much wider. This would prohibit using a resolution of 3.0 amu with spectrally complex samples. Conversely, the peak width at 0.3 amu is very narrow, but the sensitivity is low. For this reason, a compromise between peak width and sensitivity usually has to

be reached, depending on the application. The quadrupole is normally operated at a resolution of 1.0 amu for most applications.

The biggest impacts on abundance sensitivity derive from the motion and kinetic energy of the ions as they enter and exit the quadrupole. The characteristics of ion motion at the low mass boundary is different from the high mass boundary and is therefore reflected in poorer abundance sensitivity at the low mass side compared with the high mass side. In addition, the velocity (and therefore the kinetic energy) of the ions entering the quadrupole can affect the ion motion and, as a result, could have a direct impact on the abundance sensitivity. For this reason, factors that affect the kinetic energy of the ions, such as high plasma potential and the use of lens components to accelerate the ion beam can degrade the instrument's abundance sensitivity[4].

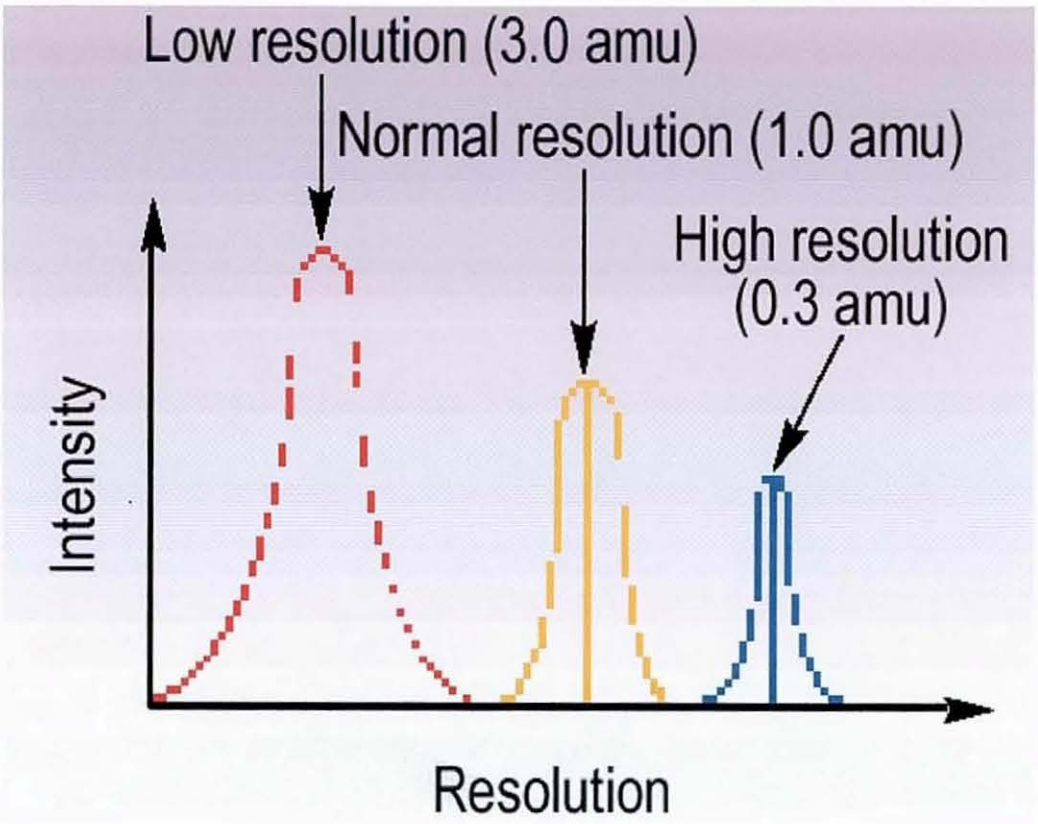

Figure 1.5. Sensitivity comparison of a quadrupole operated at 3.0, 1.0 and 0.3 amu resolution. Reproduced from R. Thomas, Spectroscopy, 2001, 16 (10), 44.

1.2.5. Detector

The detector is located at the far end of the mass spectrometer. Its purpose is to detect, amplify and measure the analyte ions passing through the mass spectrometer. A number of different ion detection designs have been used in ICP-MS. The detector is usually positioned off-axis to minimise the background from the radiation and neutral species coming from the ICP[1, 14].

The most common ion detectors used are Channeltron electron multipliers. Electron multipliers consist of an open, curved glass tube flared at one end to form a cone. The internal surface of the tube is coated with a semiconductor material such as lead oxide. For the detection of positive ions the cone is biased at a high negative potential (~ - 3 kV) and the collector electrode, beyond the output end of the tube, is held at ground. The resistance of the interior coating varies with position along the tube. Thus, when a voltage is applied, a potential gradient is established. When a positive ion leaves the mass analyser, it is attracted to the negative potential of the cone and will subsequently strike the surface. Upon impact, one or more secondary electrons are ejected and accelerated down the tube towards ground potential. This process is repeated many times as the secondary electrons move down the tube towards the collector containing up to 10^8 electrons[1].

The Faraday cup is another sort of detector used in ICP-MS instruments where ultra-trace detection limits are not required. The ion beam from the mass analyser is directed into a simple metal electrode, or Faraday cup. In this approach, there is no control over the applied voltage. The Faraday cup can only be used for high ion currents and the lower working range is in the order of 10^4 counts/s. This means that if a Faraday cup is to be used as the only detector, the sensitivity of the ICP-MS might be severely compromised. For this reason, Faraday cups are normally used in conjunction with a Channeltron or discrete dynode detector to extend the dynamic range of the instrument[14].

Another detector used for ICP-MS instruments is the discrete dynode electron multiplier which is often called an active film multiplier; it works in a similar way to the Channeltron, but uses discrete dynodes to carry out the electron multiplication. When an ion emerges from the quadrupole, it sweeps through a curved path before it strikes the first dynode. On striking the first dynode, it liberates secondary electrons. The electron optic design of the dynode produces acceleration of these secondary electrons to the next dynode, where they generate more electrons. This process is repeated at each dynode, generating a pulse of electrons that is finally captured by the multiplier collector or anode[14].

ICP-MS using the pulse counting measurement mode is usually capable of about five orders of linear dynamic range. This means that ICP-MS calibration curves generally are linear from some parts per trillion (ppt) levels to as much as a few hundred parts per billion (ppb). However, a number of ways exist to extend the dynamic range of ICP-MS by three to four orders of magnitude to work from sub ppt to as much as 100 part per million (ppm). These approaches involve using two detectors, filtering the ion beam, using two scans with one detector and using one scan with one detector[14].

1.3. Data acquisition

In ICP-MS, raw data in the form of counts per second (cps) signal intensities are collected either by peak jumping (hopping) or by continuously scanning.

In peak jumping mode, the mass spectrometer is used to collect data at a number of fixed mass positions (usually 1-3) for each isotope of interest. The location of the central position of the peak is particularly important since it is used to locate the starting point for the measurement of each peak. The peak height is measured at each single point of measurement. The advantage of this mode is that the data are collected for the analytes

of interest and the time is not wasted collecting data for isotopes which are not of interest. This can, however, also be a major disadvantage of using the peak hopping mode since no record is available for additional isotopes that might have important roles as interference or matrix species and this may result in missing data because the spectra cannot be fully examined. In theory, the peak hopping mode of measurement should provide a number of advantages where only a small number of isotopes are required, the isotopes of interest are spread across the mass range and isotope ratio measurements are made. The dwell time on each isotope can be varied according to the isotopic abundance, thus improving the counting statistics on the smaller isotope. This mode is usually used for quantitative and semi-quantitative analysis[1].

An alternative mode of operation is by using the scanning mode to collect data for a relatively large number of points so that the peak shape is defined for each isotope and the area under the curve is integrated. A complete spectrum containing information for all isotopes within the mass range 4-240 amu can be collected and stored. Continuous scanning is used to evaluate the shapes of signal peaks and for qualitative identification of the elements present in a sample. The advantage here is that the data are available over a wide mass range that can be used for archival purposes. In addition, interfering peaks are more easily identified if complete spectral information is available[1].

1.4. Interferences

The appearance of any contamination from the sample preparation or from residual gases and products of any plasma reactions may be harmful for the reliability and the accuracy of the analysis by ICP-MS. As the ICP is operating in an open atmosphere, this may lead to a greater variety of additional interferences. In addition, the extent of interference problems depends on the sample matrix and the analyte level of interest. The significance of the interference problems varies with the matrix under investigation. Simple aqueous solutions with low salt concentrations may

be easy to analyse. Quantitative multielement analysis of complex materials such as blood or milk may lead to a variety of unforeseen interferences. Special attention must also be paid to the interference problems when organic compounds are involved. Many attempts have been made to cope with interference problems using several strategies. However, none of these techniques realises a general solution to the problem and in most cases, they offer a chance to get rid of problems from a group of interferences or for selected elements in special matrices. Therefore, interference problems are still the most significant weakness of the quadrupole ICP-MS. The interferences in ICP-MS can be divided into two main groups:

- Spectral or spectroscopic interferences.
- Non-spectral or non-spectroscopic interferences.

Evans and Giglio[15] have published a comprehensive review of spectral and non-spectral interferences in ICP-MS. Todoli and Mermet[16] have reviewed the effect of the acid on the different stages taking place during the whole analytical process in the atomic spectroscopy.

1.4.1. Spectral interferences

Spectral interference generally means that the coincidence of contributions from different species with the same nominal mass. Spectral interferences may be subdivided into different types: isobaric overlap, molecular (polyatomic) ions, refractory oxide ions and doubly charged ions interferences[1].

Isobaric interferences exist when two elements have isotopes of essentially the same mass. In fact, the masses differ by very small fractions of atomic mass unit (amu) but cannot be separated by quadrupole mass analysers. Most elements in the periodic table have one or several isotopes free from isobaric overlap except indium. The most inconvenient example of an isobaric interference is the coincidence of $^{40}Ar^{+}$ and $^{40}Ca^{+}$. To overcome isobaric interferences, an isotope of the

element of interest, free of interference, can be selected. In most cases, however, this will not be the isotope of the highest abundance, so that the detection limit will be worsened by the selection of a minor isotope. If this is not possible, a correction of the total analyte signal must be done for the contribution from the interfering mass. Alternatively isobaric overlaps may be resolved by using a collision/reaction cell[17] (See Chapter 4).

Polyatomic interferences resulting from the combination of two or more species can cause serious interference problems. Argon, hydrogen, and oxygen are the dominant species present in the ICP and these may combine with each other or with elements from the analyte matrices to form polyatomic ions. A large number of polyatomic ion peaks can be yielded by the recombinations of the matrix itself. These combinations are, generally speaking, significant below mass 82 amu[1].

Recognising and eliminating these molecular ions interferences may become crucial to the success of the analysis. The appearance of the majority of molecular interferences depends on the sample itself, operating parameters for the plasma and nebuliser systems and also on the chemicals used in sample preparation step. Minimising the amount of water vapour reaching the plasma, e.g. using a temperature regulated spray chamber[18] can reduce many of the polyatomic interferences that contain hydrogen and oxygen. Introducing a dry sample into the ICP by using laser ablation can minimise this problem[19]. Cold plasma techniques avoid ionisation of Ar atoms. This allows an easier detection of elements that normally suffer from Ar interferences in standard plasma mode[20]. The cool plasma technique is only applicable to elements that are easily ionised and to samples with no complex matrices. Additionally, sensitivity is lower compared with normal plasma conditions. Mixed gas plasmas, whereby a second gas such as nitrogen is added to one or more of the gas streams have been studied with a view to reducing polyatomic ions[21]. A high-resolution mass spectrometer can be employed to distinguish between the analyte and interfering ion signals[22]. The use of a

collision/reaction cell is another approach to remove interfering species (See Chapter 4).

Refractory oxides occur as a result of incomplete dissociation of the sample matrix or from recombination in the plasma tail. These oxides are found at +16, +32 and +48 amu from the main peak. Elements with high oxide bond strengths usually give the greatest yield of refractory oxide ions. The levels of oxides are estimated with respect to the elemental peak; a ratio of MO^+/M^+ no greater than 5% is generally expected. For metal oxide ion formation, the RF forward power and nebuliser gas flow rate have a significant effect on the level of metal oxide ions generated. As with most interference effects in ICP-MS, the extent of the problem depends on the sample matrix and the analyte level of interest; oxide ion interferences are generally at low levels but matrix oxide peaks may interfere with some trace analyses[1].

The appearance of doubly charged ion formation in the ICP is dependent upon the second ionisation energy of the element. Only those elements with a second ionisation energy below that of the first ionisation energy of argon (15.76 eV) may undergo any significant degree of doubly charged ion formation. At normal operating conditions, the level of doubly changed ions is less than 1%. This interference generates a number of isotopic overlaps. Fortunately, the number of elements affected is few and to avoid this problem, an alternative isotope of the element of interest is used, if available, if not, interference corrections are needed[1].

1.4.2. Non spectral interferences

Non spectral interferences are derived from the sample matrix and are characterised by an enhancement or suppression of the analyte signal as a result of factors influencing the sample transport, ionisation, ion extraction or ion throughput in the resulting ion beam. The degree of enhancement or suppression is dependent upon the mass and ionisation energy of the matrix element. Such interferences can be broadly divided

into two categories: physical effects resulting from high levels of dissolved solid and matrix induced suppression in the ion beam[1, 15].

Suppression of the analyte signal can be caused by deposition of salt on the sampler and skimmer cones, which substantially affects the sampling process. To reduce this type of signal suppression, the system can be primed by allowing the sampling cone to partially clog thereby achieving a pseudo steady-state where the rate of deposition is equalled by the rate of dissociation[15].

An excess of a heavy, easily ionisable element in the sample matrix can cause serious analyte signal suppression. The presence of such matrix elements is thought to cause a change in the ion transmission, which subsequently suppresses the analyte signal. It has been suggested that space charge effects in the ion beam play a major role. The most severe effects are caused by heavy matrix elements with low ionisation potentials whilst light analyte elements with high ionisation potentials are most severely affected[15].

A number of approaches can be employed to overcome the effects of interfering matrix elements. A common technique to cope with such non-linearity is internal standardisation by selected elements such as Rh or In. The internal standard should be similar to the elements of interest in various properties such as mass, ionisation energy and oxide formation. Methods such as liquid chromatography, solvent extraction and co-precipitation can be used to separate the analyte from the interfering matrix, with the additional benefit of analyte pre-concentration. Matrix matching of samples and standards, and optimisation of the ion lens settings can also reduce suppression effects[15].

1.5. Calibration

The ICP-MS can not give an absolute value for the concentration of an element or isotope but is always a comparative technique. The

measurement of an isotope of an analyte is achieved by comparison of the measured counts for this isotope in unknown samples with those from a substance containing a known amount of the element or isotope.

1.5.1. Qualitative analysis

The facility to collect signals for all masses during a series of scans or peak jumps can be used for a purely qualitative examination of a sample. The spectra can then be visually examined for the presence or absence of an analyte, and to identify possible sources of interference. Sample matrices should always be subject to qualitative analysis prior to full quantification[1].

1.5.2. Semi-quantitative analysis

Semi-quantitative analysis is a useful tool for the rapid determination of bulk sample compositions. A plot of mass against sensitivity yields a relatively smooth curve if degree of ionisation and isotopic abundance are taken into account. This response curve can be used to calibrate the instrument to provide semi-quantitative data. In practice, this calibration method is ideal as a survey tool, particularly if an unfamiliar matrix or sample type is to be analysed or if only the approximate levels of the components are required. The profile of the response curve is usually defined using 6-8 elements suitably spread across the mass range. The responses for each element are corrected for isotopic abundance, concentration and degree of ionisation and a second order curve fitted to the data[1].

1.5.3. Quantitative analysis

1.5.3.1. External calibration

Calibration in ICP-MS is most commonly achieved by external standardisation. The signal intensities of all analyte isotopes are measured in a blank as well as in several standards with different, known analyte concentrations that cover the concentration range of interest. The linear

relationship between the signal intensity and the concentration is used to establish a calibration curve that can be used to calculate the concentration of the analytes in samples of unknown composition. External calibration minimises effort but often sacrifices the accuracy and the precision of the analysis. This results from the matrix effects that might cause an enhancement or suppression of the analyte signals. One common approach is to match the matrices of the standards and unknowns[1].

This method of external calibration was mainly used in this thesis and the calibration functions were derived according to the method described in Miller and Miller[23]. The calibration functions, as shown in Appendix I, were formulated into an EXCEL97 spreadsheet and all the calculations were carried out in EXCEL97.

The detection limit based on the 3 times the standard deviation of the blank is a flawed estimated and it is not usually attainable. This has been discussed by Sharp and co-workers[24] where they considered a more realistic estimate of the noise that effects measurements in ICP-MS. Where real samples are analysed the estimate of uncertainty should include the contribution from the estimation of the calibration curve. This is the method proposed by Miller and Miller[23] and is used in this thesis. The detection limits are much higher than those reported in manufacturers data sheets (3 times the standard deviation of the blank), but are more representative of true method detection limits. It should be noted that the detection limit reported using this approach directly reflects the concentration range of the calibration standards.

1.5.3.2. Internal standardisation

Modern ICP-MS instruments provide stable signals for extended periods of time. However, instrument drift (i.e. most commonly a decrease of signal intensity with time) does occur and has to be corrected for in order to ensure good quality quantitative analysis. This drift correction may be

achieved by internal standardisation, i.e. the normalisation of all data to a non-analyte isotope present in the same or known concentrations in all samples and standards. Ideally, internal standards should be non-interfered species of similar mass and ionisation potential to the analyte. Isotopes commonly used as internal standards in solution ICP-MS include ^{9}Be, ^{45}Sc, ^{89}Y, ^{103}Rh, ^{115}In and ^{209}Bi.

1.5.3.3. Standard addition

This method of calibration provides an effective way to minimise the matrix effects. This technique involves taking the sample, dividing it into equal aliquots, and adding to each increasing amounts of a reagent containing the analyte(s) under consideration. The increments usually consist of equal volumes and a minimum of four mixtures is required per sample[1].

1.5.3.4. Isotope dilution

The method of isotope dilution requires an element that has at least two stable isotopes. A spike of stable enriched isotope of the element is added to the sample. The spiked sample and un-spiked sample are analysed by ICP-MS and this determines the ratio of the isotopes. From the amount added and the isotopic ratio measured, the concentration of the element can be deduced. The isotopic ratios are not altered by element losses because both isotopes are from the same element and therefore behave in same way.

References

1. K. E. Jarvis, A. L. Gray and R. S. Houk, *Handbook of Inductively Coupled Plasma Mass Spectrometry*, Blackie Academic & Professional, Glasgow, 1992.
2. *Inductively Coupled Plasma Mass Spectrometry*, eds. A. Montaser, Wiley-VCH, New York, 1998.
3. *Inductively Coupled Plasma Mass Spectrometry and its Applications*, eds. S. J. Hill, Sheffield Academic Press, Sheffield, 1999.
4. R. Thomas, *Spectroscopy*, 2001, **16 (10)**, 44.
5. R. Thomas, *Spectroscopy*, 2001, **16 (5)**, 56.
6. B. L. Sharp, *J. Anal. At. Spectrom.*, 1988, **3**, 613.
7. B. L. Sharp, *J. Anal. At. Spectrom.*, 1988, **3**, 939.
8. P. Smichowski and S. Farias, *Microchem. J.*, 2000, **67**, 147.
9. D. Gunther, S. E. Jackson and H. P. Longerich, *Spectrochim. Acta, Part B*, 1999, **54**, 381.
10. R. Thomas, *Spectroscopy*, 2001, **16 (6)**, 26.
11. R. Thomas, *Spectroscopy*, 2001, **16 (9)**, 38.
12. R. Thomas, *Spectroscopy*, 2001, **16 (7)**, 26.
13. P. Turner, D. Mills, E. Schroder, G. Lapitajs, G. Jung, L. Iacone, D. Haydar and A. Montaser, *Instrumentation for Low- and High-Resolution ICP-MS,* in Inductively Coupled Plasma Mass Spectrometry, eds. A. Montaser, WILEY-VCH, New York, 1998, pp. 442.
14. R. Thomas, *Spectroscopy*, 2002, **17 (4)**, 34.
15. E. H. Evans and J. J. Giglio, *J. Anal. At. Spectrom.*, 1993, **8**, 1.
16. J. L. Todoli and J. M. Mermet, *Spectrochim. Acta, Part B*, 1999, **54**, 895.
17. L. J. Moens, F. F. Vanhaecke,D. R. Bandura, V. I. Baranov and S. D. Tanner, *J. Anal. At. Spectrom.*, 2001, **16**, 991.
18. H. P. Longerich and W. Diegor, *J. Anal. At. Spectrom.*, 2001, **16**, 1196.

19. B. Hattendorf and D. Gunther, *J. Anal. At. Spectrom.*, 2000, **15**, 1125.

20. C. J. Park and J. K. Suh, *J. Anal. At. Spectrom.*, 1997, **12**, 573.

21. C. J. Amarasiriwardena, N. Lupoli, V. Potula, S. Korrick and H. Hu, *Analyst*, 1998, **123**, 441.

22. T. Townsend, *J. Anal. At. Spectrom.*, 2000, **15**, 307.

23. J. N. Miller and J. C. Miller, *Statistics and Chemometrics for Analytical Chemistry*, 4th edn., Pearson Education Limited, England, 2000, ch. 5, pp.107.

24. C. P. Ingle, P. K. Appelblad, M. A. Dexter, H. J. Reid and B. L. Sharp, *J. Anal. At. Spectrom.*, 2001, **16**, 1076.

Chapter 2:

Bayesian Analysis of Inductively Coupled Plasma Mass Spectra

2.1. Introduction

Inductively coupled plasma mass spectrometry (ICP-MS) is the most powerful technique for multielement determinations in different matrices[1-3] but suffers from both spectral and non-spectral interferences which limit the accuracy, precision and reproducibility of the analytical data obtained. The nature of the interferences is complex and it is difficult to know and identify exactly all of them as each analyte has its own interferences in a particular matrix and this makes the problems more complicated. Quantitative analysis by ICP-MS usually involves choosing an isotope of the analyte of interest based on the criteria that it has the highest sensitivity and is free from interferences. This is not easy as sometimes the main isotope suffers from interferences. Many attempts have been made to correct spectral interferences (See Section 1.4.1) and in most cases, they were developed for individual applications. It can be mentioned here that there is not a unique solution for interference problems, but there are different solutions and these depend on the type of interferences encountered.

Spectral interferences are probably the largest class of interferences in ICP-MS and are caused by atomic or molecular ions that have the same m/z as the analytes of interest. Current ICP-MS instrumental software corrects for all known atomic "isobaric" interferences caused by overlapping isotopes of different elements, but does not correct for most polyatomic interferences. These are derived from precursors having numerous sources such as: the sample matrix, the reagents used for sample preparation, the plasma gases and entrained atmospheric gases. The major interferences are well documented, but on-going improvements in instrumental sensitivity continue to reveal species that were previously unknown or not measurable. A number of tables have been published listing many types of interferences[4-10] and Evans and Giglio[11] have published a comprehensive review of interferences in ICP-MS.

Vaughan and Horlick[4] presented spectral interferences for almost all the elements in the periodic table. Extensive tables indicating potential interferences caused by oxide, hydroxide and doubly charge ions were listed. In addition, Tan and Horlick[5] investigated the background species for water and for 5% solutions of nitric acid, hydrochloric acid and sulphuric acid in the mass range 1-84 amu and extensive tables was presented for the main polyatomic ion interferences in these matrices. It was found that the spectral backgrounds for HCl and H_2SO_4 are quite complex compared with the spectral background for HNO_3. Furthermore, Hutton and co-workers[6] catalogued the effect of common interferences for the elements from Li through to Ge using a double focusing ICP-MS. Moreover, Townsend[9] used magnetic sector ICP-MS to determine the first row transition metals, except Ti, in water, urine, plant, tissue and rock certified reference materials. De Boer[7] employed a spectral fitting procedure to reduce the interferences from polyatomic ions in the mass range 51-88. May and Weidmeyer[8] reported the most harmful polyatomic ion interferences accounted in ICP-MS in different matrices.

The use of chemometric approaches to deal with spectral interferences in ICP-MS has been reported and various multivariate calibration techniques have been proposed[12-20]. The application of multivariate correction methods suffer, in most cases, from incomplete knowledge of the interferences involved. Limited numbers of interferences have been addressed and in many cases artificial samples were employed. In real analysis, the relevant interferences should be taken into account, as they might derive mainly from the matrix samples.

Principal component analysis has been applied for the determination of the rare earth elements[12, 13] and it also has been used for the determination of Ni in serum and urine where several polyatomic interferences arising from the presence of calcium, sodium and potassium can interfere with the determination[14]. In addition, another mathematical approach to interference correction was being proposed and tested. De

Loos-Vollebregt and associates [15] developed a software approach based on multicomponent analysis to measure the total mass spectra including the determination of the elements in the mass range 6-250 amu in different salt matrices in ground water. However, this approach was not able to cope with too many species that might combine in any one analyte signal, which means that a complex sample such as a biological material might not be determined using this method. In another paper[16], these authors developed an updated version of the multicomponent analysis software that incorporated routines for automated interpretation of mass spectra and a database of interferents. By using the information available in the full mass range scan (6-238 amu); this fully automated approach reported concentrations in the sample solution for all analytes. Furthermore, a spectral fitting programme has been described by de Boer[7] to reduce polyatomic ion interferences in the mass range 51-88 for a number of salt solutions. It was shown that some molecular ions have a mathematical relationship with the presence of a component atomic ion. Grotti *et al.*[17] described a multi-linear regression approach for the investigation and quantification of interferences caused by sodium, calcium, chloride and sulfur when these matrix elements are present together in the sample, at concentration levels ranging from 0.5 to 1000 mg l^{-1}. The spectral interferences were studied by monitoring the changes in the isotope ratio (signal ratio for mono-isotopic analytes) with varying matrix composition. All the expected interfering effects caused by the considered matrix elements were found; however, the dependence of their magnitude on matrix composition was found to be a complex function.

The first attempt to use a computer programme to deal with spectral interferences (oxide, hydroxide and doubly charge ions) was introduced by Vaughan and Horlick[18]. This model simplified the problem by looking at a limited number of species and ignoring some important species such as argide ions. Even the ions, which were included, were not quantified in their contributions. An additional programme (MS InterView) has been developed by Burton and Horlick[19, 20]. This programme enables the user to

display, manage and access elemental spectral interferences as pictoral data. It was written originally for Apple Macintosh; however, another version has been written for Windows. The programme offers a listing of interferences broken down into the following categories: isobaric, oxides, doubly charged, background dependent and matrix dependent species. Interference information was provided for all masses of all elements and was easily accessed through a periodic table window. The programme has a database that lists as many known interferences as possible up to the date of its launch and it is possible to expand this database by adding more interfering ions. This programme does not provide an answer for the magnitude of the interferences at a selected mass.

2.2. Bayesian analysis

ICP-MS instruments provide a huge amount of information on the elemental content of a sample. This information usually is fit for its intended purpose. The measurements in ICP-MS, in fact, do not provide such information directly rather they provide data. This data does not provide a complete representation of the real world, but an approximation that may be biased and is certainly modified by the presence of noise. Given the data, it is inferred what the real world is like, and then through a model information is derived (requiring a linear calibration model to link the data and concentrations). However, there are problems arising from the noise associated with the data that limits the precision. When the data is plotted on mass scales, it is found that more than one species can contribute to the counts in any particular measurement channel. Further, the sensitivity for different species may be matrix dependent. These factors combine to scramble the data obtained from the ICP-MS, particularly for complex samples[21].

The probability of a particular data point occurring in a predicted or "mock" spectrum with a known noise distribution is readily calculated and this is known as the likelihood. However experiments yield the data and from this

the true spectrum must be inferred, this quantity is known as the posterior. The two are linked by Bayes' theorem as:

prob(S and D) = prob(S) x prob(D given S) = prob(D) x prob(S given D)

↑ ↑ ↑ ↑

prior *likelihood* *predictive* *posterior*

The predictive is a number that indicates how effectively the calculated spectrum fits the data. It is arrived at by integrating the posterior over the whole space of possible spectra. The prior encapsulates the question that is to be asked of the data and forces recognition that the ultimate quality of an answer depends as much on the question as on the data. The prior attempts to identify that spectrum that best fits the data whilst making the least commitment to missing data[21].

The application of Bayesian analysis, and in particular, the Massive Inference (MI™) algorithm, as described by Sibisi and Skilling[22], to the deconvolution of ICP-MS rare earth spectra in the mass range from 140-176 amu has been investigated[21]. The basic principles of Bayesian analysis were outlined and it was shown that an important feature of this approach is that previous knowledge, and indeed experience, are incorporated in a systematic way into the analysis. An excellent description of the Bayesian approach has been provided by Daniell[23] who also describes the role of, and need for, a statistical prior that is independent of the data, but extracts from it information without dependence on missing data.

Bayesian analysis is based on the following principles: opinions are expressed in probabilities, data are collected and these data change the prior probabilities, and through the operation of Bayes's theorem, yield posterior probabilities[23].

In the case of ICP-MS experiments, the data set can be very large and it becomes a challenge to find the maximum of a function with a large number of variables. Therefore, there is a need to use mathematical algorithms to simplify the conversion of data to conclusions. Massive Inference offers rapid and consistent data recovery, it is robust, portable and can be easily transferred from one sample scenario to another. However, a good knowledge of the sample is essential in order to have a good component menu to tackle the problems of polyatomic ion interferences.

Massive Inference is an enhanced algorithm that builds upon maximum entropy. It is based on Bayesian statistics and provides a consistent probabilistic theory to obtain unbiased results, without making any unsubstantiated assumptions. This is particularly desirable if there is no additional information to justify these hypotheses. If, on the other hand, additional prior knowledge is available, it can be effectively incorporated into the computation, leading to more stringent confidence intervals.

2.3. Aims and objectives

In the present study, a mathematical model was used to reduce the effects of polyatomic ion interferences, i.e. the Massive Inference (MI^{TM}) algorithm. This chapter describes the analysis of mass spectra over the range 46 - 88 amu which represents a significant part of the spectrum that is particularly prone to molecular ion interferences. Although studying a limited mass range might be considered to be against the ethos of multivariate analysis, it does, as will be seen, restrict the amount of data to be processed to more manageable proportions. An additional justification is that this mass range accounts for the transition metals, with the exception of mono isotopic Sc, and the important additional elements Ga, Ge, As, Se, Br, Kr, Rb and Sr and therefore encompasses a significant proportion of the biologically active trace elements. In addition, the effects

of mass bias are estimated and corrected to verify the effectiveness of the deconvolution algorithm.

2.4. Experimental

2.4.1. Standard solutions and reference materials

Multielement standards CLMS-2A and CLMS-4 (Spex, Stanmore, Middlesex, UK) and the certified reference materials TORT 1 - Lobster Hepatopancreas, NIST 1547 - Peach Leaves and NIST 1577b - bovine liver were used in this study. The multielement standard CLMS-2A consists of Ag, Al, As, Ba, Be, Ca, Cd, Co, Cr, Cs, Cu, Fe, Ga, K, Li, Mn, Mg, Na, Ni, Pb, Rb, Se, Sr, Tl, U, V and Zn and the CLMS-4 contains B, Ge, Mo, Nb, P, Re, S, Si, Ta, Ti, W and Zr. The certified reference materials were purchased from Promochem (Welwyn Garden City, Herts, UK).

Dilutions were carried out with high purity acid (see below) and 18 MΩ Milli-Q water (Millipore, MA, USA). The weights of TORT 1, NIST 1547 and NIST 1577b taken were 0.496g, 0.551g and 0.492g respectively. The CRM samples were microwave digested in 5ml high purity nitric acid ("Aristar", Merck, Poole, Dorset, UK). The microwave used was a Perkin Elmer 'Multiwave' system fitted with 50 ml quartz vessels capable of 70 bar working pressure (75 bar cut off). The microwave-operating programme is shown in Table 2.1.

All samples were diluted with 18 MΩ de-ionised water to 50ml prior to measurement. The final acid concentration was nominally 7 % v/v (based on dilution). Calibration standards were prepared by mixing the two multielement standards that contained all of the elements within the study in mass range (mass 46-88). Seven standards were prepared with concentrations for all elements of: 0.1, 0.3, 1.0, 3.0, 10, 30 and 100 $\mu g\ l^{-1}$. Standards, blank and a procedural blank were prepared in the same acid

concentration. 50 μg l^{-1} of Rh was used as the internal standard and 2% v/v nitric acid was used as the wash solution.

Table 2.1. Optimised microwave digestion programme.

Step	Power (W)	Time (min)
1	0 to 500	5
2	500	5
3	500-1000	0
4	1000	20
5	0	15

2.4.2. Instrumentation

All samples were analysed using an ELAN 6000 ICP-MS (Perkin-Elmer SCIEX, Thornhill, Ontario, Canada). The ICP-MS operating conditions are listed in Table 2.2.

2.4.3. Bayesian spectral deconvolution algorithm

Spectral deconvolution was carried out using the *Massive Inference (MI™)* programme supplied by MaxEnt Solutions Ltd., Tresawsam, Killaha East, Kenmare, Co. Kerry, Ireland.

This programme requires two input files in order to carry out the data analysis (isotopes abundances are stored in a reference database[24]), i. e.

- Data file: this consists of the raw counts or the mass bias corrected counts and the standard deviations at each mass.
- Component menu file: this contains the collection of possible components that have significant contributions in the selected mass region. Note that it isn't necessary to know every species in order to obtain useful information from the algorithm.

The output from the programme contains the following information:

- The relative abundances of all species in the menu at each mass.
- The evidence (E).
- The total predicted count for each component with the error in this count and the probability that the species has been detected by the algorithm.
- The spectral fit at each mass in the region studied.
- Correlation matrix for the selected species.

A brief description of the operating procedure for the Massive Inference programme is presented in Appendix II.

Table 2.2. Operating conditions for ELAN 6000

Rf power/W	1050
Gases / l min^{-1}	
Plasma	14.0
Auxiliary	0.80
Nebuliser	0.77
Acquisition Parameters	
Sweeps per reading	20
Readings per replicate	1
Number of replicates	3
Scanning mode	Peak jump
Dwell time per analyte/ms	50

2.4.4. Initial strategy for inferring the species contributing to the observed mass spectrum

The MI algorithm requires an estimate of the noise or standard deviation of each signal as part of its input data. It follows that a basic criterion for

estimating the closeness between the predicted (the so-called *mock* spectrum) and observed spectrum is to take the difference between them and scale this to the standard deviation. The upper value for this parameter at any mass is in fact logically given by the signal to noise ratio (S/N). The MI algorithm is internally consistent in this respect and if a single species, which cannot possibly contribute to the observed spectrum (e.g. use Pb as a dummy species for the mass range 46 - 88), is used to try to predict the spectrum then MI returns the S/N at each mass. The effect of any species on reducing this number towards zero is an indication of its contribution at a particular mass. The *Evidence,* Prob(D), which is formally the probability of the data, indicates how well the actual data accounts for the spectra (potentially a very large number) that can be synthesised from the proposed menu of species. This parameter therefore represents the goodness of fit for the spectrum as a whole, rather than the fit at individual masses, with more positive values close to zero indicating improved prediction (Table 2.3).

The following steps were followed:

1. Run MI on the spectral data with a dummy species (e.g. Pb) to establish the S/N at each mass (Figures 2.1A-D).
2. Run MI on the spectral data with individual selected species in the mass range studied to see if MI predicts any contribution for such species. From this step a group of species that involve the elemental and many of the polyatomic ions are selected. It should be mentioned here that some of the polyatomic ions selected (because they improve prediction) must, however, be excluded from consideration if it is known in advance that they do not exist in the samples (e.g. Hf^{+2}).
3. Run MI again with a menu containing all the selected species from step 2. Species are retained if the algorithm indicates a high probability of detection (close to 100%) and a significant contribution to the total count at the relevant masses.
4. To verify that the process of selecting the species menu has been successful the procedure can be reversed. Thus carry out further runs

of MI, this time removing one species at a time from the composite menu and monitoring the effects.

Progress through Steps 1 - 4 is guided by the simple expedients of looking at the E value and spectral fit at each mass in turn (See Table 2.3 and Figures 2.2A-D and 2.3A-D), however, other parameters also have to be considered and may force reconsideration of earlier conclusions. The calibration data in terms of linearity and error and the derived analytical data from reference materials must be considered.

2.4.5. Choosing the component menus

The selection of the components in the menu was important, because the MI programme used the menu to search for the composition of the components. If any component was missed out in the menu, then the count numbers might be unreasonable for the given sample. Different component menus gave different predicted counts for the each species in the menu.

When the MI programme was run with component menus containing only the elemental species in the mass range studied, the S/N at some masses, such as m/z=76 in the 100ppb standard and the biological reference materials, was reduced but did not become close to zero which indicates that the data was not fully optimised (as shown in Figures 2.2A-D). More complicated component menus were developed based on the steps previously mentioned (See Section 2.4.4.) and Table 2.4 presents the component menus used for the standard solutions and biological samples.

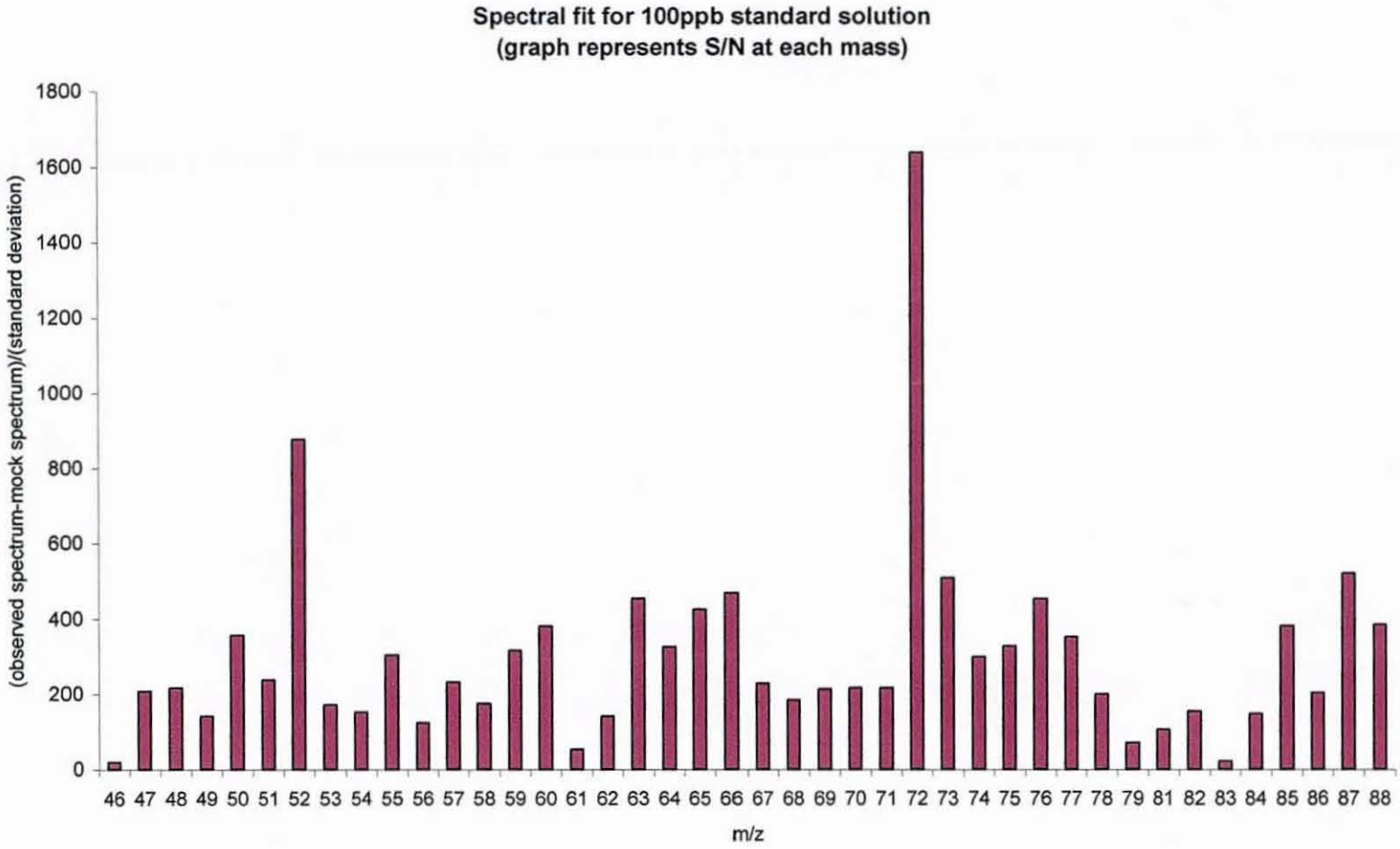

Figure 2.1A. Spectral fit for 100ppb standard solution derives from dummy menu.

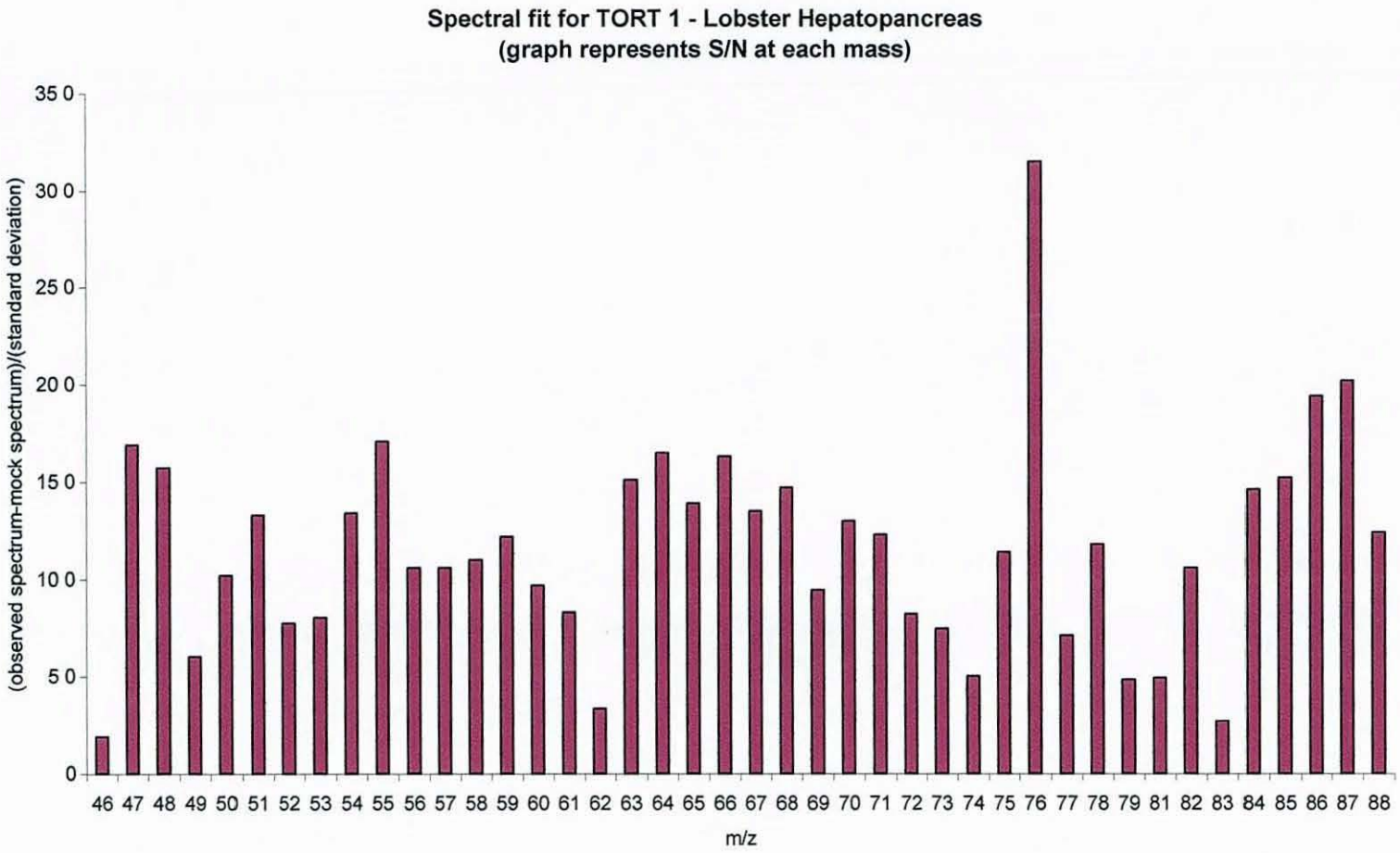

Figure 2.1B. Spectral fit for TORT 1 - Lobster Hepatopancreas Marine derives from dummy menu.

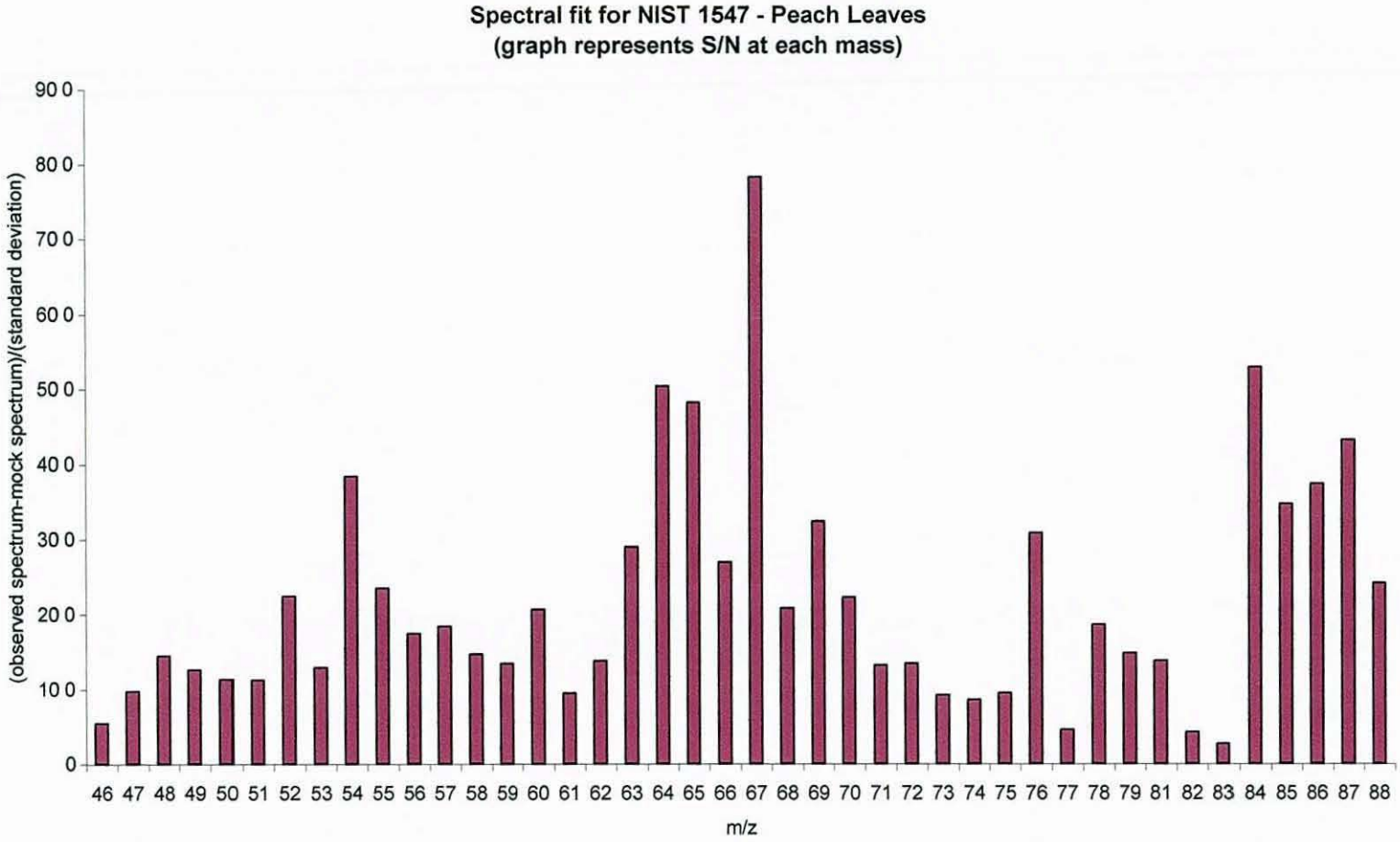

Figure 2.1C. Spectral fit for NIST 1547 - Peach Leaves derives from dummy menu.

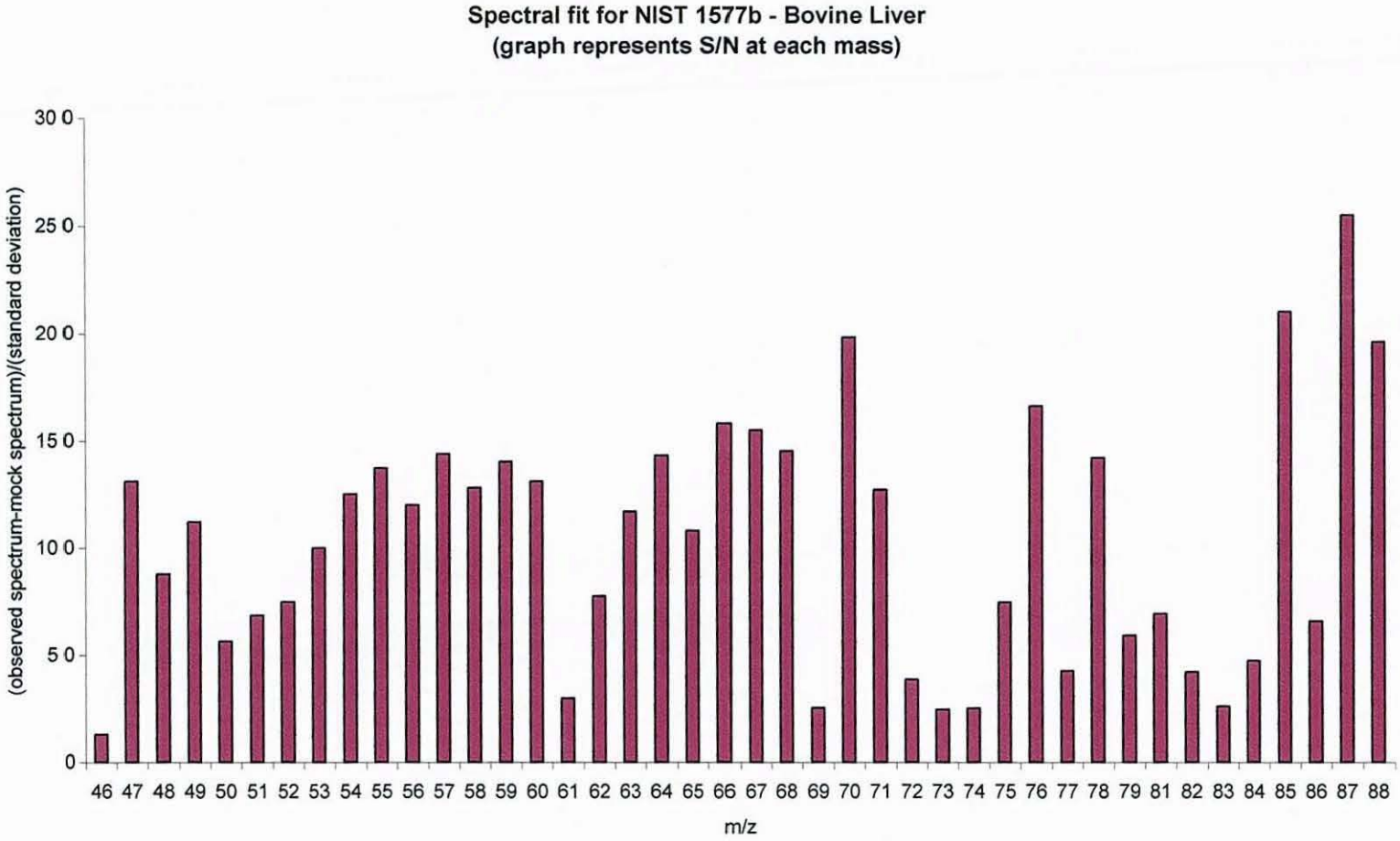

Figure 2.1D. Spectral fit for NIST 1577b - Bovine Liver derives from dummy menu.

Table 2.3. Evidence values for 100ppb standard solution and biological samples.

	Evidence derive from			
	Dummy data	**Elemental data**	**Raw data**	**Mass bias data**
100 ppb	1.83×10^{11}	-41666	-603	-562
TORT 1	8.49×10^{11}	-66126	-690	-670
NIST 1547	5.50×10^{11}	-200176	-795	-771
NIST 1577b	4.71×10^{11}	-37878	-591	-542

Table 2.4. Species contributing to the "mock" spectrum for standard solutions and biological samples

Species	Standard Solutions	TORT 1	NIST 1547	NIST 1577b
Ti	•	•	•	•
V	•	•	•	•
Cr	•	•	•	•
Mn	•	•	•	•
Fe	•	•	•	•
Co	•	•	•	•
Ni	•	•	•	•
Cu	•	•	•	•
Zn	•	•	•	•
Ga	•	•	•	•
Ge	•	•	•	•
As	•	•	•	•
Se	•	•	•	•
Rb	•	•	•	•
Sr	•	•	•	•
Ar_2	•	•	•	•
Ar_2H	•		•	•
Ar_2H_2	•			
ArC			•	•
ArC_2	•			
ArCa	•			
ArCl			•	
ArCN				•
ArCNH	•			
ArCO	•	•		
ArN	•			
ArN_2	•			•

ArN_2H		•		
ArNa	•			
ArNO		•	•	
ArNOH		•	•	•
ArO	•			
ArO_2	•			
ArO_2H	•	•	•	•
ArOH			•	
ArS			•	•
$ArSH_2$	•			
ArV	•			
Ba^{++}	•		•	
Br	•	•	•	•
Ca	•	•	•	
CaOH	•	•		
$CClH_3$		•	•	
Cl_2		•		
ClN	•			
ClO	•			•
ClO_2H	•			
CrO	•			
CuO	•			
FeO	•			
GaO	•			
GeO	•			
HNCl	•			
Kr	•	•	•	•
N_2O		•	•	
Na_2O	•	•		
NO_2	•			
NO_2H		•	•	•
ScO	•			
Si_2	•		•	•
SiO_2	•		•	
SiO_2H	•		•	
SN	•			•
SO	•			•
SO_2H	•	•	•	•
SO_3		•		
SOH	•	•	•	•
TiOH	•			
ZnO	•			

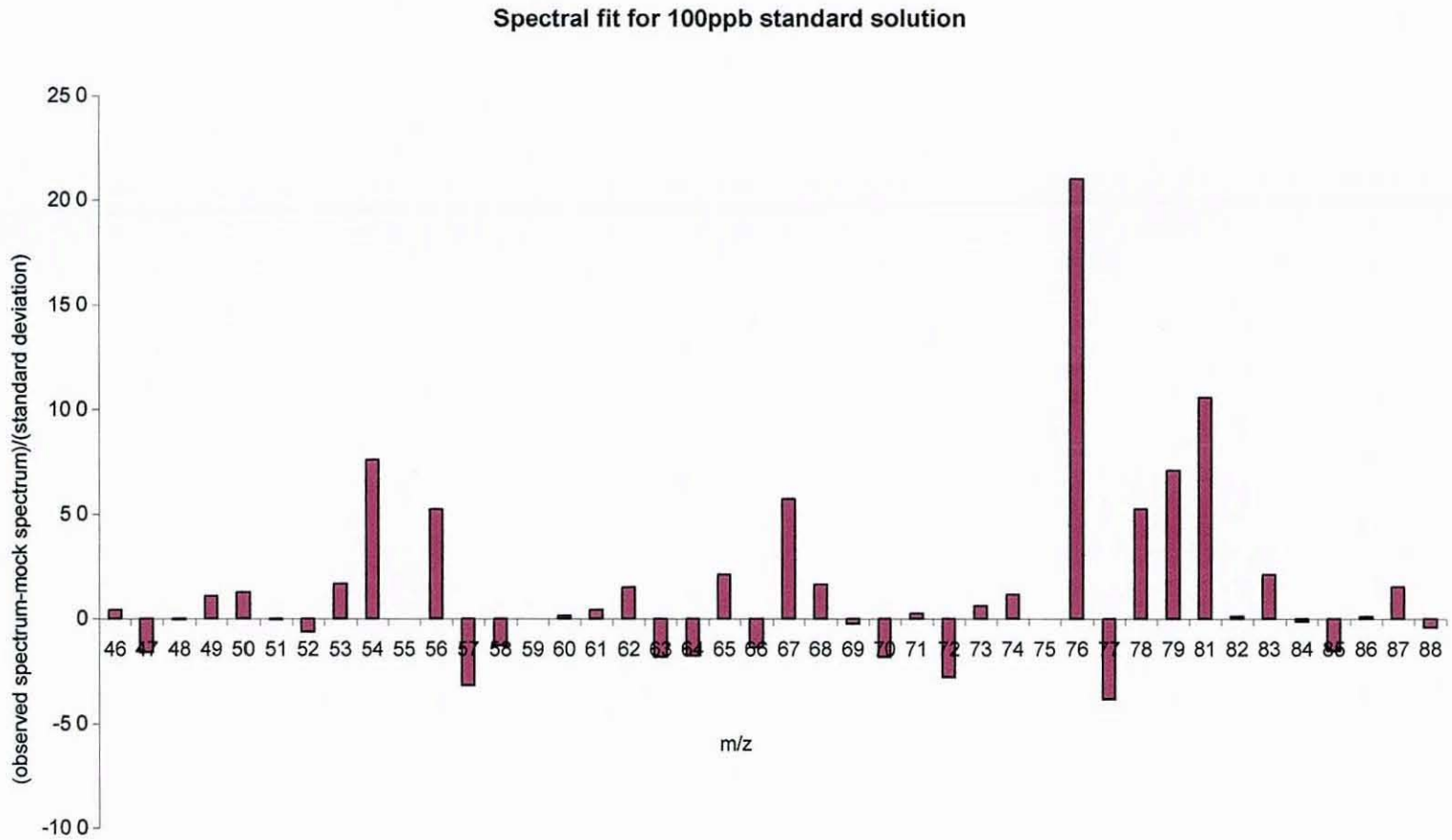

Figure 2.2A. Spectral fit for 100ppb standard solution derives from elemental menu.

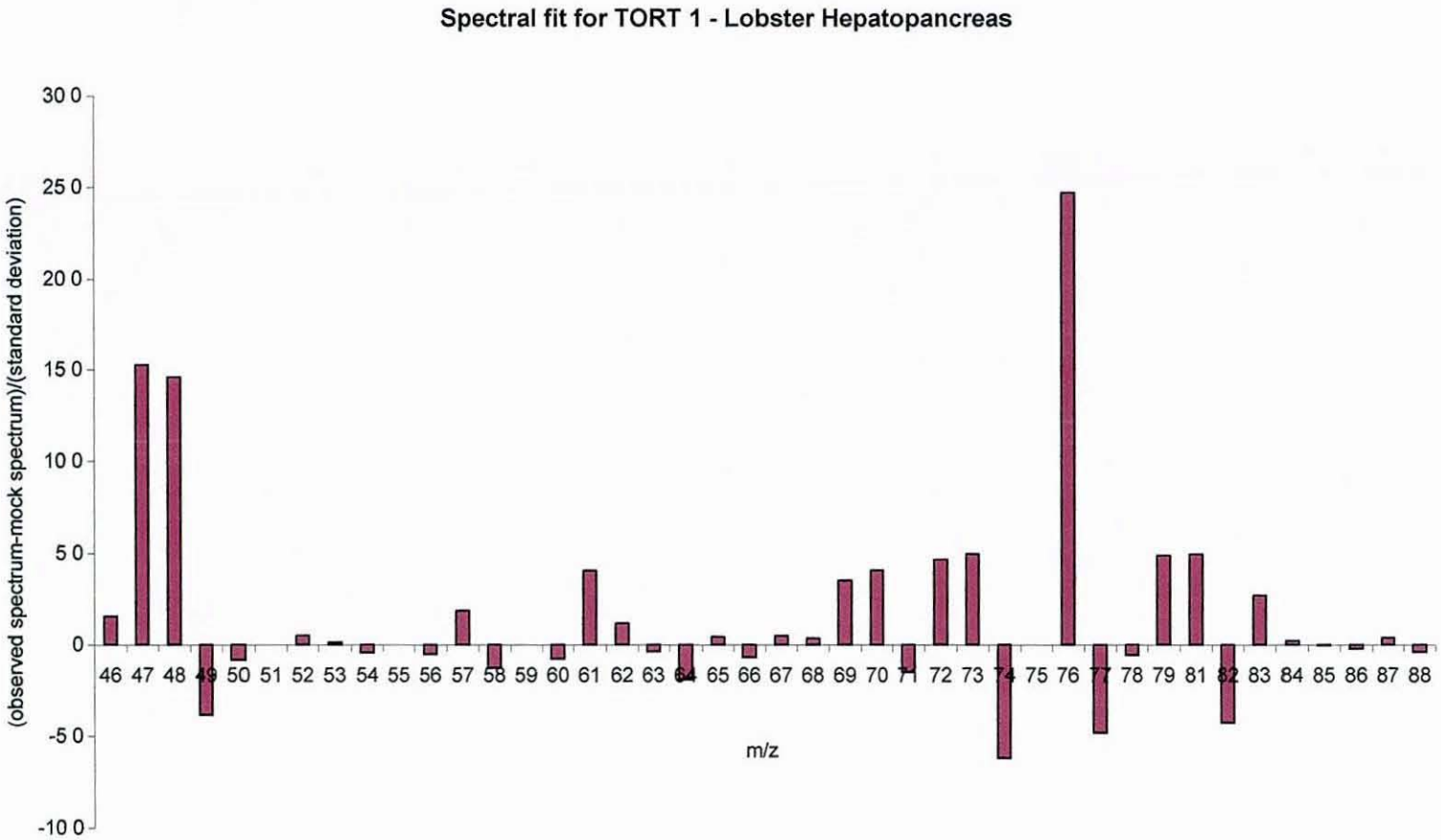

Figure 2.2B. Spectral fit for TORT 1 - Lobster Hepatopancreas Marine derives from elemental menu.

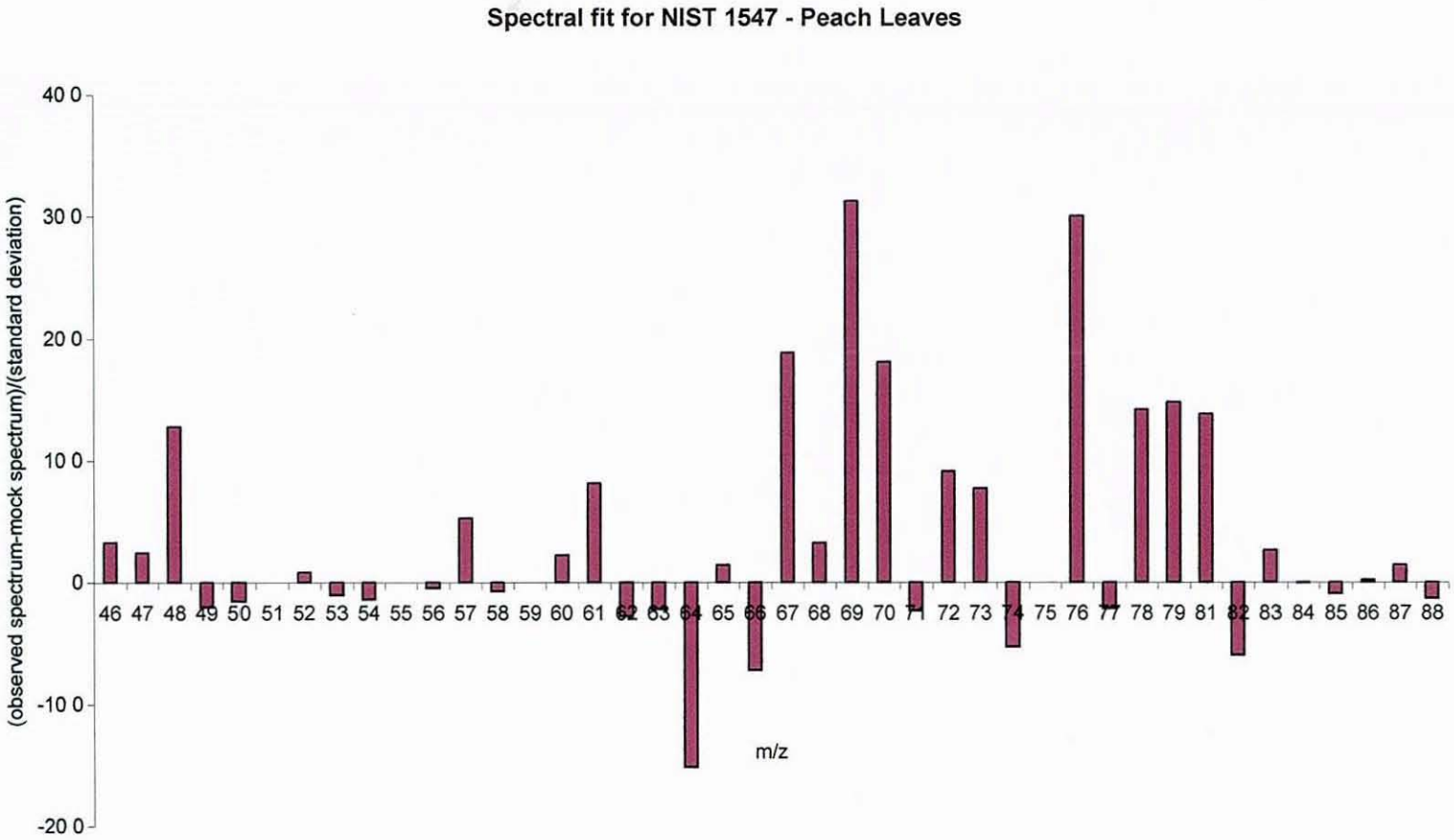

Figure 2.2C. Spectral fit for NIST 1547 - Peach Leaves derives from elemental menu.

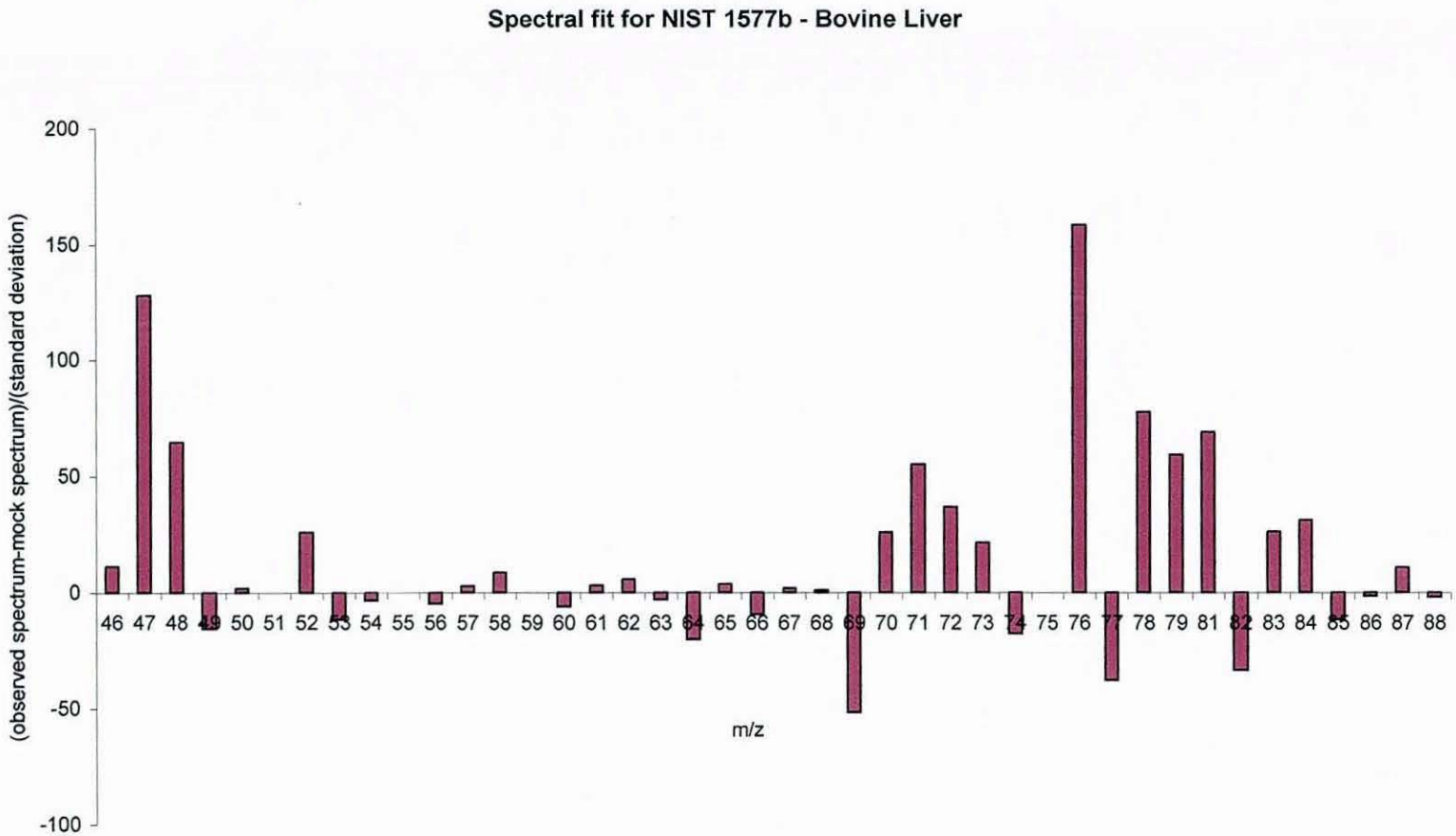

Figure 2.2D. Spectral fit for NIST 1577b - Bovine Liver derives from elemental menu.

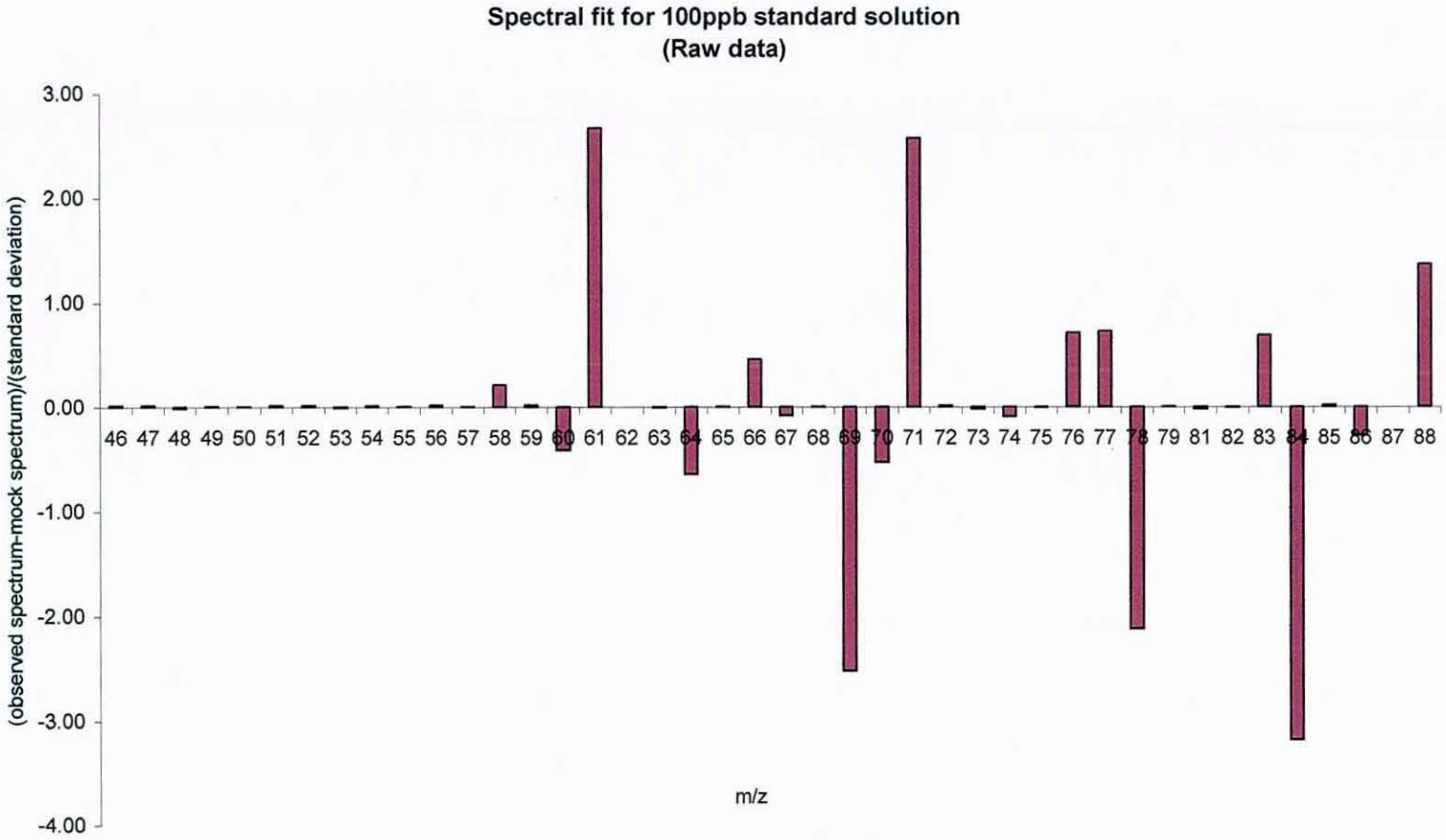

Figure 2.3A. Spectral fit for raw data for 100ppb standard solution derives from species menu (See Table 2.4).

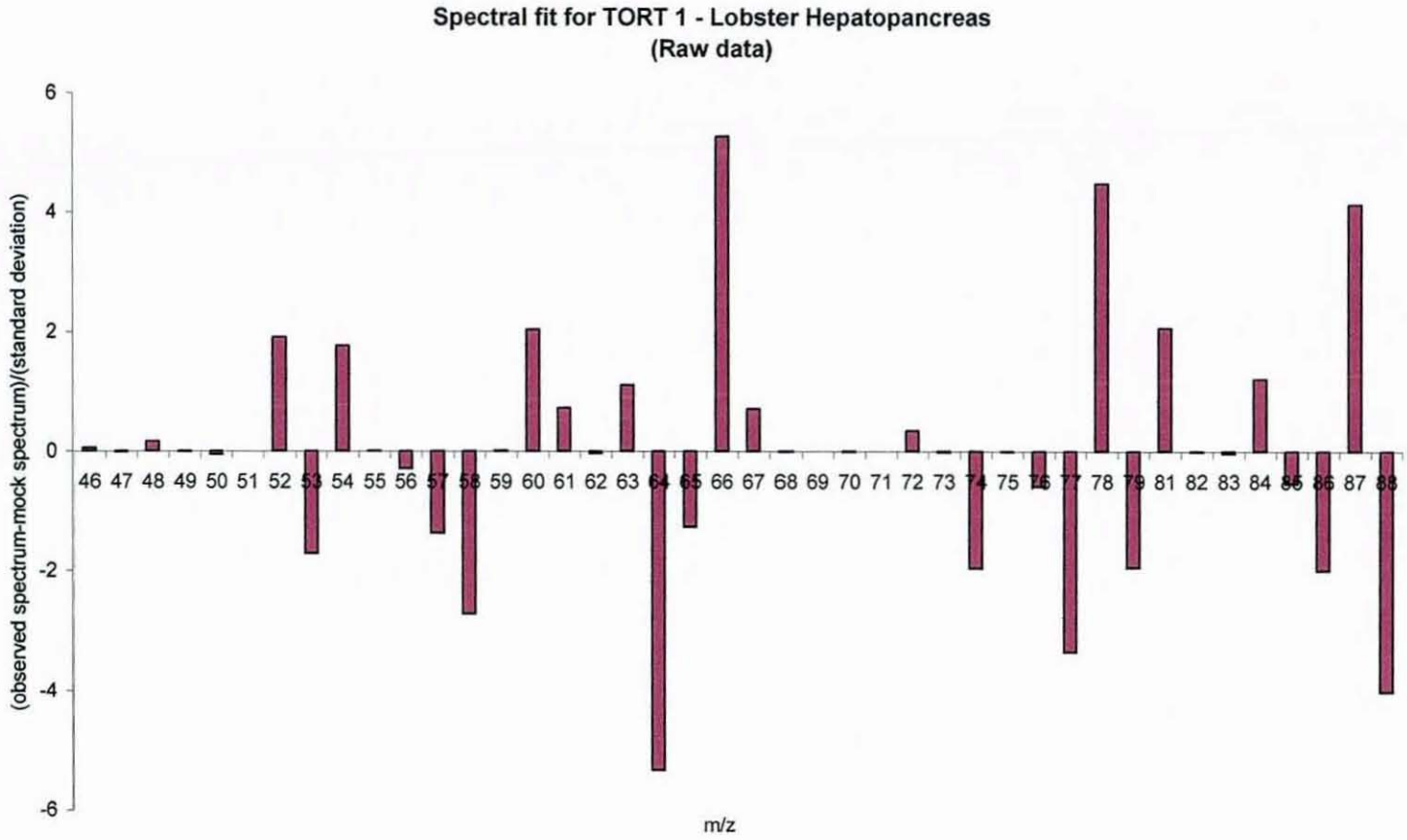

Figure 2.3B. Spectral fit for raw data for TORT 1 - Lobster Hepatopancreas Marine derives from species menu (See Table 2.4).

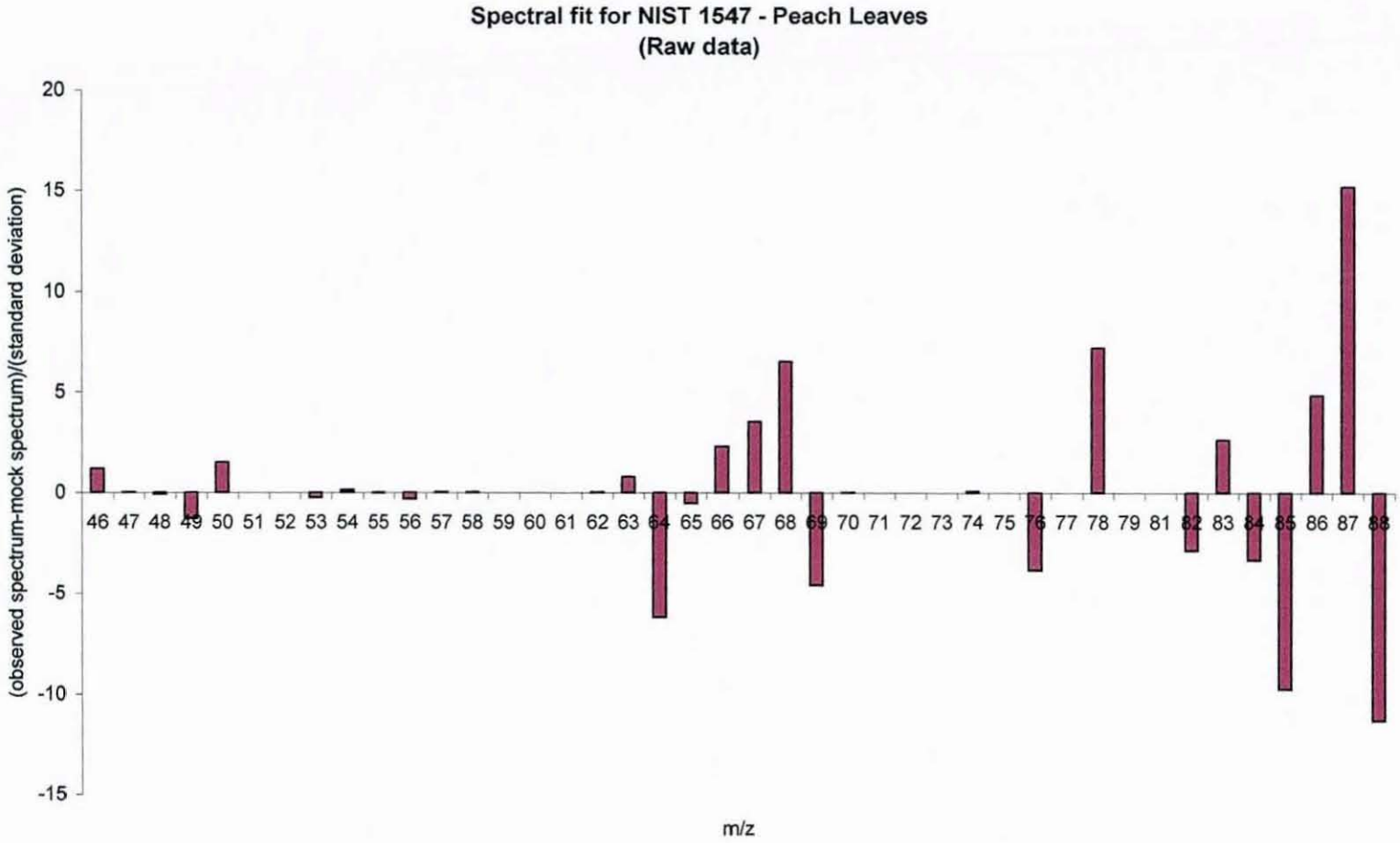

Figure 2.3C. Spectral fit for raw data for NIST 1547 - Peach Leaves derives from species menu (See Table 2.4).

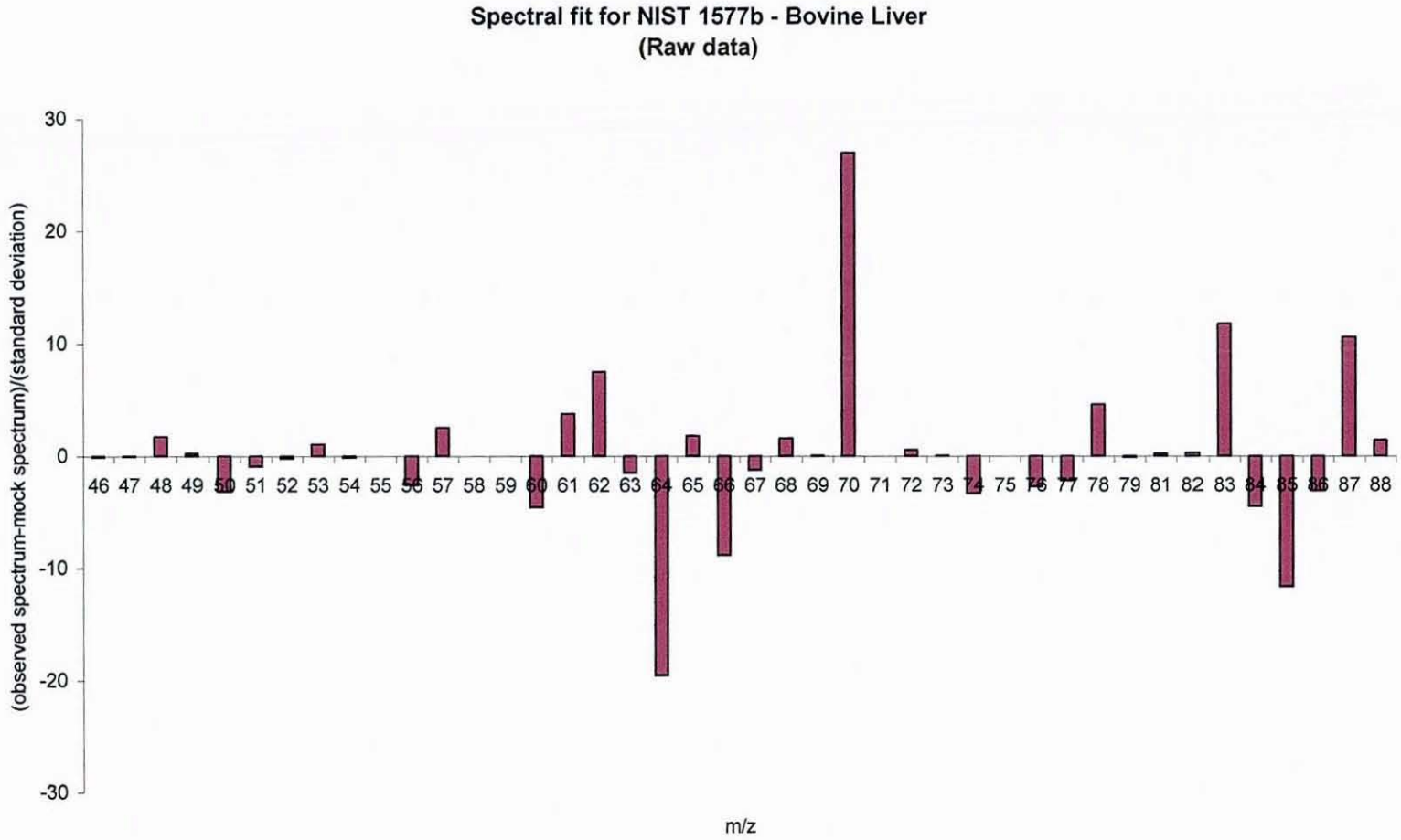

Figure 2.3D. Spectral fit for raw data for NIST 1577b - Bovine Liver derives from species menu (See Table 2.4).

2.5. Results and discussion for raw data

The total predicted count for each component was used to plot calibration curves. The calibration functions were derived according to the method described in Miller and Miller[25] (See Appendix I). The calibration functions were formulated into an EXCEL97 spreadsheet; all the calculations were carried out in EXCEL97. Appendix III shows an example of the calibration spreadsheet results. Table 2.5A shows the calibration functions for the elements in the mass range studied and Table 2.5B show the certified analytical data for these elements for the biological materials.

Table 2.5A. The calibration functions for raw data.

Element	Intercept (a)	Slope (b)	R^2
V	461	5115	0.9998
Cr	4173	5444	0.9999
Mn	311	6684	1
Fe	156937	6834	0.9924
Co	-412	5840	0.9999
Ni	364	4501	0.9999
Cu	-709	2836	0.9817
Zn	2854	2004	0.9990
As	25	782	0.9999
Se	342	710	0.9999
Rb	5298	11885	0.9997
Sr	1461	14689	0.9997

Overall, the results obtained in Table 2.5B were generally far from the documented values for most elements especially for the mono-isotopic As and Se in all samples and Sr in NIST 1577b. The exclusion of mass 80 may affect the determination of Se, which has an isobaric overlap with $^{40}Ar_2$. Mn, Fe, Co, Zn, and Rb results show a better agreement as compared with other elemental components. The estimation of V, Cr, Ni,

and Cu were poor in some samples. These results were derived directly from the data collected from the ICP-MS instrument; however, it was thought that these data might have been affected by mass bias. A further investigation was carried out using MI with mass bias corrected data.

2.6. Study of the mass bias effect

Knowledge of the isotopic abundances of the elements provides useful information for identifying molecular ion species. However, the relative abundances are not accurately reflected by the instrument because of a mass dependent instrumental response that is quantified through measurement of the mass bias. There are three algorithms that may be applied to the correction of mass bias in ICP-MS; these are based upon linear, power law and exponential relationships between the mass bias and the mass difference. For example, Longerich *et al.*[26] found empirically that the power law correction worked well for Pb isotope ratio measurements, using Tl as an internal standard. Taylor *et al.*[27] found the power law and the exponential function to be more successful for correction of mass bias than the linear function for U isotope ratio measurements by multiple collector ICP-MS. Begley and Sharp[28] applied the linear and power law equations and preferred the latter for correcting the mass bias for Pb isotope ratio measurements, using Tl as an internal standard. Park *et al.*[29] used linear, power law and exponential equations to correct the mass bias for Cd isotope ratio measurements by double focusing sector field ICP-MS and found all these to yield equivalent results. De Boer *et al.*[30] incorporated a mass bias correction into their spectral fitting procedure to improve Sn isotope ratio measurements.

Table 2.5B. Analytical results for raw data for biological samples¶.

Element	TORT 1 - Lobster Hepatopancreas Marine			NIST 1547 - Peach Leaves			NIST 1577b - Bovine Liver		
	Certified Value $\mu g\ g^{-1}$	Found Value $\mu g\ g^{-1}$	% of Error	Certified Value $\mu g\ g^{-1}$	Found Value $\mu g\ g^{-1}$	% of Error	Certified Value $\mu g\ g^{-1}$	Found Value $\mu g\ g^{-1}$	% of Error
V	1.4 ± 0.3	1.20 ± 0 09	-14	0 37 ± 0 03	0 26 ± 0 08	-30	0.123#	0.10 ± 0.10	-19
Cr	2.4 ± 0 6	3 02 ± 0.06	26	1#	1.35 ± 0 06	35			
Mn	23 4 ± 1.0	20 6 ± 0.16	-12	98 ± 3	73 9 ± 0 60	-25	10 5 ± 1 7	11.7 ± 0.10	12
Fe	186 ± 11	165 ± 16	-11	218 ± 14	157 ± 16	-28	184 ± 15	209 ± 19	14
Co	0.42 ± 0 05	0 48 ± 0 06	14	0.07#	0 05 ± 0 06	-29	0 25#	0 29 ± 0 06	16
Ni	2.3 ± 0.3	2 80 ± 0.06	22	0 69 ± 0 09	0 44 ± 0 06	-36			
Cu	439 ± 22	320 ± 30	-27	3 7 ± 0 4	4 81 ± 0 99	30	160 ± 8	233 ± 14	46
Zn	177 ± 10	140 ± 5 6	-21	17 9 ± 0 4	16.5 ± 0.59	-7.8	127 ± 16	152 ± 5 2	20
As	24 6 ± 2 2	33 8 ± 0.26	37	0.06 ± 0.018	0.15 ± 0.05	150	0 05#	0 14 ± 0 05	180
Se	6 88 ± 0 47	10.0 ± 0.08	45	0.12 ± 0 009	0 32 ± 0 04	167	0 73 ± 0 06	1 55 ± 0 05	112
Rb				19.7 ± 1 2	17 2 ± 0 31	-13	13 7 ± 1.1	16 5 ± 0.29	20
Sr	113 ± 5	97.9 ± 1.8	-13	53 ± 4	45.7 ± 0 84	-14	0 136 ± 0.001	0.35 ± 0.12	157

¶ *The Found values and the percent of error were estimated to three and two significant figures respectively in most cases.*

 # Value not certified.

2.6.1. Method for correcting the instrumental response function from knowledge of the mass bias

The mass bias per unit mass (as defined below) was estimated by running a multielement standard and subtracting from the raw data a matrix blank (7 % HNO_3). The mass bias was then calculated for all possible isotopic pairs for each element and the results plotted against masses. After rejection of outliers, a smooth curve was obtained from the isotope ratios Cr 53-52, Ni 62-61, Cu 65-63, Se 78-77 and Sr 86-84 obtained from the top standard, see Figure 2.4. Isotopic signals were rejected if more than 5% of the total signal was derived from interfering ions. The mass bias, per unit mass, was then re-estimated from the fitted curve. The mass bias curve reflects the well-known fall-off in sensitivity of quadrupole instruments at low masses. However, this fall-off is parameter dependent (e.g. gas flow rates, sampling depth and ion lens settings) and does appear to level out at very low masses so that good sensitivity is available even for ^6Li the lowest mass isotope normally measured.

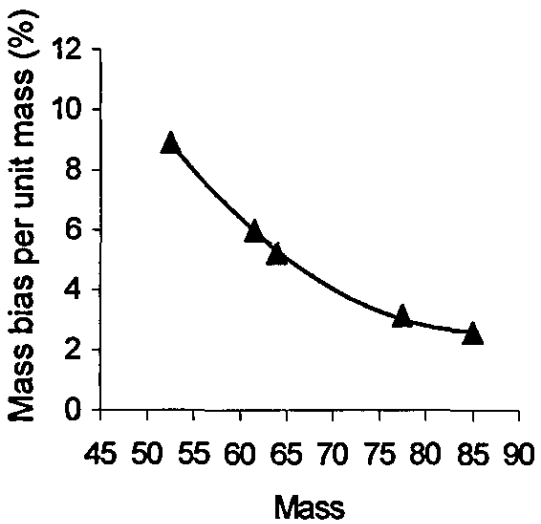

Figure 2.4. Mass bias estimation for the mass range 46-88.

The mass bias (per unit mass) is defined as:

B = (Measured Ratio - True Ratio) / (True Ratio x Δm)

where Δm is the mass difference between the measured isotopes.

Expanding this into intensity measurements at two masses *i* and *i+1* yields:

$$B_{(i+1),i} = \frac{\frac{I^A_{i+1}}{I^A_i} - \frac{I^T_{i+1}}{I^T_i}}{\frac{I^T_{i+1}}{I^T_i}} \Big/ \Delta m \qquad 1$$

where

I_i^A and I_{i+1}^A are the actual count rates at masses *i*, and *i+1* respectively.

I_i^T and I_{i+1}^T are the count rates at masses *i*, and *i+1* required to give the correct theoretical isotope ratio.

However, in a practical measurement of the isotope ratio one mass, usually the lower mass signal (I_i), effectively acts as a reference point and the bias is derived from the intensity at the other (I_{i+1}). Thus $I_i^A = I_i^T$ in equation (1). The mass bias *B*, with minor re-arrangement, is therefore given by:

$$B_{(i+1),i} = \frac{I^A_{(i+1)} - I^T_{(i+1)}}{\Delta m} \Big/ \frac{1}{I^T_{(i+1)}} \qquad 2$$

Thus to correct the relative response at two masses (as required for isotope ratio measurement) requires applications of the equation:

$$I^T_{(i+1)} = \frac{I^A_{(i+1)}}{(1 + B_{(i+1),i}\Delta m)} \qquad 3$$

In this form, equation (2) for the mass bias can be seen to be directly related to the instrument response function over the particular mass increment. The equation states that the mass bias is equal to the slope of the instrument response function normalised to the recorded intensity at the upper mass. This indicates an important conclusion that, by using the known isotopic abundances, the instrument response function can be determined over broad mass ranges without knowledge of the molar concentration of the calibrating elements or estimations of their degree of ionisation as these are constants for isotopes of the same element.

However, correcting the instrumental response over a wide range of mass requires not only that pairs of masses are unbiased with respect to each of other, but also that all masses are unbiased with respect to the first mass of the range measured. To achieve this requires establishing the relationship between $I_N{}^T$ (the count rate at mass (N) required to give the correct theoretical isotope ratio) and $I_i{}^A$ using only the measured mass biases $B_{(i+1),i}$ which for best accuracy should be determined over unit mass increments ($\Delta m = 1$). Thus as an example the sequential mass biases $B_{2,1}$ and $B_{3,2}$ are:

$$B_{2,1} = \frac{\frac{I_2^A}{I_1^A} - \frac{I_2^T}{I_1^T}}{\frac{I_2^T}{I_1^T}} \qquad 4$$

and

$$B_{3,2} = \frac{\frac{I_3^A}{I_2^A} - \frac{I_3^T}{I_2^T}}{\frac{I_3^T}{I_2^T}} \qquad 5$$

Combining equation (4) and (5) yield:

$$B_{3,2} = \frac{\frac{I_3^A}{I_2^A} - \frac{I_3^T(1+B_{2,1})}{I_2^A}}{\frac{I_3^T(1+B_{2,1})}{I_2^A}} \quad 6$$

Or

$$B_{3,2} = \frac{I_3^A - I_3^T(1+B_{2,1})}{I_3^T(1+B_{2,1})} \quad 7$$

and rearranging yields:

$$I_3^T = \frac{I_3^A}{(1+B_{2,1})(1+B_{3,2})} \quad 8$$

This can be generalised to correct over the mass range from i to $i + N$:

$$I_{i+N}^T = \frac{I_{i+N}^A}{(1+B_{(i+1),i})(1+B_{i+2,(i+1)})\ldots.(1+B_{(i+N),(i+N-1)})} \quad 9$$

Or

$$I_{i+N}^T = \frac{I_{i+N}^A}{\prod_{j=1}^{j=N}(1+B_{(i+j),(i+j-1)})} \quad 10$$

Equation (10) was applied to the raw data for multielement standard solutions and biological reference materials and the results were used as the data file for the MI programme. The output (the predicted or the mass bias corrected data) counts for each component of interest were used in the same as for the raw data. The same strategy for inferring the species contributing to the observed mass spectrum was employed (See 2.4.4.). The menu files used with mass bias corrected data for standard solutions and biological samples contain the species that have been mentioned in Table 2.4.

The evidence (Table 2.3) and spectral fit (Figures 2.5A-D) for the mass bias corrected data for 100ppb standard solution and biological samples were improved compared with those obtained with raw data (Figures 2.3A-D).

Table 2.6A. The calibration functions for mass bias corrected data.

Element	Intercept (a)	Slope (b)	R^2
V	667	4350	0.9998
Cr	3516	4532	0.9999
Mn	191	5297	1
Fe	136954	5026	0.9995
Co	-381	4316	0.9999
Ni	357	3385	1
Cu	127	2905	0.9999
Zn	1595	1402	0.9991
As	-7	449	1
Se	55	400	0.9999
Rb	4232	6314	0.9988
Sr	2384	6991	0.9995

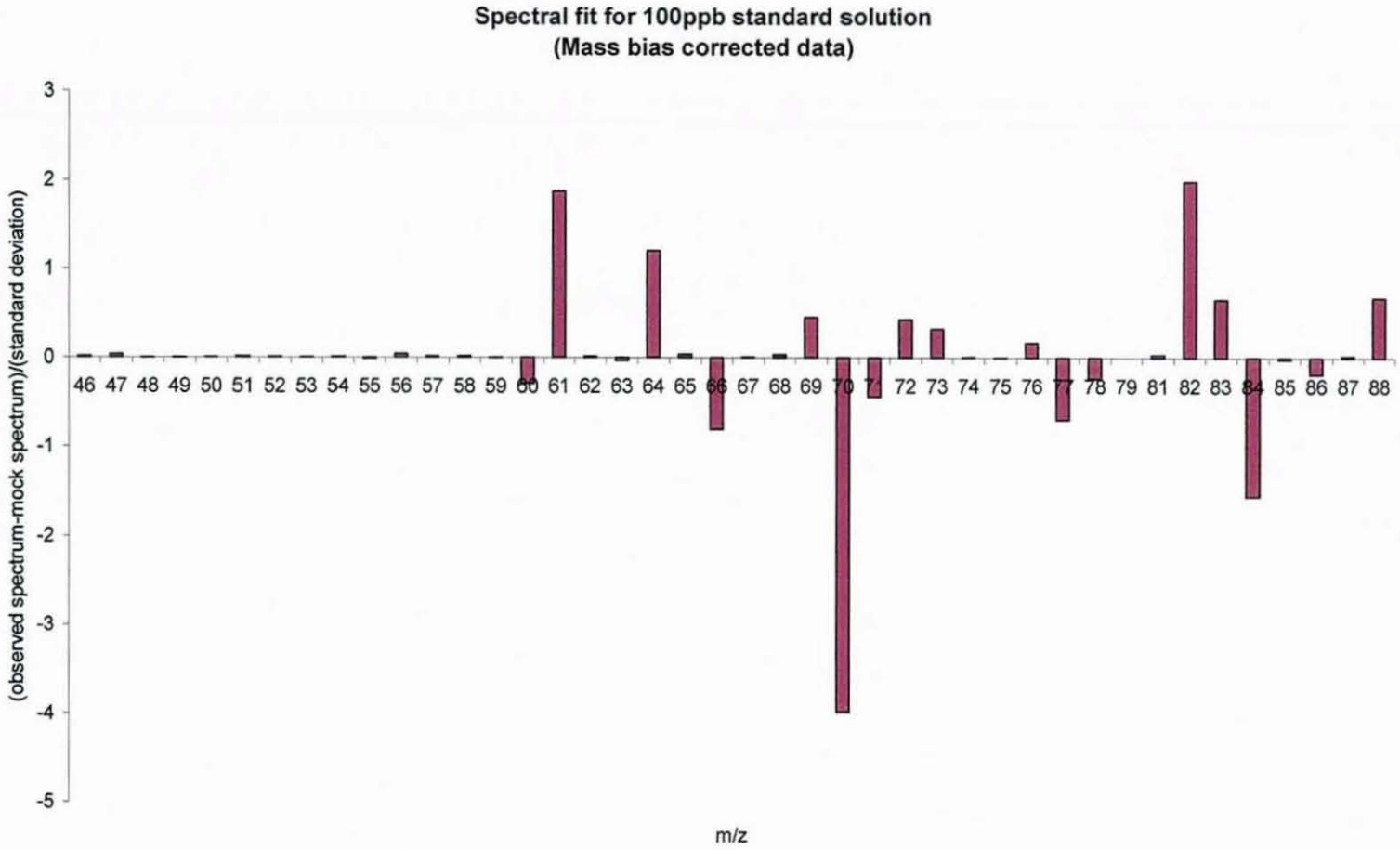

Figure 2.5A. Spectral fit for mass bias data for 100ppb standard solution derives from species menu (See Table 2.4).

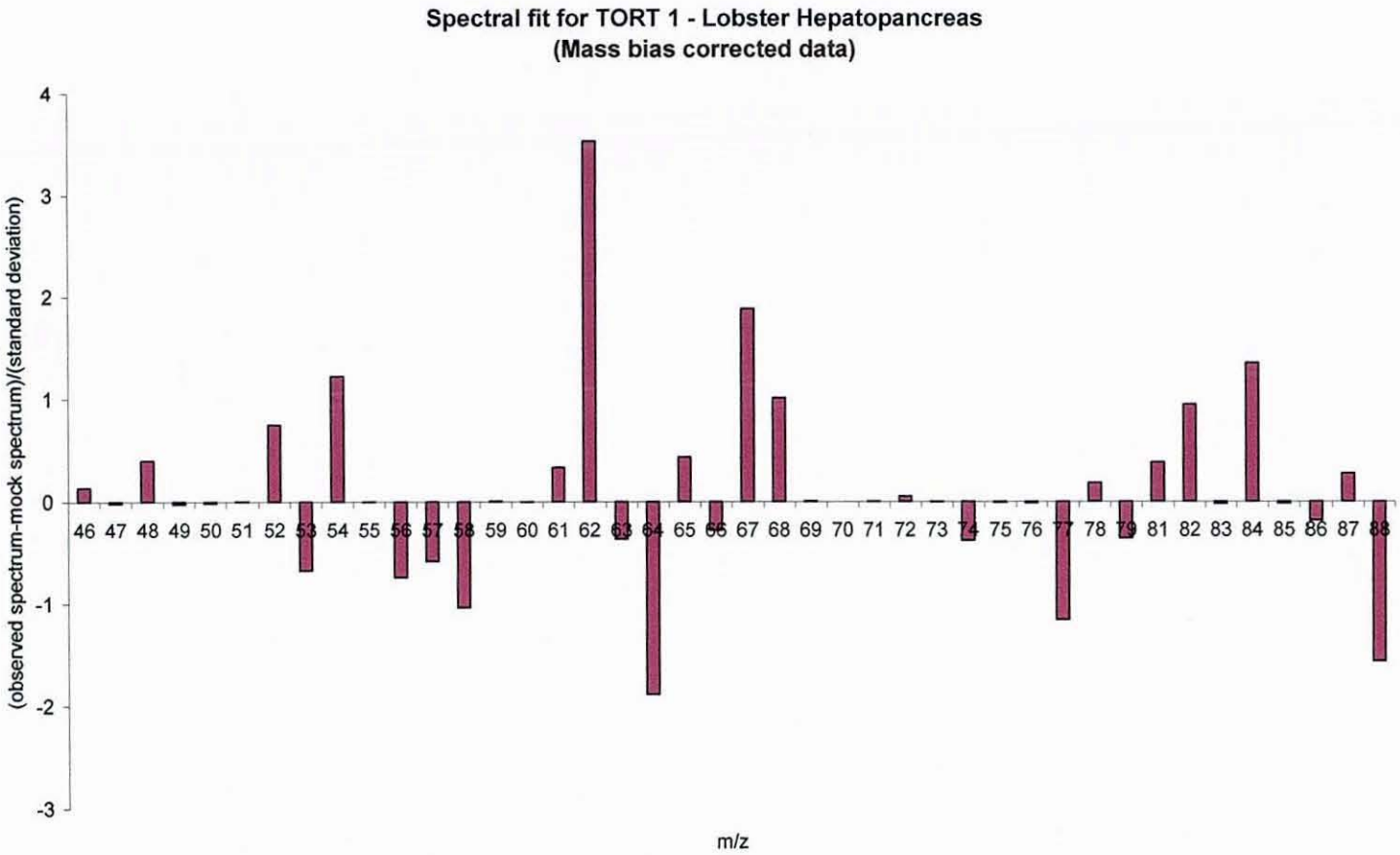

Figure 2.5B. Spectral fit for mass bias data for TORT 1 - Lobster Hepatopancreas Marine derives from species menu (See Table 2.4).

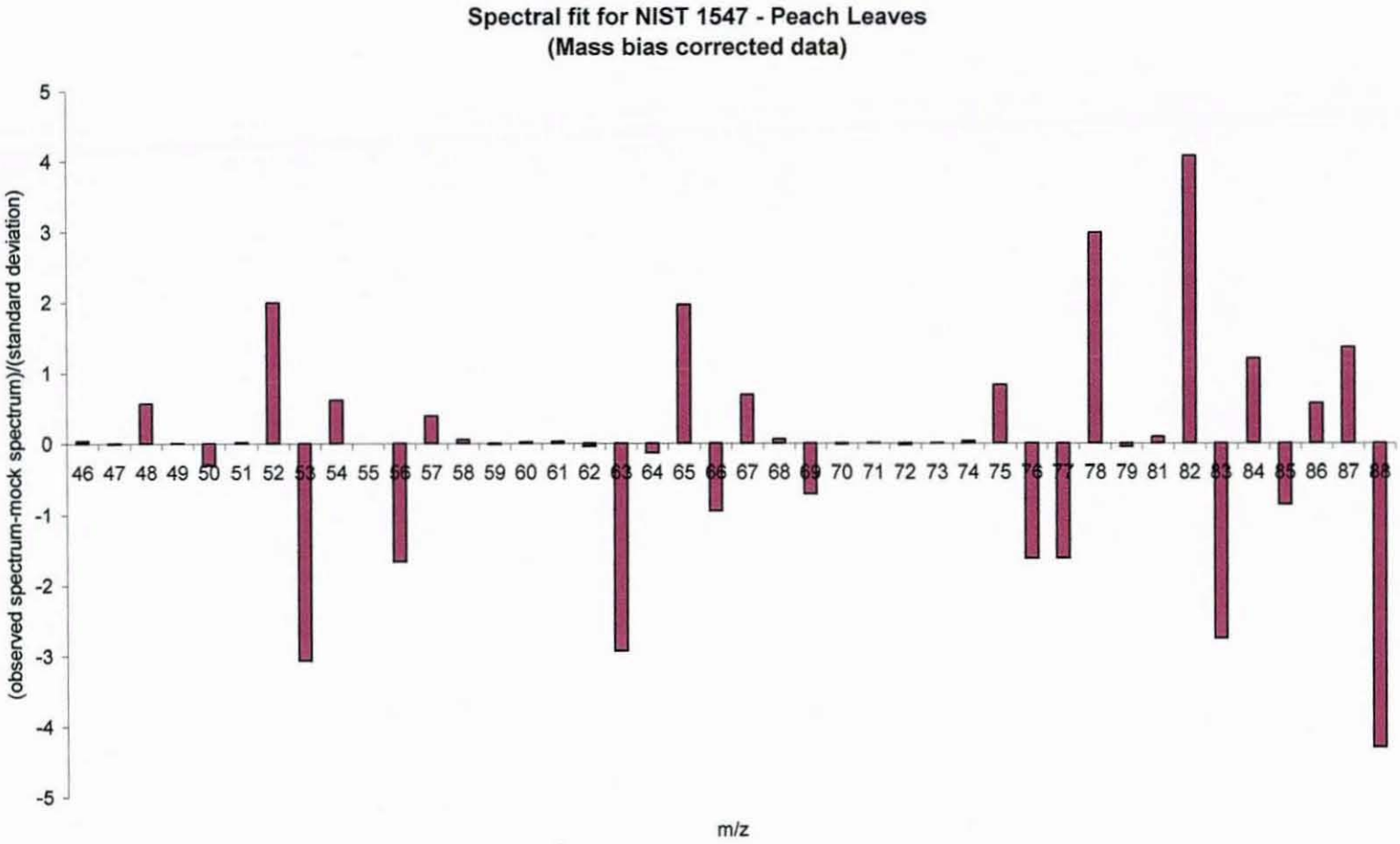

Figure 2.5C. Spectral fit for mass bias data for NIST 1547 - Peach Leaves derives from species menu (See Table 2.4).

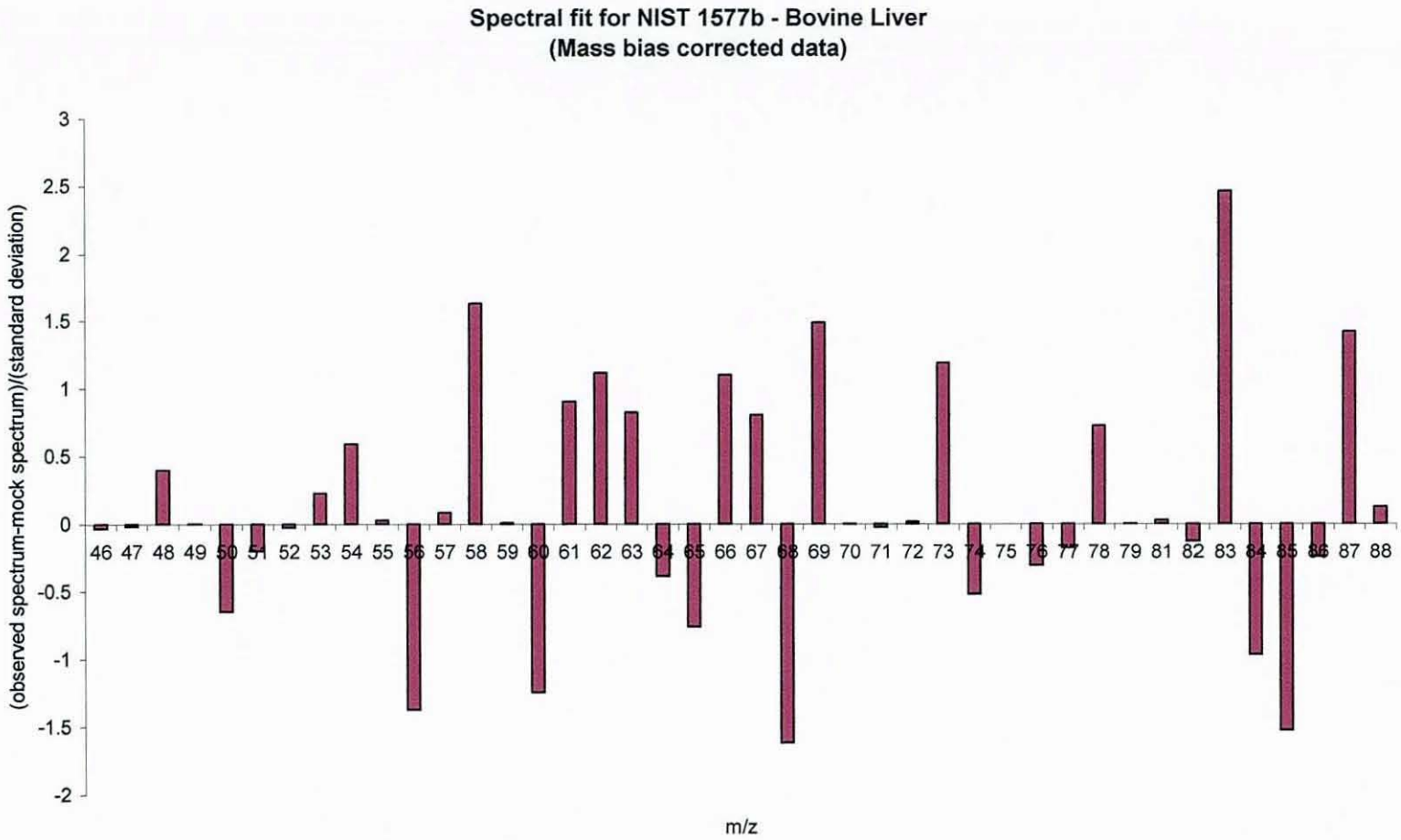

Figure 2.5D. Spectral fit for mass bias data for NIST 1577b - Bovine Liver derives from species menu (See Table 2.4).

2.7. Results and discussion for mass bias corrected data

Tables 2.6A and 2.6B show the calibration functions and the analytical data using mass bias corrected data. It can be seen that improvements in the determinations of many elements (Cr, Fe, Co, Cu, Zn and Sr) are observed compared with using raw data. As and Se in all samples and Sr in NIST1577b still give poor results. These data might be improved if isotopic ratio calculations are taken into account (See Chapter 3).

2.8. Conclusion

The aim of this work was an evaluation of the Bayesian approach to spectral deconvolution and in particular the Massive Inference algorithm. This programme offers fast searching time, flexibility in changing the component menu, consistent results especially for calibration data and good estimation for most of the tested elements. The Massive Inference algorithm is dependent upon correct selection of the component menu. The presence of the mass bias effect is deleterious, however, with proper correction, the results can be improved.

The results for some analytes were shown to be in good agreement with the documented data whereas elements such as As and Se have a large deviation from their real concentrations. Further work was necessary in order to provide a more robust procedure. The determinations reported here were carried out using the total predicted counts for each element. This sometimes causes additional noise as different interferences interfere with different isotopes of the same analyte. This suggests the use of isotope ratio calculations as a further test for the quality of prediction.

Table 2.6B. Analytical results for mass bias corrected data for biological samples¶.

Element	TORT 1 - Lobster Hepatopancreas Marine			NIST 1547 - Peach Leaves			NIST 1577b - Bovine Liver		
	Certified Value $\mu g\ g^{-1}$	Found Value $\mu g\ g^{-1}$	% of Error	Certified Value $\mu g\ g^{-1}$	Found Value $\mu g\ g^{-1}$	% of Error	Certified Value $\mu g\ g^{-1}$	Found Value $\mu g\ g^{-1}$	% of Error
V	1 4 ± 0 3	1 22 ± 0 11	-13	0.37 ± 0 03	0.27 ± 0.10	-27	0.123#	0 10 ± 0.11	-19
Cr	2.4 ± 0 6	2.93 ± 0.07	22	1#	1 22 ± 0 06	22			
Mn	23.4 ± 1.0	20 6 ± 0.19	-12	98 ± 3	73 9 ± 0 73	-25	10 5 ± 1.7	11.7 ± 0.11	11
Fe	186 ± 11	178 ± 6	-4.3	218 ± 14	170 ± 5 9	-22	184 ± 15	210 ± 7 3	14
Co	0.42 ± 0 05	0 46 ± 0 08	9 5	0 07#	0 08 ± 0 07	14	0 25#	0 29 ± 0.08	16
Ni	2.3 ± 0 3	2 60 ± 0 05	13	0 69 ± 0 09	0.40 ± 0.04	-42			
Cu	439 ± 22	329 ± 3.9	-25	3.7 ± 0.4	3 33 ± 0 07	-10	160 ± 8	150 ± 1.9	-6.3
Zn	177 ± 10	156 ± 6.5	-12	17.9 ± 0 4	16 7 ± 0 66	-6 7	127 ± 16	143 ± 5 9	13
As	24 6 ± 2.2	33.4 ± 0.30	36	0 06 ± 0 018	0 13 ± 0 06	117	0 05#	0 12 ± 0 06	140
Se	6 88 ± 0.47	9.88 ± 0 12	44	0.12 ± 0 009	0 26 ± 0 07	117	0.73 ± 0 06	1 51 ± 0 08	107
Rb				19.7 ± 1.2	16.7 ± 0.74	-15	13.7 ± 1.1	15 4 ± 0 69	12
Sr	113 ± 5	102 ± 3.1	-9 7	53 ± 4	49.1 ± 1.47	-7.4	0.136 ± 0.001	0 21 ± 0.12	54

¶ *The Found values and the percent of error were estimated to three and two significant figures respectively in most cases.*

 # Value not certified.

References

1. K. E. Jarvis, A. L. Gray and R. S. Houk, *Handbook of Inductively Coupled Plasma Mass Spectrometry*, Blackie Academic & Professional, Glasgow, 1992.
2. *Inductively Coupled Plasma Mass Spectrometry*, eds. A. Montaser, Wiley-VCH, 1998.
3. *Inductively Coupled Plasma Mass Spectrometry and its Applications*, eds. S. J. Hill, Sheffield Academic Press, 1999.
4. M. A. Vaughan and G. Horlick, *Appl. Spectrosc.*, 1986, **40**, 434.
5. S. H. Tan and G. Horlick, *Appl. Spectrosc.*, 1986, **40**, 445.
6. N. M. Reed, R. O. Cairns and R. C. Hutton, *J. Anal. At. Spectrom.*, 1994, **9**, 881.
7. J. L. M. de Boer, *Spectrochim. Acta, Part B*, 1997, **52**, 389.
8. T. W. May and R. H. Wiedmeyer, *At. Spectrosc.*, 1998, 19, 150.
9. T. Townsend, *J. Anal. At. Spectrom.*, 2000, **15**, 307.
10. The Element ICP-MS, http://www.finnigan.de/products/downld/, September 2002.
11. E. H. Evans and J. J. Giglio, *J. Anal. At. Spectrom.*, 1993, **8**, 1.
12. M. A. Vaughan and G. Horlick, *Appl. Spectrosc.*, 1990, **44**, 587.
13. M. Vaughan and D. M. Templeton, *Appl. Spectrosc.*, 1990, **44**, 1685.
14. S. X. Xu, L. Stuhne-Sekalec and D. M. Templeton, *J. Anal. At. Spectrom.*, 1993, **8**, 445.
15. E. H. Van, S. Bosch and M. T. C. De Loos-Vollebregt, *Spectrochim. Acta, Part B*, 1994, **49**, 1347.
16. E. H. Van, S. Bosch and M. T. C. De Loos-Vollebregt, *Spectrochim. Acta, Part B*, 1996, **51**, 591.
17. M. Grotti, C. Gnecco and F. Bonfiglioli, *J. Anal. At. Spectrom.*, 1999, **14**, 1171.
18. M. A. Vaughan and G. Horlick, *Appl. Spectrosc.*, 1987, **41**, 523.
19. L. L. Burton and G. Horlick, *Spectrochim. Acta, Part B*, 1992, **47**, E1621.

20. L. L. Burton and G. Horlick, *Spectrochim. Acta, Part B*, 1993, **48**, E1063.

21. B. L. Sharp, J. Batey, I. S. Begley, D. Gregson, J. Skilling, A. B. Sulaiman and G. Verbogt, *J. Anal. At. Spectrom.*, 1999, **14**, 99.

22. S. Sibisi, and J. Skilling, *J. R. Statist. Soc. B*, 1997, **59**, 217.

23. G.J. Daniell, in *Maximum Entropy in Action*, eds. B. Buck, and V.A. Macaulay, Clarendon Press, Oxford, 1991.

24. K. J. R. Rosman and P. D. P. Taylor, *J. Anal. At. Spectrom.*, 1999, **14**, 5N.

25. J. N. Miller and J. C. Miller, *Statistics and Chemometrics for Analytical Chemistry*, 4th edn., Pearson Education Limited, England, 2000, ch. 5, pp.107.

26. H. P. Longerich, B. J. Fryer and D. F. Strong, *Spectrochim. Acta, Part B*, 1987, **42**, 39.

27. P. D. P. Taylor, P. De Bievre, A. J. Walder and A. Entwistle, *J. Anal. At. Spectrom.*, 1995, **10**, 395.

28. S. Begley and B. L. Sharp, *J. Anal. At. Spectrom.*, 1997, **12**, 395.

29. C. J. Park, K. H. Cho, J. K. Suh and M. S. Han, *J. Anal. At. Spectrom.*, 2000, **15**, 567.

30. J. L. M. de Boer, P. de Joode and R. Ritsman, *J. Anal. At. Spectrom.*, 1998, **13**, 971.

Chapter 3:

Further Development of Bayesian Deconvolution of ICP-MS

3.1. Introduction

The analytical data for the biological reference materials presented in Chapter 2 shows that there are some deviations from the documented values. It was thought that, employing the known isotopic ratios as an additional test of the quality of prediction could improve the results obtained. Deviations from natural abundance values are an indication of spectral interference problems. If the component menu contains all the species that have a significant contribution to the spectrum, the isotopic ratios should be close to the natural abundance values. The predicted counts for each analyte or isotope can then be used to determine their concentrations.

As mentioned earlier, the selection of the potential components in the analysis menu is vitally important and affects the outcome of the final results. MI uses the component menu, but can also be used to search for the composition of the components. The menu file is just like a key to a door, when this key cannot open the door, just change to another one. Knowledge of the sample matrix is helpful in establishing a good component menu for the samples.

It can be seen that different component menus give different estimations (mock or predicted counts) for the elemental components and therefore the results in Chapter 2 obtained for the biological reference materials show deviations for some analytes from the documented values. These results indicate that the menus were not fully optimised.

3.2. Aims and objectives

This chapter continues to describe the analysis of mass spectra over the range 46 - 88 amu using the Massive Inference (MI^{TM}) algorithm. Two sets of data were investigated (raw data and mass bias corrected data derived from the method employed to correct the instrument response function from knowledge of the mass bias as in Chapter 2). The evidence, spectral

fit values and the deviations of the isotopic ratios from the natural abundance values for each component were used to guide the search. The found concentration of each analyte in the samples was compared with the documented value.

3.3. Experimental

All the experimental details (standard solutions and reference materials, sample preparation, instrumentation and the *Massive Inference (MI^{TM})* programme) were described in Chapter 2 (See 2.4.).

3.3.1. Strategy for inferring the species contributing to the observed mass spectrum

The strategy described in Chapter 2 (See 2.4.4.) was further developed. There are various strategies that might be applied to deriving the species menu, but here the incremental approach was chosen as it provided a clearer picture of the individual species contributions. Isotopic abundances provide information on the relative contributions of given species at different masses and are key factors in the synthesis of possible spectra (the predictive[1]). However, they are not particularly helpful in ranking the relative importance of various species at particular masses because this depends directly on the concentrations of the components present in a particular sample.

The following steps were followed:

1. Take the lowest mass point in the spectrum (e.g. mass 46), select the element with the highest abundance isotope at this mass (Ti), add this element to the blank menu, run the MI algorithm and observe the spectral fit and E value achieved. Note the magnitude of the remaining residual and its percentage reduction.
2. Repeat step 1 at the same mass for each possible element and molecular ion and then for other masses throughout the selected range. Molecular ions can be selected on the basis of published

information[2-8] and knowledge of the sample (note, it is unlikely that all the species will be known).

3. Run MI with a composite menu of species selected from Step 2. The deviation of the mock data from the real spectrum should, for a good fit, be less than two standard deviations at each mass.
4. To verify that the process of selecting the species menu has been successful the procedure can be reversed. Thus carry out further runs of MI, this time removing one species at a time from the composite menu. It will often be observed that a species will improve the fit at masses at which it has no direct spectral contribution. This is an entirely predictable outcome of multi-variant spectral analysis. Where two species share any common portion of the spectrum and have fixed abundances, the counts allocated to one will affect the other across its isotopic range.

Steps 1 - 4 obviously involve a considerable effort in data processing, but it only has to be done once for a given sample type and is entirely within the spirit of Bayesian analysis, i.e. modification of conclusions based on previous findings. Further, it provides a degree of confidence that the menu is the minimum that can account for the observed spectrum.

Table 3.1 summarises the species contributing to the "mock" spectrum at each mass for the standard and sample solutions for both raw data and mass bias corrected data in the mass range studied. All the elemental species in the standards and those found in the samples are certified in the reference materials with the exception of Ti and Rb in TORT 1, Ge in NIST 1547, Cr and Ni in NIST 1577b. Moreover, it can be seen that most of the polyatomic interferences are, not surprisingly, derived from Ar or N (HNO_3).

Two menus were derived for the standards and for each sample type, one based on the raw data and the other on the mass bias corrected data. These menus were for the most part similar varying by 2 or 3 species in each case.

Table 3.1. Species contributing to the "mock" spectrum for standard solutions and biological samples

Species	Standard Solutions		TORT 1 - Lobster Hepatopancreas Marine		NIST 1547 - Peach Leaves		NIST 1577b - Bovine Liver	
	RD menu	MB menu	RD menu	MB menu	RD menu	MB menu	RD menu	MB menu
Ti	•	•	•	•				
V	•	•	•	•	•	•	•	•
Cr	•	•	•	•	•	•	•	•
Mn	•	•	•	•	•	•	•	•
Fe	•	•	•	•	•	•	•	•
Co	•	•	•	•	•	•	•	•
Ni	•	•	•	•	•	•	•	•
Cu	•	•	•	•	•	•	•	•
Zn	•	•	•	•	•	•	•	•
Ga	•	•	•	•				
Ge	•	•			•	•		
As	•	•	•	•	•	•	•	•
Se	•	•	•	•	•	•	•	•
Rb	•	•	•	•	•	•	•	•
Sr	•	•	•	•	•	•	•	•
Ar_2	•	•	•	•	•	•	•	•
Ar_2H	•	•	•	•	•	•	•	•
ArAl	•	•						
ArBe						•	•	•
ArC			•	•	•	•	•	•
ArCa	•	•						
ArCH	•	•						

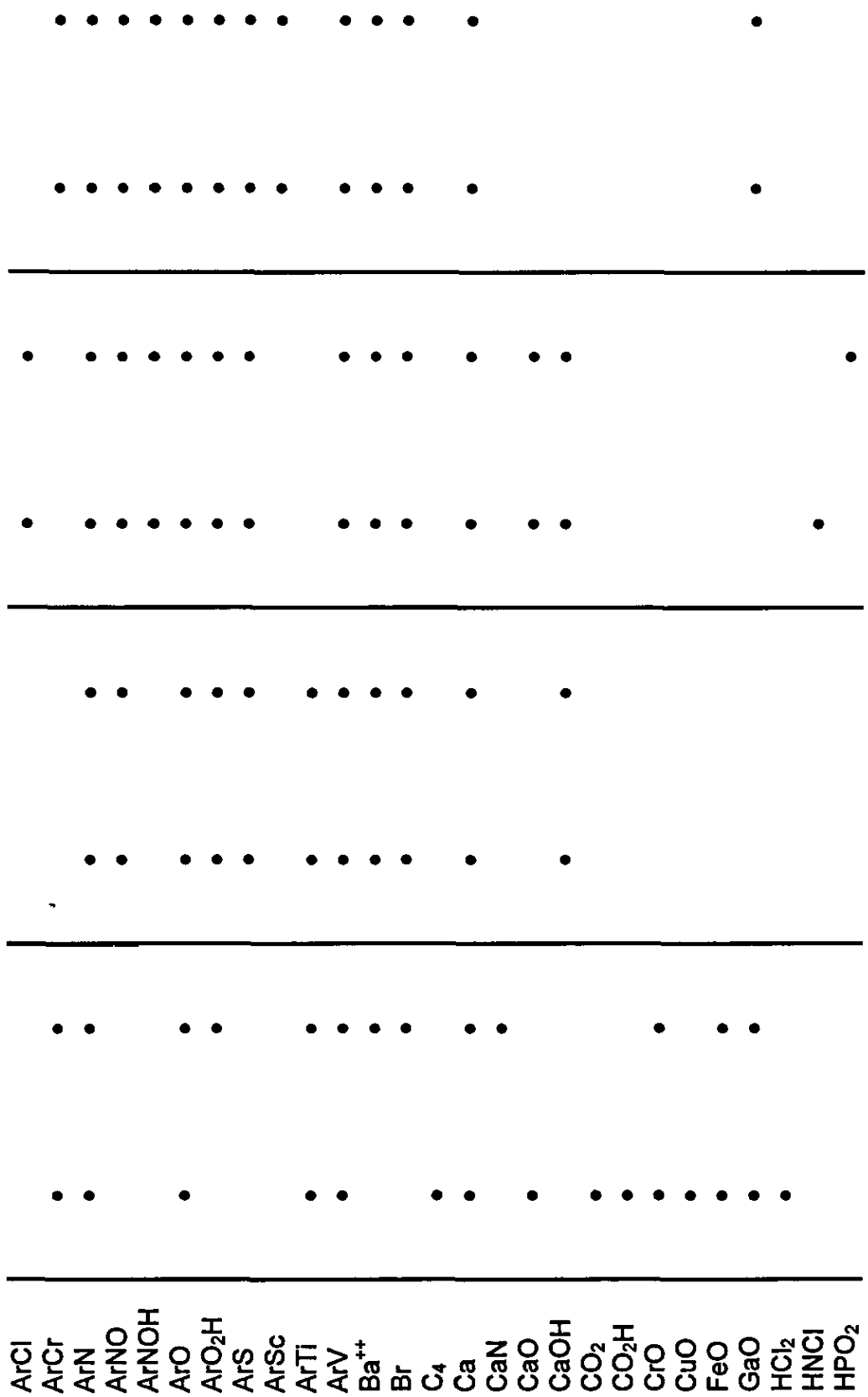
ArCl
ArCr
ArN
ArNO
ArNOH
ArO
ArO2H
ArS
ArSc
ArTi
ArV
Ba++
Br
C4
Ca
CaN
CaO
CaOH
CO2
CO2H
CrO
CuO
FeO
GaO
HCl2
HNCl
HPO2

KCl	•	•	•	•				
Kr					•	•	•	•
Mg_2	•							
N_2O	•	•	•	•	•	•	•	•
Na_2	•	•						
Na_2O	•							
NaCl		•						
NCCl	•							
NO_2	•							
NO_2H		•	•	•	•	•	•	•
POH		•	•	•	•	•	•	•
SiO	•	•	•	•				
SN	•				•			
SO		•		•		•	•	•
SO_2H	•		•		•			
SO_3			•	•				
SOH					•			
TiO		•	•	•				
TiOH				•				

RD menu = Raw data menu is the list of species that MI infers from the raw data.

MB menu = Mass bias corrected data menu is the list of species that MI infers from the mass bias corrected data.

Progress through Steps 1 - 4 is guided by the simple expedients of looking at the E value and spectral fit at each mass in turn (See Table 3.2 and Figures 3.1A-D), however, other parameters also have to be considered and may force reconsideration of earlier conclusions. Firstly, calibration data in terms of linearity and error and the derived analytical data from reference materials must be considered. Secondly, a fully modelled spectrum should closely reflect the known isotopic abundances of the contributing species (not least because these are used in the predictive process), however, as will be shown these are particularly difficult to rationalise for all elements in the data set. If these criteria are not met then the species menu is re-examined to find the source of the problem.

Table 3.2. Evidence values for 100ppb standard solution and biological samples.

	Evidence derive from	
	Raw data	**Mass bias data**
100 ppb	-685	-594
TORT 1	-753	-574
NIST 1547	-788	-697
NIST 1577b	-830	-550

It can be seen from Table 3.2 that the E values derived from the mass bias corrected data for the 100ppb standard solution and biological samples are lower than those values obtained from the raw data (E value represents the goodness of fit for the spectrum as a whole with more positive values close to zero indicating improved prediction). The spectral fit at each mass in the region studied is given in Figures 3.1A-D which show that these fits for the mass bias corrected data are superior to the fits obtained from the raw data (the spectral fits at each mass should be reduced towards zero in the ideal world and this indicates that the data are fully optimised).

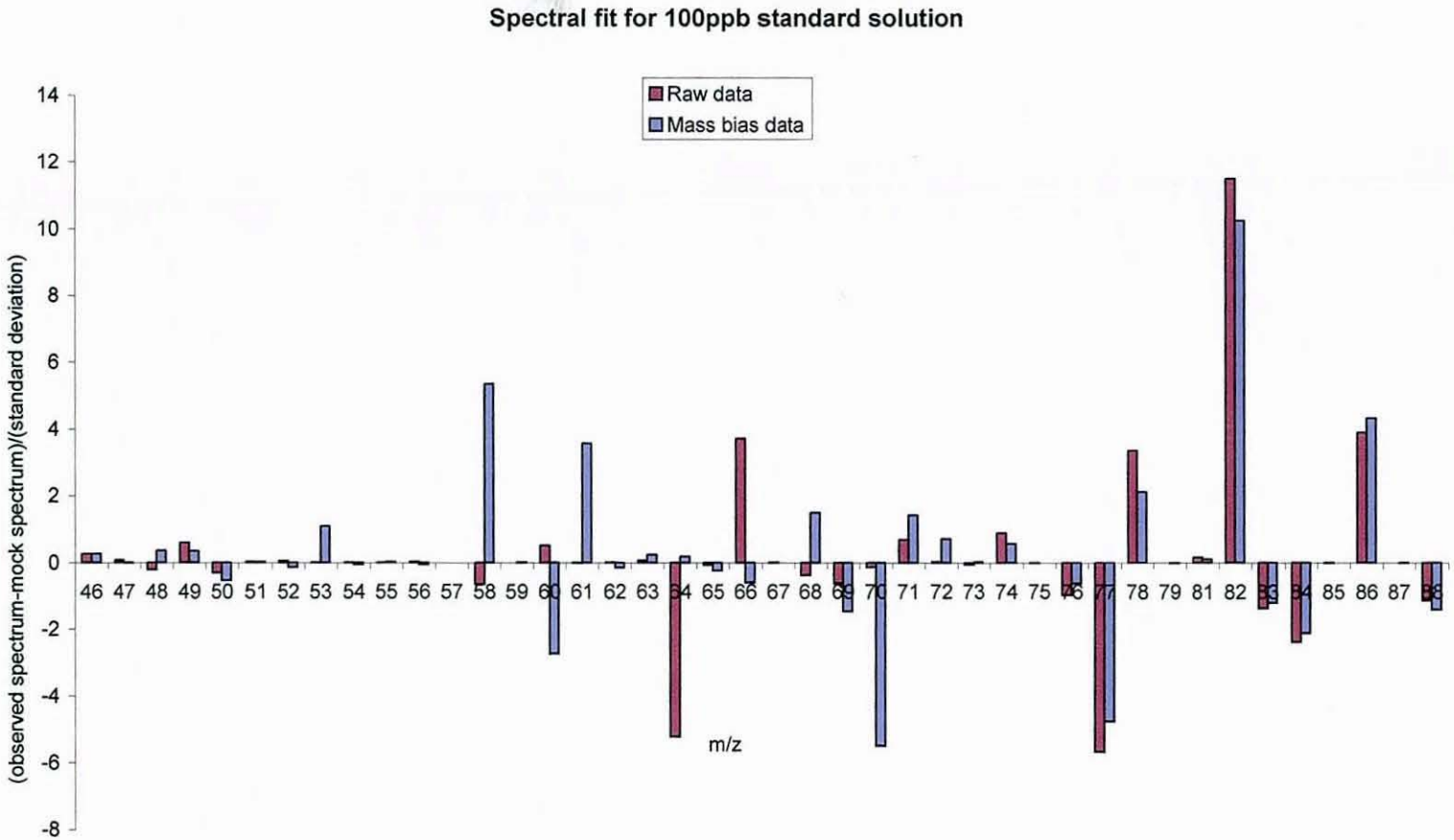

Figure 3.1A. Spectral fit for 100ppb standard solution for raw data and mass bias corrected data.

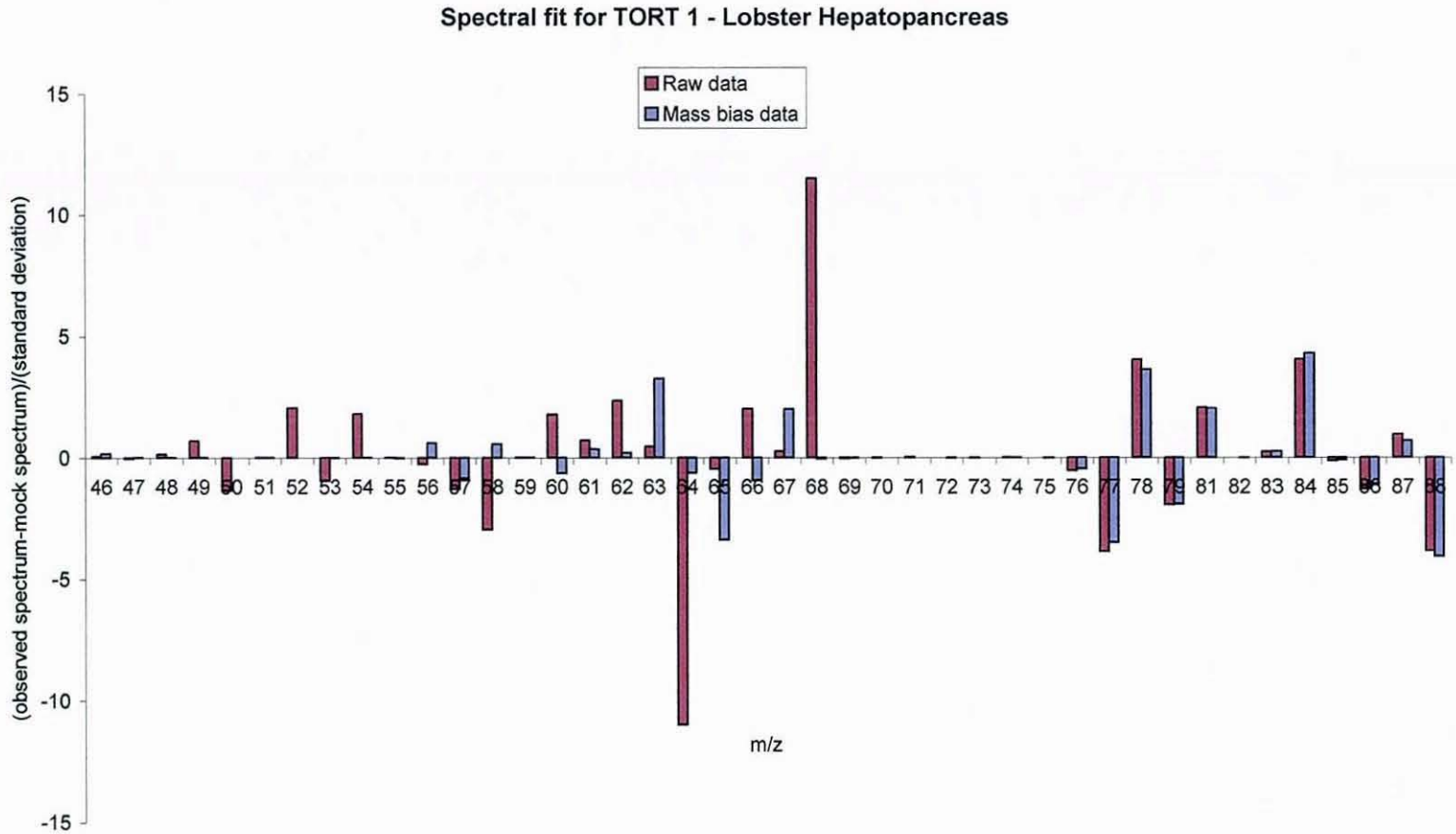

Figure 3.1B. Spectral fit for TORT 1 - Lobster Hepatopancreas Marine for raw data and mass bias corrected data.

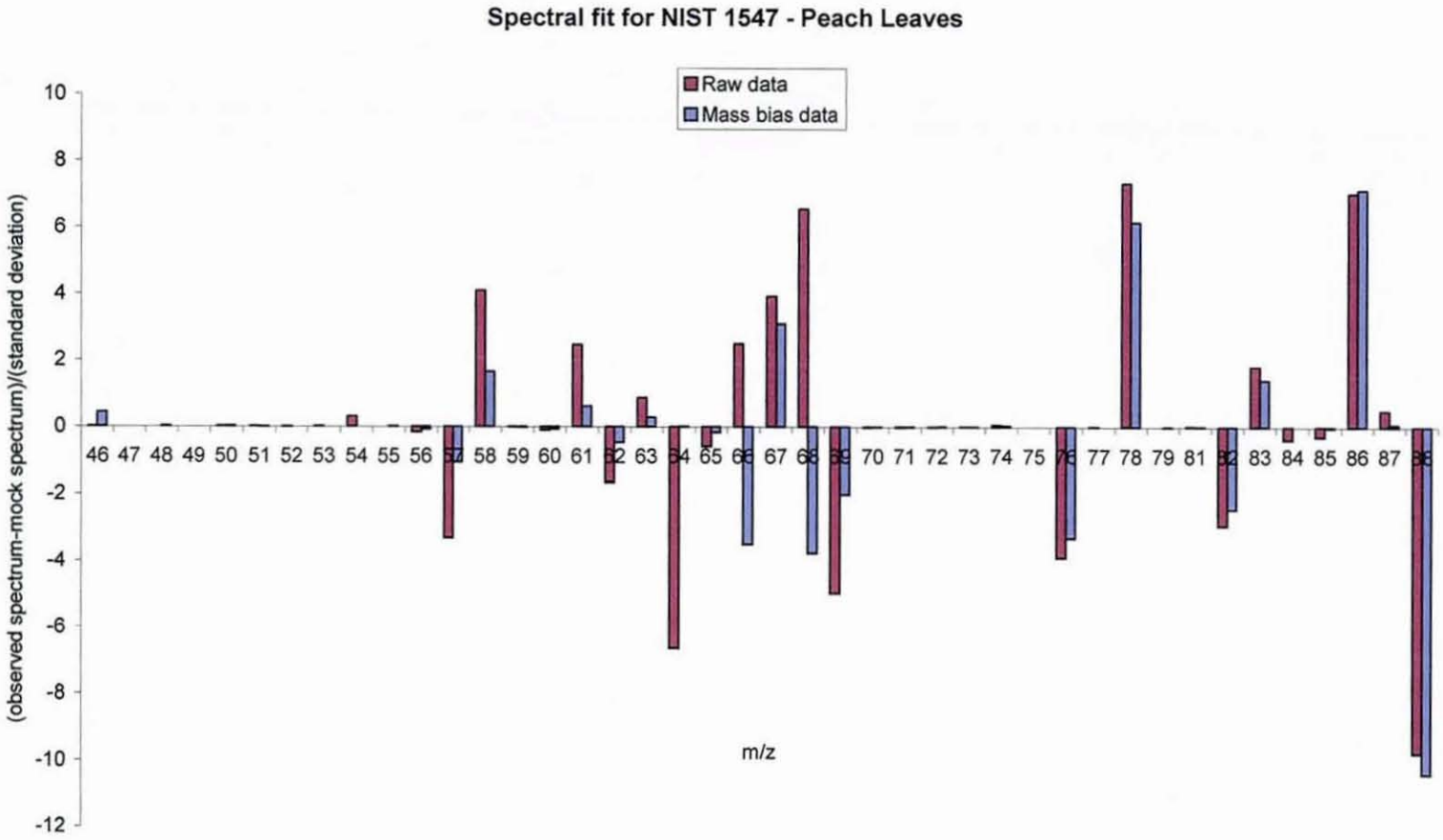

Figure 3.1C. Spectral fit for NIST 1547 - Peach Leaves for raw data and mass bias corrected data.

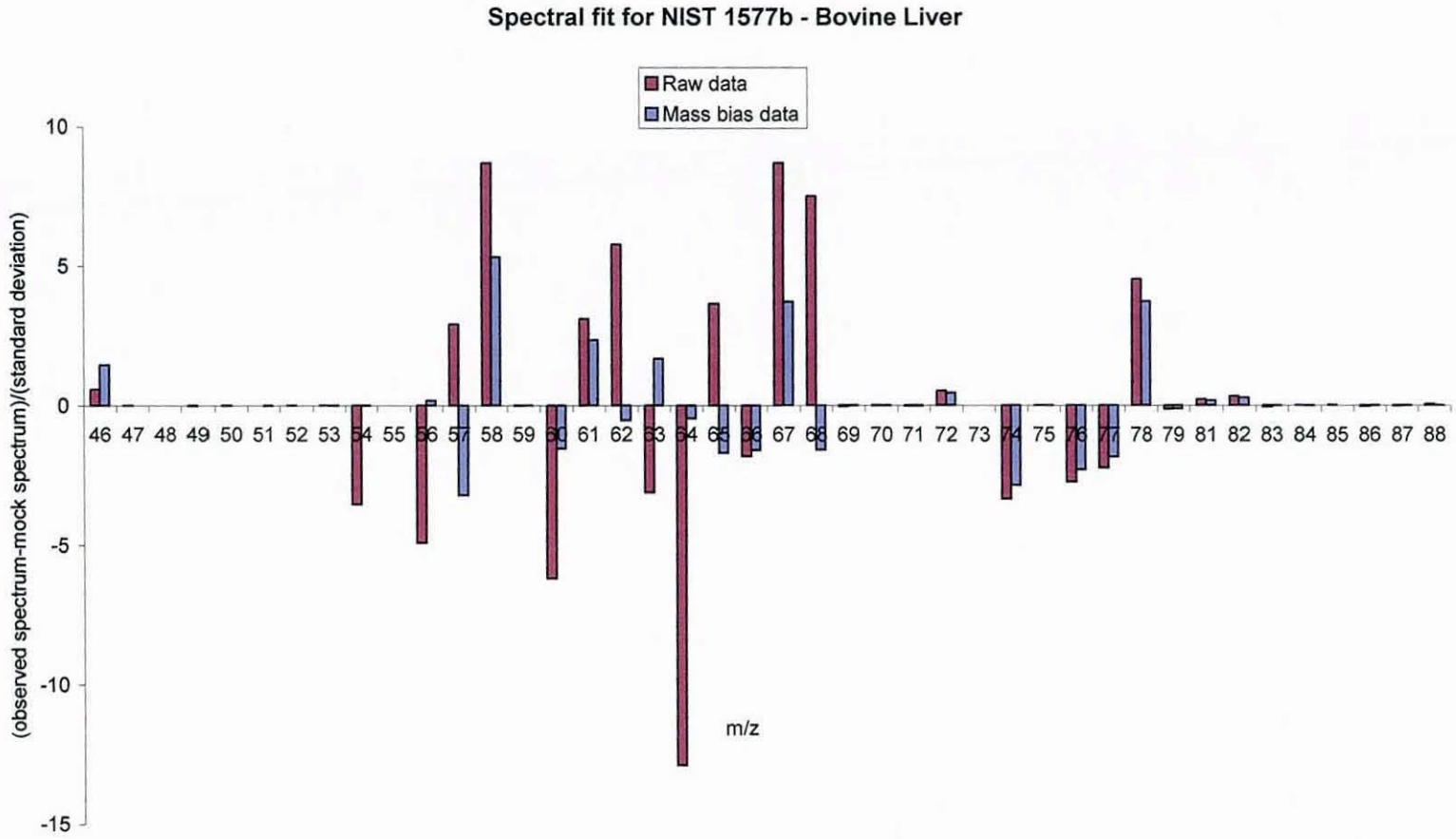

Figure 3.1D. Spectral fit for NIST 1577b - Bovine Liver for raw data and mass bias corrected data.

3.4. Results and discussion

3.4.1. Spectral interferences

Tables 3.3A-H show the possible interferences for the 100ppb standard solution, TORT 1, NIST 1547 and NIST 1577b for both raw and mass bias corrected data. To calculate the percentage of the contribution of each species at each mass, the computed total count for a species was multiplied by its natural isotopic abundance and this number divided by the instrumental count for that mass (species contributing less than 0.01% are omitted). The final column of the table provides the summation of these percentages and generally a sum close to 100% was indicative of achieving good analytical and isotopic data. This leads to one of the most significant advantages of this approach to spectral analysis, namely, that a fully synthesised spectrum requires no blank subtraction. This is so because the non-specific background continuum from the instrument is very low (≤ 1 cps) and so all the observed counts are attributed to molecular ions. However, where the procedural blank indicates significant levels of contamination (i.e. correctly synthesised isotope ratios can be derived from this blank) then it should be subtracted in the normal manner.

The species yielding a contribution of ≥ 25 % of the total count are highlighted in Tables 3.3A-H. For the standard solutions (Table 3.3A) these include the well-known interferences from ^{54}ArN, ^{56}CaO, $^{76}Ar_2$, $^{78}Ar_2$, ^{79}CuO, $^{81}Ar_2H$, ^{83}ArTi and ^{83}ArCa. NIST 1577b (Table 3.3G) is a relatively "clean" sample, but new interferences are introduced by the sample matrix and the relative importance of others changes because of the different elemental composition compared with the standard. Thus $^{46}N_2O$, $^{47}NO_2H$, ^{48}SO, ^{48}POH, ^{49}ArBe (this species is strongly indicated by the algorithm, probability of detection 100%, but for obvious reasons its actual existence must be doubted, it is probably a surrogate for an unknown species), ^{49}SO, ^{50}SO, ^{52}ArC, $^{138}Ba^{++}$, ^{71}ArNOH, ^{72}ArS, $^{73}ArO_2H$, $^{76}Ar_2$, $^{78}Ar_2$, ^{79}Br, ^{81}Br, $^{81}Ar_2H$, ^{83}Kr, ^{83}ArSc (see comment above for ^{49}ArBe), ^{84}Kr and ^{87}GaO are the major contributions. NIST 1547 (Table 3.3E) is rather

similar to NIST 1577b, but chloride species make an appearance and the major contributions are: ^{46}SN, $^{47}NO_2H$, ^{48}POH, ^{49}SOH, $^{50}ClNH$, $^{57}CaOH$, $^{61}CaOH$, $^{134}Ba^{++}$, $^{136}Ba^{++}$, $^{138}Ba^{++}$, $^{70}ArNO$, $^{71}ArNOH$, ^{72}ArS, $^{73}ArO_2H$, $^{75}ArCl$, $^{76}Ar_2$, $^{77}ArCl$, $^{78}Ar_2$, ^{79}Br, ^{81}Br, $^{81}Ar_2H$, ^{82}Kr and ^{83}Kr. Interestingly the presence of ClO^+ could not be confirmed, but these are not chloride matrices and the V was present at ng ml^{-1} levels in the final solution and so dominated the observed signal. It has to be recognised that, ions that might be quite prominent in the blank spectrum can be swamped by the elemental signal (and its attendant noise) in the sample spectrum. TORT 1 (Table 3.5C) is the most complex of the sample matrixes and has the highest elemental concentrations with Si, Ca and Ti contributing as their oxides. The list of principal interferences includes ^{46}SiO, $^{47}NO_2H$, ^{48}POH, $^{61}CaOH$, ^{62}TiO, $^{138}Ba^{++}$, $^{70}ArNO$, ^{72}ArS, $^{73}ArO_2H$, $^{76}Ar_2$, $^{78}Ar_2$, ^{79}Br, ^{81}Br and $^{83}ArTi$.

Correcting the data for the effect of mass bias does not change the menus of species significantly. The changes are for the standards: add ^{54}CaN, ^{56}ArO, ^{79}Br, remove ^{54}ArN, ^{56}CaO, ^{79}CuO; NIST 1577b: add $^{49}NO_2H$; NIST 1547: add $^{46}N_2O$, $^{49}ArBe$, ^{50}SO, ^{60}CaO, remove ^{46}SN, ^{49}SOH, $^{50}ClNH$, and for TORT 1: add ^{50}POH.

Some species inferred by the algorithm are unexpected, their actual presence could be confirmed by using a high resolution instrument, but it seems likely that there are, as yet unknown species contributing to the spectrum.

Table 3.3A. Possible interference's for raw data of the 100ppb standard solution

M/Z	Contributing Species	Σ of %
46	^{46}**Ti$_{8.253}$(70.79)**, ^{46}Ca$_{0.004}$(0.01), $^{\#}$SiO(16.48), $^{\#}$COOH(5.27), ^{12}C^{16}O^{18}O$_{0.395}$(1.83), ^{32}S^{14}N$_{94.668}$(1.29), ^{14}N^{16}O^{16}O$_{99.152}$(1.27), ^{23}Na^{23}Na$_{100}$(1.17), $^{\#}$NNO(0.58)	98.69
47	^{47}**Ti$_{7.442}$(97.17)**, ^{12}C^{16}O^{18}OH$_{0.395}$(2.65), $^{\#}$SiO(0.08), ^{13}C^{16}O^{18}O$_{0.004}$(0.03), $^{\#}$SN(0.02), $^{\#}$NOO(0.01), ^{14}N^{15}N^{18}O$_{0.002}$(0.01)	99.97
48	^{48}**Ti$_{73.723}$(90.29)**, ^{48}Ca$_{0.187}$(0.05), ^{12}C^{12}C^{12}C^{12}C$_{95.672}$(5.53), ^{24}Mg^{24}Mg$_{62.394}$(4.21), ^{34}S^{14}N$_{4.194}$(0.01)	100.09
49	^{49}**Ti$_{5.412}$(83.27)**, ^{24}Mg^{25}Mg$_{15.798}$(13.19), ^{12}C^{12}C^{12}C^{13}C$_{4.256}$(3.05), ^{36}Ar^{12}CH$_{0.336}$(0.07)	99.58
50	^{50}**Ti$_{5.182}$(45.36)**, ^{50}**Cr$_{4.345}$(43.30)**, ^{50}V$_{0.250}$(2.41), ^{24}Mg^{26}Mg$_{17.394}$(8.52), ^{36}Ar^{14}N$_{0.339}$(0.47), ^{12}C^{12}C^{13}C^{13}C$_{0.071}$(0.03)	100.09
51	^{51}**V$_{99.750}$(99.88)**, ^{25}Mg^{26}Mg$_{2.202}$(0.11)	99.99
52	^{52}**Cr$_{83.789}$(99.70)**, ^{36}Ar^{16}O$_{0.339}$(0.22), ^{26}Mg^{26}Mg$_{1.212}$(0.07), ^{38}Ar^{14}N$_{0.060}$(0.01)	100.00
53	^{53}**Cr$_{9.501}$(89.16)**, ^{40}Ar^{12}CH$_{98.495}$(10.83)	99.99
54	^{54}**Fe$_{5.845}$(34.97)**, ^{54}Cr$_{2.365}$(9.36), ^{40}**Ar^{14}N$_{99.231}$(55.48)**, ^{38}Ar^{16}O$_{0.060}$(0.14), ^{40}Ar^{13}CH$_{1.096}$(0.05)	100.00
55	^{55}**Mn$_{100}$(99.95)**, ^{40}Ar^{15}N$_{0.368}$(0.04)	99.99

56	**$^{56}Fe_{91.754}$(49.86)**, **$^{40}Ca^{16}O_{96.707}$(30.93)**, $^{40}Ar^{16}O_{99\ 361}$(19.19)	99.98
57	**$^{57}Fe_{2.119}$(98.43)**, $^{40}Ca^{17}O_{0\ 039}$(0.97), $^{40}Ar^{17}O_{0\ 040}$(0.60)	100.00
58	**$^{58}Ni_{68.077}$(98.11)**, $^{58}Fe_{0\ 282}$(0.75), #CaO(1.33), $^{40}Ar^{18}O_{0\ 199}$(0.19)	100.38
59	**$^{59}Co_{100}$(99.89)**, $^{43}Ca^{16}O_{0\ 140}$(0.11)	100.00
60	**$^{60}Ni_{26.223}$(91.80)**, $^{44}Ca^{16}O_{2\ 085}$(8.07)	99.87
61	**$^{61}Ni_{1.140}$(84.93)**, $^{14}N^{12}C^{35}Cl_{74\ 659}$(14.99), #CaO(0.09)	100.01
62	**$^{62}Ni_{3.634}$(82.39)**, $^{23}Na^{23}Na^{16}O_{99.760}$(17.33), $^{44}Ca^{18}O_{0\ 004}$(0.21), #NCCl(0.07)	100.00
63	**$^{63}Cu_{69\ 173}$(99.89)**, $^{14}N^{12}C^{37}Cl_{23\ 875}$(0.10)	99.99
64	**$^{64}Zn_{48.636}$(96.95)**, $^{64}Ni_{0\ 926}$(3.79), $^{48}Ca^{16}O_{0\ 190}$(0.85), $^{23}Na^{23}Na^{18}O_{0\ 200}$(0.01)	101.61
65	**$^{65}Cu_{30\ 833}$(91.22)**, $^{32}S^{16}O^{16}OH_{94\ 555}$(8.79)	100.01
66	**$^{66}Zn_{27.903}$(98.51)**, $^{50}Cr^{16}O_{4\ 340}$(0.52), #SOOH(0.18)	99.21
67	**$^{67}Zn_{4.101}$(71.67)**, $^{40}Ar^{27}Al_{99\ 600}$(23.39), $^{34}S^{16}O^{16}OH_{4.189}$(4.93)	99.99
68	**$^{68}Zn_{18.755}$(87.13)**, $^{52}Cr^{16}O_{83\ 589}$(13.07)	100.20

69	**$^{69}Ga_{60.108}$(100.17)**, $^{53}Cr^{16}O_{9\ 477}$(0.13)	100.30
70	**$^{70}Ge_{21.848}$(98.11)**, $^{70}Zn_{0\ 623}$(1.17), $^{54}Fe^{16}O_{5\ 786}$(0.62), $^{54}Cr^{16}O_{2\ 364}$(0.17)	100.07
71	**$^{71}Ga_{39.892}$(97.92)**, $^{35}Cl^{35}ClH_{57\ 405}$(1.76)	99.68
72	**$^{72}Ge_{27.543}$(93.03)**, $^{56}Fe^{16}O_{91\ 500}$(6.93), $^{36}Ar^{36}Ar_{0\ 001}$(0.04)	100.00
73	**$^{73}Ge_{7.735}$(90.35)**, $^{35}Cl^{37}ClH_{36\ 714}$(9.08), $^{57}Fe^{16}O_{2\ 195}$(0.58)	100.01
74	**$^{74}Ge_{36.287}$(87.61)**, $^{74}Se_{0\ 894}$(0.30), $^{39}K^{35}Cl_{70\ 663}$(11.76), #FeO(0.02)	99.69
75	**$^{75}As_{100}$(99.16)**, $^{37}Cl^{37}ClH_{5\ 870}$(0.84)	100.00
76	**$^{76}Ge_{7.614}$(42.27)**, $^{76}Se_{9\ 373}$(6.74), **$^{36}Ar^{40}Ar_{0.677}$(40.73)**, #KCl(10.41), $^{36}Ar^{40}Ca_{0\ 330}$(0.07)	100.22
77	**$^{77}Se_{7.632}$(100.81)**, $^{36}Ar^{40}ArH_{0\ 677}$(0.78), $^{40}K^{37}Cl_{0\ 002}$(0.02)	101.61
78	**$^{78}Se_{23.773}$(67.05)**, **$^{38}Ar^{40}Ar_{0.120}$(28.89)**, $^{41}K^{37}Cl_{1\ 631}$(2.32), #ArCa(0.05)	98.31
79	**$^{63}Cu^{16}O_{69.004}$(99.13)**, $^{38}Ar^{40}ArH_{0\ 120}$(0.87), #ArCa(0.01)	100.01
81	**$^{40}Ar^{40}ArH_{99.192}$(93.82)**, $^{65}Cu^{16}O_{30\ 756}$(6.03)	99.85
82	**$^{82}Se_{8.732}$(90.19)**, #ArCa(1.88), $^{36}Ar^{46}Ti_{0\ 027}$(0.48), $^{40}Ar^{40}Ar^{2}H_{0\ 020}$(0.01)	92.56

83	**$^{36}Ar^{47}Ti_{0.025}$(55.33), $^{40}Ar^{43}Ca_{0.139}$(49.64)**, $^{65}Cu^{18}O_{0\ 062}$(1.39)	106.36
84	**$^{84}Sr_{0\ 561}$(92.19)**, $^{40}Ar^{44}Ca_{2\ 082}$(5.40), $^{\#}$ArTi(4.02)	101.61
85	**$^{85}Rb_{72.172}$(89.37)**, $^{69}Ga^{16}O_{59\ 956}$(10.63)	100.00
86	**$^{86}Sr_{9.861}$(90.91)**, $^{40}Ar^{46}Ti_{7\ 968}$(7.13), $^{69}Ga^{17}O_{0\ 024}$(0.03), $^{36}Ar^{50}Cr_{0\ 015}$(0.01)	98.08
87	**$^{87}Rb_{27.832}$(65.76)**, $^{87}Sr_{7\ 001}$(18.77), $^{71}Ga^{16}O_{39\ 804}$(13.51), $^{40}Ar^{47}Ti_{7\ 271}$(1.88), $^{36}Ar^{51}V_{0\ 339}$(0.09)	100.01
88	**$^{88}Sr_{82\ 581}$(92.36)**, $^{40}Ar^{48}Ti_{73\ 505}$(7.91), $^{\#}$ArCr(0.02)	100.29

Table 3.3B. Possible interference's for mass bias corrected data of the 100ppb standard solution

M/Z	Contributing Species	Σ of %
46	**$^{46}Ti_{8.253}$(63.97)**, $^{23}Na^{23}Na_{100}$(20.45), $^{\#}$SiO(14.10), $^{\#}$NNO(0.14)	98.66
47	**$^{47}Ti_{7.442}$(87.14)**, $^{14}N^{16}O^{16}OH_{99\ 142}$(12.80), $^{\#}$SiO(0.07)	100.01
48	**$^{48}Ti_{73.723}$(93.55)**, $^{32}S^{16}O_{94\ 792}$(6.22), $^{31}P^{16}OH_{99\ 750}$(0.03), $^{\#}$NOOH(0.01)	99.81
49	**$^{49}Ti_{5\ 412}$(98.95)**, $^{\#}$SO(0.73), $^{14}N^{16}O^{18}OH_{0\ 398}$(0.08)	99.76
50	**$^{50}Ti_{5.182}$(61.37)**, **$^{50}Cr_{4.345}$(34.06)**, $^{50}V_{0\ 250}$(2.13), $^{34}S^{16}O_{4\ 200}$(2.58)	100.14
51	**$^{51}V_{99.750}$(99.99)**	99.99
52	**$^{52}Cr_{83.789}$(99.60)**, $^{36}Ar^{16}O_{0\ 339}$(0.41)	100.01
53	**$^{53}Cr_{9.501}$(99.36)**	99.36
54	**$^{54}Fe_{5.845}$(26.36)**, $^{54}Cr_{2\ 365}$(11.56), **$^{40}Ca^{14}N_{96\ 581}$(61.71)**, $^{38}Ar^{16}O_{0\ 060}$(0.32)	99.95
55	**$^{55}Mn_{100}$(99.94)**, $^{40}Ca^{15}N_{0\ 359}$(0.05)	99.99
56	**$^{56}Fe_{91.754}$(45.30)**, **$^{40}Ar^{16}O_{99\ 361}$(54.69)**, $^{42}Ca^{14}N_{0\ 648}$(0.04)	100.03

57	**$^{57}Fe_{2.119}$(97.29)**, $^{40}Ar^{17}O_{0.040}$(1.86), #CaN(0.85)	100.00
58	**$^{58}Ni_{68.077}$(88.08)**, $^{58}Fe_{0.282}$(0.81), $^{23}Na^{35}Cl_{75.770}$(6.57), $^{44}Ca^{14}N_{2.082}$(0.84), $^{40}Ar^{18}O_{0.199}$(0.64)	96.94
59	**$^{59}Co_{100}$(100.00)**	100.00
60	**$^{60}Ni_{26.223}$(94.80)**, $^{23}Na^{37}Cl_{24.230}$(5.91)	100.71
61	**$^{61}Ni_{1.140}$(93.32)**	93.32
62	**$^{62}Ni_{3.634}$(95.83)**, $^{46}Ti^{16}O_{7.981}$(2.71), $^{48}Ca^{14}N_{0.189}$(1.56)	100.10
63	**$^{63}Cu_{69.173}$(99.77)**, $^{47}Ti^{16}O_{7.282}$(0.17)	99.94
64	**$^{64}Zn_{48.636}$(90.08)**, $^{64}Ni_{0.926}$(4.86), $^{48}Ti^{16}O_{73.623}$(5.00)	99.94
65	**$^{65}Cu_{30.833}$(99.74)**, $^{49}Ti^{16}O_{5.487}$(0.30), $^{130}Ba^{++}{}_{0.110}$(0.02)	100.06
66	**$^{66}Zn_{27.903}$(99.33)**, $^{50}Ti^{16}O_{5.387}$(0.72), $^{50}Cr^{16}O_{4.340}$(0.04), $^{132}Ba^{++}{}_{0.100}$(0.04)	100.13
67	**$^{67}Zn_{4.101}$(74.84)**, $^{40}Ar^{27}Al_{99.600}$(20.33), $^{134}Ba^{++}{}_{2.420}$(4.85), #TiO(0.01)	100.03
68	**$^{68}Zn_{18.755}$(93.81)**, $^{136}Ba^{++}{}_{7.850}$(4.30), $^{52}Cr^{16}O_{83.589}$(1.08)	99.19
69	**$^{69}Ga_{60.108}$(97.20)**, $^{138}Ba^{++}{}_{71.700}$(3.47) $^{53}Cr^{16}O_{9.477}$(0.01)	100.68

70	**$^{70}Ge_{21.848}$(101.18)**, $^{70}Zn_{0\ 623}$(1.33), $^{54}Fe^{16}O_{5\ 786}$(0.02), $^{54}Cr^{16}O_{2\ 364}$(0.01)	102.54
71	**$^{71}Ga_{39.892}$(99.34)**	99.34
72	**$^{72}Ge_{27.543}$(99.69)**, $^{56}Fe^{16}O_{91\ 500}$(0.22), $^{36}Ar^{36}Ar_{0\ 001}$(0.04)	99.95
73	**$^{73}Ge_{7.735}$(98.29)**, $^{40}Ar^{16}O^{16}OH_{99\ 113}$(1.68), $^{57}Fe^{16}O_{2\ 195}$(0.02)	99.99
74	**$^{74}Ge_{36.287}$(96.50)**, $^{74}Se_{0\ 894}$(0.29), $^{39}K^{35}Cl_{70\ 663}$(3.00)	99.79
75	**$^{75}As_{100}$(100.00)**	100.00
76	**$^{76}Ge_{7.614}$(47.42)**, $^{76}Se_{9\ 373}$(6.68), **$^{36}Ar^{40}Ar_{0.677}$(43.25)**, #KCl(2.71), $^{36}Ar^{40}Ca_{0\ 330}$(0.07)	100.13
77	**$^{77}Se_{7.632}$(100.67)**, $^{36}Ar^{40}ArH_{0\ 677}$(0.71)	101.39
78	**$^{78}Se_{23\ 773}$(67.25)**, **$^{38}Ar^{40}Ar_{0.120}$(31.02)**, $^{41}K^{37}Cl_{1\ 631}$(0.61), #ArCa(0.05)	98.93
79	**$^{79}Br_{50.697}$(99.70)**, $^{38}Ar^{40}ArH_{0\ 120}$(0.81), #ArCa(0.01)	100.52
81	$^{81}Br_{49\ 317}$(13.16), **$^{40}Ar^{40}ArH_{99.192}$(86.73)**	99.89
82	**$^{82}Se_{8.732}$(90.96)**, #ArCa(1.91), $^{36}Ar^{46}Ti_{0\ 027}$(0.48), $^{40}Ar^{40}Ar^{2}H_{0\ 020}$(0.01)	93.36
83	**$^{36}Ar^{47}Ti_{0.025}$(53.25)**, **$^{40}Ar^{43}Ca_{0.139}$(48.82)**	102.07

84	**$^{84}Sr_{0.561}$(91.94)**, $^{40}Ar^{44}Ca_{2\ 082}$(5.50), #ArTi(4.00)	101.44
85	**$^{85}Rb_{72.172}$(89.65)**, $^{69}Ga^{16}O_{59\ 956}$(10.35)	100.00
86	**$^{86}Sr_{9.861}$(90.72)**, $^{40}Ar^{46}Ti_{7\ 968}$(7.11), $^{69}Ga^{17}O_{0\ 024}$(0.03), $^{36}Ar^{50}Cr_{0\ 015}$(0.01)	97.87
87	**$^{87}Rb_{27.832}$(66.07)**, $^{87}Sr_{7\ 001}$(18.75), $^{71}Ga^{16}O_{39\ 804}$(13.17), $^{40}Ar^{47}Ti_{7\ 271}$(1.87), $^{36}Ar^{51}V_{0\ 339}$(0.14)	100.00
88	**$^{88}Sr_{82.581}$(92.42)**, $^{40}Ar^{48}Ti_{73\ 505}$(7.91), #ArCr(0.03)	100.36

Table 3.3C. Possible interference's for raw data of TORT 1 – Lobester Hepatopancreas Marine

M/Z	Contributing Species	Σ of %
46	$^{46}Ti_{8\ 253}$(9.08), $^{46}Ca_{0\ 004}$(0.05), **$^{\#}$SiO(87.71)**, $^{\#}$NNO(2.88)	99.72
47	$^{47}Ti_{7\ 442}$(4.48), **$^{14}N^{16}O^{16}OH_{99.142}$(95.38)**, $^{\#}$SiO(0.15), $^{14}N^{15}N^{18}O_{0\ 002}$(0.012)	100.13
48	$^{48}Ti_{73\ 723}$(3.17), $^{48}Ca_{0\ 187}$(0.08), **$^{31}P^{16}OH_{99.750}$(96.62)**, $^{\#}$NOOH(0.03), $^{30}Si^{18}O_{0\ 006}$(0.01)	99.91
49	**$^{49}Ti_{5.412}$(74.28)**, $^{\#}$POH(16.16), $^{14}N^{16}O^{18}OH_{0.398}$(8.42)	98.86
50	**$^{50}Cr_{4\ 345}$(56.72)**, $^{50}Ti_{5\ 182}$(23.48), $^{50}V_{0\ 250}$(1.47), $^{31}P^{18}OH_{0\ 200}$(19.63)	101.30
51	**$^{51}V_{99.750}$(99.99)**	99.99
52	**$^{52}Cr_{83.789}$(96.20)**, $^{40}Ar^{12}C_{98\ 504}$(1.13)	97.33
53	**$^{53}Cr_{9.501}$(101.06)**, $^{40}Ar^{13}C_{1\ 096}$(0.12)	101.18
54	**$^{54}Fe_{5.845}$(98.08)**, $^{54}Cr_{2\ 365}$(0.58)	98.66
55	**$^{55}Mn_{100}$(100.00)**	100.00
56	**$^{56}Fe_{91.754}$(100.25)**	100.25

57	**$^{57}Fe_{2.119}$(79.02)**, $^{40}Ca^{16}OH_{96\ 698}$(22.20)	101.22
58	**$^{58}Ni_{68\ 077}$(73.74)**, **$^{58}Fe_{0.282}$(28.90)**, $^{\#}$CaOH(0.03)	102.67
59	**$^{59}Co_{100}$(97.58)**, $^{\#}$CaOH(2.41)	99.99
60	**$^{60}Ni_{26.223}$(97.86)**, $^{43}Ca^{16}OH_{0\ 140}$(0.31)	98.17
61	**$^{61}Ni_{1.140}$(46.65)**, **$^{44}Ca^{16}OH_{2.085}$(52.49)**	99.14
62	**$^{62}Ni_{3.634}$(59.42)**, **$^{48}Ti^{16}O_{7.981}$(33.53)**, $^{\#}$CaOH(0.02)	92.97
63	**$^{63}Cu_{69.173}$(99.68)**, $^{47}Ti^{16}O_{7\ 282}$(0.02)	99.70
64	**$^{64}Zn_{48.636}$(105.12)**, $^{64}Ni_{0\ 926}$(0.07), $^{48}Ti^{16}O_{73\ 623}$(1.48)	106.67
65	**$^{65}Cu_{30.833}$(94.34)**, $^{32}S^{16}O^{16}OH_{94\ 555}$(5.95), $^{49}Ti^{16}O_{5\ 487}$(0.04)	100.33
66	**$^{66}Zn_{27.903}$(98.32)**, $^{\#}$SOOH(0.25), $^{50}Ti^{16}O_{5\ 387}$(0.18)	98.75
67	**$^{67}Zn_{4.101}$(90.93)**, $^{34}S^{16}O^{16}OH_{4\ 189}$(8.77), $^{134}Ba^{++}{}_{2\ 420}$(0.10)	99.80
68	**$^{68}Zn_{18.755}$(92.09)**, $^{136}Ba^{++}{}_{7\ 850}$(0.07)	92.16
69	**$^{69}Ga_{60.108}$(55.50)**, **$^{138}Ba^{++}{}_{71.700}$(43.49)**, $^{\#}$SOOH(1.04), $^{36}Ar^{16}O^{16}OH_{0\ 338}$(0.02)	100.05

70	**$^{70}Zn_{0.623}$(63.54)**, **$^{40}Ar^{14}N^{16}O_{98\ 993}$(36.46)**	100.00
71	**$^{71}Ga_{39.892}$(98.75)**, $^{\#}$ArNO(1.22), $^{38}Ar^{16}O^{16}OH_{0\ 060}$(0.01)	99.98
72	**$^{40}Ar^{32}S_{94.640}$(94.10)**, $^{36}Ar^{36}Ar_{0\ 001}$(4.33), $^{40}Ar^{14}N^{18}O_{0\ 198}$(1.45)	99.88
73	**$^{40}Ar^{16}O^{16}OH_{99.113}$(98.02)**, $^{40}Ar^{33}S_{0\ 747}$(2.00), $^{\#}$ArNO(0.01)	100.03
74	**$^{74}Se_{0.894}$(73.88)**, $^{39}K^{35}Cl_{70\ 663}$(15.39), $^{40}Ar^{34}S_{4\ 193}$(7.61), $^{\#}$ArOOH(0.06)	96.94
75	**$^{75}As_{100}$(100.00)**	100.00
76	$^{76}Se_{9\ 373}$(13.29), **$^{36}Ar^{40}Ar_{0\ 677}$(86.76)**, $^{\#}$KCl(0.1)	100.06
77	**$^{77}Se_{7.632}$(105.44)**	105.44
78	**$^{78}Se_{23.773}$(65.89)**, **$^{38}Ar^{40}Ar_{0.120}$(30.66)**, $^{41}K^{37}Cl_{1\ 631}$(0.01)	96.56
79	**$^{79}Br_{50.697}$(104.02)**	104.02
81	**$^{81}Br_{49.317}$(95.76)**, $^{\#}$SOOO(0.03)	95.79
82	**$^{82}Se_{8.732}$(88.15)**, $^{\#}$SOOO(10.37), $^{36}Ar^{46}Ti_{0\ 027}$(1.49)	100.01
83	**$^{36}Ar^{47}Ti_{0.025}$(97.57)**, $^{\#}$SOOO(1.53)	99.10

84	**$^{84}Sr_{0.561}$(95.98)**, $^{\#}$ArTi(1.24), $^{\#}$SOOO(0.01)	97.23
85	**$^{85}Rb_{72.172}$(100.05)**, $^{\#}$ArTi(0.03)	100.08
86	**$^{86}Sr_{9.861}$(98.37)**, $^{\#}$ArTi(2.29)	100.66
87	**$^{87}Sr_{7.001}$(85.59)**, $^{87}Rb_{27.832}$(10.04), $^{\#}$ArTi(2.54), $^{36}Ar^{51}V_{0.339}$(1.36)	99.53
88	**$^{88}Sr_{82.581}$(100.53)**, $^{\#}$ArTi(2.56)	103.09

Table 3.3D. Possible interference's for mass bias corrected data of TORT 1 – Lobester Hepatopancreas Marine

M/Z	Contributing Species	Σ of %
46	$^{46}Ti_{8\ 253}$(6.16), $^{46}Ca_{0\ 004}$(0.01), **$^{\#}SiO$(92.41)**, $^{\#}NNO$(0.56)	99.14
47	$^{47}Ti_{7\ 442}$(3.02), **$^{14}N^{16}O^{16}OH_{99\ 142}$(96.82)**, $^{\#}SiO$(0.16)	100.00
48	$^{48}Ti_{73\ 723}$(2.46), $^{48}Ca_{0\ 187}$(0.02), **$^{31}P^{16}OH_{99.750}$(96.13)**, $^{32}S^{16}O_{94\ 792}$(1.34), $^{\#}NOOH$(0.04), $^{30}Si^{18}O_{0\ 006}$(0.01)	100.00
49	**$^{49}Ti_{5\ 412}$(66.22)**, $^{\#}POH$(18.44), $^{14}N^{16}O^{18}OH_{0\ 398}$(11.32), $^{\#}SO$(4.00), $^{36}Ar^{13}C_{0\ 004}$(0.01)	99.99
50	**$^{50}Cr_{4.345}$(38.89)**, $^{50}Ti_{5\ 182}$(23.84), $^{50}V_{0\ 250}$(1.30), **$^{31}P^{18}OH_{0.20}$(25.51)**, $^{34}S^{16}O_{4\ 200}$(8.21), $^{36}Ar^{14}N_{0\ 339}$(2.16), $^{38}Ar^{12}C_{0\ 059}$(0.09)	100.00
51	**$^{51}V_{99.750}$(99.99)**	99.99
52	**$^{52}Cr_{83.789}$(83.75)**, $^{40}Ar^{12}C_{98\ 504}$(16.20), $^{38}Ar^{14}N_{0\ 060}$(0.05), $^{\#}SO$(0.01)	100.01
53	**$^{53}Cr_{9.501}$(98.14)**, $^{40}Ar^{13}C_{1\ 096}$(1.86)	100.00
54	**$^{54}Fe_{5.845}$(80.71)**, $^{54}Cr_{2\ 365}$(0.62), $^{40}Ar^{14}N_{99\ 231}$(18.66)	99.99
55	**$^{55}Mn_{100}$(99.97)**, $^{40}Ar^{15}N_{0\ 368}$(0.04)	100.01
56	**$^{56}Fe_{91.754}$(99.42)**	99.42

57	**$^{57}Fe_{2.119}$(85.25)**, $^{40}Ca^{16}OH_{96\ 698}$(15.54)	100.79
58	**$^{58}Ni_{68.077}$(65.75)**, **$^{58}Fe_{0.282}$(33.72)**, $^{\#}$CaOH(0.03)	99.50
59	**$^{59}Co_{100}$(98.02)**, $^{\#}$CaOH(1.96)	99.98
60	**$^{60}Ni_{26.223}$(100.38)**, $^{43}Ca^{16}OH_{0\ 140}$(0.27)	100.65
61	**$^{61}Ni_{1.140}$(50.92)**, **$^{44}Ca^{16}OH_{2.085}$(48.66)**	99.58
62	**$^{62}Ni_{3.634}$(68.66)**, **$^{46}Ti^{16}O_{7.981}$(30.74)**, $^{\#}$CaOH(0.01)	99.41
63	**$^{63}Cu_{69.173}$(97.76)**, $^{46}Ti^{16}OH_{7\ 980}$(0.05), $^{47}Ti^{16}O_{7.282}$(0.02)	97.83
64	**$^{64}Zn_{48.636}$(98.47)**, $^{64}Ni_{0\ 926}$(0.09), $^{48}Ti^{16}O_{73\ 623}$(1.50), $^{\#}$TiOH(0.31)	100.37
65	**$^{65}Cu_{30\ 833}$(101.28)**, $^{48}Ti^{16}OH_{73\ 616}$(1.10), $^{49}Ti^{16}O_{5\ 4868}$(0.04)	102.42
66	**$^{66}Zn_{27.903}$(99.95)**, $^{49}Ti^{16}OH_{5\ 486}$(0.42), $^{50}Ti^{16}O_{5\ 387}$(0.20)	100.57
67	**$^{67}Zn_{4.101}$(95.70)**, $^{50}Ti^{16}OH_{5.386}$(2.71), $^{134}Ba^{++}{}_{2\ 420}$(0.10)	98.51
68	**$^{68}Zn_{18.755}$(99.96)**, $^{136}Ba^{++}{}_{7\ 850}$(0.08)	100.04
69	**$^{69}Ga_{60.108}$(53.23)**, **$^{138}Ba^{++}{}_{71.700}$(46.68)**, $^{50}Ti^{18}OH_{0\ 011}$(0.08), $^{36}Ar^{16}O^{16}OH_{0\ 338}$(0.02)	100.01

70	**$^{70}Zn_{0.623}$(72.59), $^{40}Ar^{14}N^{16}O_{98.993}$(27.40)**	99.99
71	**$^{71}Ga_{39\ 892}$(99.03)**, #ArNO(0.93), $^{38}Ar^{16}O^{16}OH_{0\ 060}$(0.01)	99.97
72	**$^{40}Ar^{32}S_{94.640}$(94.43)**, $^{36}Ar^{36}Ar_{0\ 001}$(4.14), $^{40}Ar^{14}N^{18}O_{0\ 198}$(1.13)	99.70
73	**$^{40}Ar^{16}O^{16}OH_{99.113}$(98.45)**, $^{40}Ar^{33}S_{0\ 747}$(2.04), #ArNO(0.01)	100.50
74	**$^{74}Se_{0.894}$(71.70)**, $^{39}K^{35}Cl_{70\ 663}$(17.07), $^{40}Ar^{34}S_{4\ 193}$(7.85), #ArOOH(0.06)	96.68
75	**$^{75}As_{100}$(100.01)**	100.01
76	$^{76}Se_{9\ 373}$(13.14), **$^{36}Ar^{40}Ar_{0.677}$(86.88)**, #KCl(0.12)	100.14
77	**$^{77}Se_{7.632}$(104.90)**	104.90
78	**$^{78}Se_{23.773}$(65.86)**, **$^{38}Ar^{40}Ar_{0.120}$(31.04)**, $^{41}K^{37}Cl_{1\ 631}$(0.01)	96.91
79	**$^{79}Br_{50.697}$(103.95)**	103.95
81	**$^{81}Br_{49.317}$(95.83)**, #SOOO(0.03)	95 86
82	**$^{82}Se_{8.732}$(88.60)**, #SOOO(9.93), $^{36}Ar^{46}Ti_{0\ 027}$(1.48)	100.01
83	**$^{36}Ar^{47}Ti_{0.025}$(97.55)**, #SOOO(1.46)	99.01

84	$^{84}Sr_{0.561}$**(95.81)**, #ArTi(1.24), #SOOO(0.01)	97.06
85	$^{85}Rb_{72.172}$**(100.03)**, #ArTi(0.03)	100.06
86	$^{86}Sr_{9.861}$**(98.27)**, #ArTi(2.30)	100.57
87	$^{87}Sr_{7.001}$**(85.59)**, $^{87}Rb_{27\ 832}$(10.05), #ArTi(2.55), $^{36}Ar^{51}V_{0\ 339}$(1.48)	99.67
88	$^{88}Sr_{82.581}$**(100.71)**, #ArTi(2.57)	103.28

Table 3.3E. Possible interference's for raw data of NIST 1547 - Peach Leaves

M/Z	Contributing Species	Σ of %
46	$^{46}Ca_{0.004}$(0.03), $^{32}S^{14}N_{94.668}$**(98.48)**, #NNO(1.48)	99.99
47	$^{14}N^{16}O^{16}OH_{99.142}$**(97.64)**, #SN(2.33), $^{14}N^{15}N^{18}O_{0.002}$(0.02)	99.99
48	$^{48}Ca_{0.187}$(0.04), $^{31}P^{16}OH_{99.750}$**(99.82)**, $^{34}S^{14}N_{4.194}$(0.13), #NOOH(0.01)	100.00
49	$^{32}S^{16}OH_{94.782}$**(91.85)**, #POH(7.28), $^{14}N^{16}O^{18}OH_{0.398}$(0.80), $^{34}S^{15}N_{0.016}$(0.07)	100.00
50	$^{50}Cr_{4.345}$(17.85), $^{50}V_{0.250}$(0.31), $^{35}Cl^{14}NH_{75.482}$**(58.48)**, $^{31}P^{18}OH_{0.200}$(22.64), #SOH(0.64), $^{36}S^{14}N_{0.020}$(0.07), $^{38}Ar^{12}C_{0.059}$(0.02)	100.01
51	$^{51}V_{99.750}$**(97.04)**, $^{34}S^{16}OH_{4.200}$(2.76), #ClNH(0.18)	99.98
52	$^{52}Cr_{83.789}$**(88.27)**, $^{40}Ar^{12}C_{98.504}$(6.94), $^{37}Cl^{14}NH_{24.138}$(4.80)	100.01
53	$^{53}Cr_{9.501}$**(98.99)**, $^{40}Ar^{13}C_{1.096}$(0.76), #ClNH(0.18), #SOH(0.06)	99.99
54	$^{54}Fe_{5.845}$**(99.66)**, $^{54}Cr_{2.365}$(0.26)	99.92
55	$^{55}Mn_{100}$**(100.00)**	100.00
56	$^{56}Fe_{91.754}$**(98.99)**, $^{40}Ca^{16}O_{96.707}$(1.11)	100.10

57	$^{57}Fe_{2.119}$**(68.99)**, $^{40}Ca^{16}OH_{96.698}$**(32.79)**, $^{40}Ca^{17}O_{0\ 039}$(0.01)	101.79
58	$^{58}Fe_{0.282}$**(58.00)**, $^{58}Ni_{68.077}$**(37.26)**, $^{\#}$CaO(1.84), $^{\#}$CaOH(0.11)	97.21
59	$^{59}Co_{100}$**(73.28)**, $^{\#}$CaOH(23.09), $^{43}Ca^{16}O_{0\ 140}$(3.64)	100.01
60	$^{60}Ni_{26.223}$**(74.54)**, $^{44}Ca^{16}O_{2\ 085}$(23.92), $^{43}Ca^{16}OH_{0\ 140}$(1.58)	100.04
61	$^{61}Ni_{1\ 140}$(11.37), $^{44}Ca^{16}OH_{2.085}$**(85.97)**, $^{\#}$CaO(0.04)	97.38
62	$^{62}Ni_{3.634}$**(100.12)**, $^{44}Ca^{18}O_{0\ 004}$(0.92), $^{\#}$CaOH(0.16)	101.20
63	$^{63}Cu_{69.173}$**(99.69)**, $^{44}Ca^{18}H_{0\ 004}$(0.01)	99.70
64	$^{64}Zn_{48.636}$**(101.04)**, $^{64}Ni_{0\ 926}$(0.15), $^{48}Ca^{16}O_{0\ 190}$(0.13)	101.32
65	$^{65}Cu_{30\ 833}$**(89.93)**, $^{32}S^{16}O^{16}OH_{94\ 555}$(8.81), $^{130}Ba^{++}{}_{0\ 110}$(0.91), $^{48}Ca^{16}O\ H_{0\ 190}$(0.47)	100.12
66	$^{66}Zn_{27.903}$**(98.58)**, $^{132}Ba^{++}{}_{0.100}$(0.41), $^{36}Ar^{14}N^{16}O_{0\ 338}$(0.05), $^{\#}$SOOH(0.04)	99.08
67	$^{67}Zn_{4.101}$**(59.06)**, $^{134}Ba^{++}{}_{2.420}$**(39.55)**, $^{34}S^{16}O^{16}OH_{4\ 189}$(0.81), $^{36}Ar^{14}N^{16}OH_{0\ 338}$(0.08)	99.50
68	$^{68}Zn_{18.755}$**(65.67)**, $^{136}Ba^{++}{}_{7.850}$**(31.17)**, $^{38}Ar^{14}N^{16}O_{0\ 060}$(0.01), $^{36}Ar^{32}S_{0\ 323}$(0.01)	96.86
69	$^{138}Ba^{++}{}_{71.700}$**(101.53)**	101.53

70	$^{70}Zn_{0.623}$(12.06), $^{70}Ge_{21.848}$(1.75), **$^{40}Ar^{14}N^{16}O_{98.993}$(86.19)**, $^{38}Ar^{32}S_{0.057}$(0.01)	100.01
71	**$^{40}Ar^{14}N^{16}OH_{98.983}$(98.87)**, #ArNO(1.08), $^{36}Ar^{35}Cl_{0.258}$(0.04), $^{38}Ar^{16}O^{16}OH_{0.060}$(0.01)	100.00
72	$^{72}Ge_{27.543}$(16.83), **$^{40}Ar^{32}S_{94.640}$(78.33)**, $^{36}Ar^{36}Ar_{0.001}$(2.55), $^{40}Ar^{14}N^{18}O_{0.198}$(1.25), #ArNOH(0.97)	99.93
73	$^{73}Ge_{7.735}$(8.68), **$^{40}Ar^{16}O^{16}OH_{99.113}$(89.28)**, $^{40}Ar^{33}S_{0.747}$(1.12), $^{40}Ar^{14}N^{18}OH_{0.198}$(0.84), #ArCl(0.08), #ArNO(0.01)	100.01
74	**$^{74}Ge_{36.287}$(80.61)**, $^{74}Se_{0.894}$(3.16), $^{40}Ar^{34}S_{4.193}$(12.48), #ArOOH(0.16), #ArNOH(0.01)	96.42
75	**$^{75}As_{100}$(55.67)**, **$^{40}Ar^{35}Cl_{75.467}$(44.01)**, $^{40}Ar^{16}O^{18}OH_{0.397}$(0.34)	100.02
76	$^{76}Se_{9.373}$(0.57), $^{76}Ge_{7.614}$(0.31), **$^{36}Ar^{40}Ar_{0.677}$(100.39)**	101.27
77	**$^{77}Se_{7.632}$(43.95)**, **$^{40}Ar^{37}Cl_{24.133}$(48.48)**, $^{36}Ar^{40}ArH_{0.677}$(7.55)	99.98
78	$^{78}Se_{23.773}$(7.05), $^{78}Kr_{0.351}$(0.04), **$^{38}Ar^{40}Ar_{0.120}$(88.98)**	96.07
79	**$^{79}Br_{50.697}$(99.94)**, $^{38}Ar^{40}ArH_{0.120}$(0.06)	100.00
81	**$^{81}Br_{49.317}$(66.17)**, **$^{40}Ar^{40}ArH_{99.192}$(33.82)**	99.99
82	**$^{82}Se_{8.732}$(72.33)**, **$^{82}Kr_{11.581}$(34.47)**, $^{40}Ar^{40}Ar^{2}H_{0.020}$(0.23)	107.03
83	**$^{83}Kr_{11.496}$(93.13)**	93.13

84	**$^{84}Sr_{0.561}$(98.75)**, $^{84}Kr_{57.004}$(1.32)	100.07
85	**$^{85}Rb_{72.172}$(100.08)**	100.08
86	**$^{86}Sr_{9.861}$(98.08)**, $^{86}Kr_{17.302}$(0.02), $^{\#}$ArV(0.02)	98.12
87	**$^{87}Rb_{27.832}$(51.82)**, **$^{87}Sr_{7.001}$(42.97)**, $^{36}Ar^{51}V_{0.339}$(5.10)	99.89
88	**$^{88}Sr_{82.581}$(104.06)**	104.06

Table 3.3F. Possible interference's for mass bias corrected data of NIST 1547 - Peach Leaves

M/Z	Contributing Species	Σ of %
46	$^{46}Ca_{0.004}$(0.02), $^{\#}$**NNO(99.21)**	99.23
47	$^{14}N^{16}O^{16}OH_{99.142}$**(98.51)**, $^{14}N^{15}N^{18}O_{0.002}$(1.51), $^{38}Ar^{9}Be_{0.060}$(0.02)	100.04
48	$^{48}Ca_{0.187}$(0.04), $^{31}P^{16}OH_{99.750}$**(91.34)**, $^{32}S^{16}O_{94.792}$(8.60), $^{\#}$NOOH(0.01)	99.99
49	$^{40}Ar^{9}Be_{99.600}$**(80.08)**, $^{\#}$SO(11.21), *POH(7.64), $^{14}N^{16}O^{18}OH_{0.398}$(1.08)	100.01
50	$^{50}Cr_{4.345}$(12.38), $^{50}V_{0.250}$(0.28), $^{34}S^{16}O_{4.200}$**(58.84)**, $^{31}P^{18}OH_{0.200}$**(27.05)**, $^{36}Ar^{14}N_{0.339}$(1.39), $^{38}Ar^{12}C_{0.059}$(0.04)	99.98
51	$^{51}V_{99.750}$**(99.96)**, $^{\#}$SO(0.04)	100.00
52	$^{52}Cr_{83.789}$**(77.78)**, $^{40}Ar^{12}C_{98.504}$(22.01), $^{\#}$SO(0.12), $^{38}Ar^{14}N_{0.060}$(0.08)	99.99
53	$^{53}Cr_{9.501}$**(97.29)**, $^{40}Ar^{13}C_{1.096}$(2.70)	99.99
54	$^{54}Fe_{5.845}$**(82.64)**, $^{54}Cr_{2.365}$(0.28), $^{40}Ar^{14}N_{99.231}$(17.08)	100.00
55	$^{55}Mn_{100}$**(99.99)**, $^{40}Ar^{15}N_{0.368}$(0.01)	100.00
56	$^{56}Fe_{91.754}$**(98.92)**, $^{40}Ca^{16}O_{96.707}$(1.14)	100.06

57	**$^{57}Fe_{2.119}$(75.00), $^{40}Ca^{16}OH_{96.698}$(25.56),** $^{40}Ca^{17}O_{0\ 039}$(0.01)	100.57
58	**$^{58}Fe_{0.282}$(68.20), $^{58}Ni_{68\ 077}$(28.36),** $^{\#}$CaO(2.23), $^{\#}$CaOH(0.10)	98.89
59	**$^{59}Co_{100}$(74.39),** $^{\#}$CaOH(20.93), $^{43}Ca^{16}O_{0\ 140}$(4.72)	100.04
60	**$^{60}Ni_{26.223}$(65.26), $^{44}Ca^{16}O_{2.085}$(33.24),** $^{43}Ca^{16}OH_{0\ 140}$(1.53)	100.03
61	$^{61}Ni_{1\ 140}$(10.59), **$^{44}Ca^{16}OH_{2\ 085}$(88.70),** $^{\#}$CaO(0.07)	99.36
62	**$^{62}Ni_{3.634}$(98.74),** $^{44}Ca^{18}O_{0\ 004}$(1.44), $^{\#}$CaOH(0.18)	100.36
63	**$^{63}Cu_{69.173}$(99.89),** 44$Ca^{18}OH_{0\ 004}$(0.01)	99.90
64	**$^{64}Zn_{48.636}$(95.26),** $^{64}Ni_{0\ 926}$(0.17), $^{31}P^{16}O^{16}OH_{99\ 511}$(4.35), $^{48}Ca^{16}O_{0\ 190}$(0.22)	100.00
65	**$^{65}Cu_{30.833}$(98.64),** $^{130}Ba^{++}{}_{0\ 110}$(0.79), $^{48}Ca^{16}O\ H_{0\ 190}$(0.59), $^{\#}$POOH(0.02)	100.04
66	**$^{66}Zn_{27.903}$(100.85),** $^{132}Ba^{++}{}_{0\ 100}$(0.37), $^{36}Ar^{14}N^{16}O_{0\ 338}$(0.04), $^{31}P^{16}O^{18}OH_{0\ 399}$(0.03)	101.29
67	**$^{67}Zn_{4.101}$(62.55), $^{134}Ba^{++}{}_{2.420}$(36.98),** $^{36}Ar^{14}N^{16}OH_{0\ 338}$(0.07)	99.60
68	**$^{68}Zn_{18.755}$(71.74), $^{136}Ba^{++}{}_{7\ 850}$(30.06),** $^{38}Ar^{14}N^{16}O_{0\ 060}$(0.01), $^{36}Ar^{32}S_{0\ 323}$(0.01)	101.82
69	**$^{138}Ba^{++}{}_{71.700}$(100.61)**	100 61

70	$^{70}Zn_{0.623}$(13.86), $^{70}Ge_{21.848}$(1.63), **$^{40}Ar^{14}N^{16}O_{98.993}$(84.49)**, $^{38}Ar^{32}S_{0.057}$(0.01)	99.99
71	**$^{40}Ar^{14}N^{16}OH_{98.983}$(98.91)**, #ArNO(1.08), $^{36}Ar^{35}Cl_{0.258}$(0.04), $^{38}Ar^{16}O^{16}OH_{0.060}$(0.01)	100.04
72	$^{72}Ge_{27.543}$(16.32), **$^{40}Ar^{32}S_{94.640}$(78.94)**, $^{36}Ar^{36}Ar_{0.001}$(2.43), $^{40}Ar^{14}N^{18}O_{0.198}$(1.27), #ArNOH(0.98)	99.94
73	$^{73}Ge_{7.735}$(8.55), **$^{40}Ar^{16}O^{16}OH_{99.113}$(89.31)**, $^{40}Ar^{33}S_{0.747}$(1.15), $^{40}Ar^{14}N^{18}OH_{0.198}$(0.86), #ArCl(0.08), #ArNO(0.01)	99.96
74	**$^{74}Ge_{36.287}$(80.35)**, $^{74}Se_{0.894}$(2.98), $^{40}Ar^{34}S_{4.193}$(12.92), #ArOOH(0.16), #ArNOH(0.01)	96.42
75	**$^{75}As_{100}$(54.83)**, **$^{40}Ar^{35}Cl_{75.467}$(44.96)**, $^{40}Ar^{16}O^{18}OH_{0.397}$(0.35)	100.14
76	$^{76}Se_{9.373}$(0.54), $^{76}Ge_{7.614}$(0.31), **$^{36}Ar^{40}Ar_{0.677}$(100.21)**	101.06
77	**$^{77}Se_{7.632}$(42.45)**, **$^{40}Ar^{37}Cl_{24.133}$(50.25)**, $^{36}Ar^{40}ArH_{0.677}$(7.46)	100.16
78	$^{78}Se_{23.773}$(6.84), $^{78}Kr_{0.351}$(0.04), **$^{38}Ar^{40}Ar_{0.120}$(89.82)**	96.70
79	**$^{79}Br_{50.697}$(99.93)**, $^{38}Ar^{40}ArH_{0.120}$(0.06)	99.99
81	**$^{81}Br_{49.317}$(66.26)**, **$^{40}Ar^{40}ArH_{99.192}$(33.75)**	100.01
82	**$^{82}Se_{8.732}$(70.58)**, **$^{82}Kr_{11.581}$(35.02)**, $^{40}Ar^{40}Ar^{2}H_{0.020}$(0.23)	105.83
83	**$^{83}Kr_{11.496}$(94.65)**	94.65

84	**$^{84}Sr_{0.561}$(98.66)**, $^{84}Kr_{57\ 004}$(1.34)	100.00
85	**$^{85}Rb_{72.172}$(100.01)**	100.01
86	**$^{86}Sr_{9.861}$(98.06)**, $^{86}Kr_{17\ 302}$(0.02), $^{\#}$ArV(0.02)	98.10
87	**$^{87}Rb_{27.832}$(51.87)**, **$^{87}Sr_{7.001}$(43.00)**, $^{36}Ar^{51}V_{0\ 339}$(5.12)	99.99
88	**$^{88}Sr_{82.581}$(104.32)**	104.32

Table 3.3G. Possible interference's for raw data of NIST 1577b - Bovine Liver

M/Z	Contributing Species	Σ of %
46	$^{46}Ca_{0.004}$(0.06), $^{\#}$**NNO(95.64)**	95.70
47	$^{14}N^{16}O^{16}OH_{99.142}$**(99.87)**, $^{14}N^{15}N^{18}O_{0.002}$(0.14)	100.01
48	$^{48}Ca_{0.187}$(0.56), $^{32}S^{16}O_{94.792}$**(53.11)**, $^{31}P^{16}OH_{99.750}$**(45.75)**, $^{\#}$NOOH(0.45), $^{36}Ar^{12}C_{0.336}$(0.13)	100.00
49	$^{40}Ar^{9}Be_{99.600}$**(49.79)**, $^{\#}$**SO(25.71)**, $^{14}N^{16}O^{18}OH_{0.398}$(23.00), $^{\#}$POH(1.42), $^{36}Ar^{13}C_{0.004}$(0.09)	100.01
50	$^{50}Cr_{4.345}$**(48.36)**, $^{50}V_{0.250}$(0.54), $^{34}S^{16}O_{4.200}$**(48.72)**, $^{31}P^{16}OH_{0.200}$(1.82), $^{38}Ar^{12}C_{0.059}$(0.50), $^{\#}$NOOH(0.03)	99.97
51	$^{51}V_{99.750}$**(99.97)**, $^{\#}$SO(0.02)	99.99
52	$^{52}Cr_{83.789}$**(54.18)**, $^{40}Ar^{12}C_{98.504}$**(45.83)**, $^{\#}$SO(0.02)	100.03
53	$^{53}Cr_{9.501}$**(92.36)**, $^{40}Ar^{13}C_{1.096}$(7.66)	100.02
54	$^{54}Fe_{5.845}$**(102.62)**, $^{54}Cr_{2.365}$(0.22)	102.84
55	$^{55}Mn_{100}$**(99.99)**	99.99
56	$^{56}Fe_{91.754}$**(104.09)**	104.09

57	**$^{57}Fe_{2.119}$(97.99)**	97.99
58	**$^{58}Fe_{0.282}$(60.78)**, **$^{58}Ni_{68\ 077}$(32.45)**	93.23
59	**$^{59}Co_{100}$(99.98)**	99.98
60	**$^{60}Ni_{26.223}$(104.73)**	104.73
61	**$^{61}Ni_{1.140}$(89.66)**	89.66
62	**$^{62}Ni_{3.634}$(92.54)**	92.54
63	**$^{63}Cu_{69.173}$(102.68)**	102.68
64	**$^{64}Zn_{48.636}$(109.00)**, $^{64}Ni_{0\ 926}$(0.02)	109.02
65	**$^{65}Cu_{30.833}$(96.65)**	96.65
66	**$^{66}Zn_{27.903}$(101.16)**	101.16
67	**$^{67}Zn_{4.101}$(94.38)**, $^{134}Ba^{++}{}_{2\ 420}$(0.02), $^{36}Ar^{14}N^{16}OH_{0\ 338}$(0.01)	94.41
68	**$^{68}Zn_{18.755}$(94.80)**, $^{136}Ba^{++}{}_{7\ 850}$(0.01)	94.81
69	**$^{138}Ba^{++}{}_{71.700}$(99.76)**, $^{38}Ar^{14}N^{16}OH_{0\ 060}$(0.23), $^{36}Ar^{16}O^{16}OH_{0\ 338}$(0.03)	100.02

70	**$^{70}Zn_{0.623}$(82.82)**, $^{40}Ar^{14}N^{16}O_{98\ 993}$(17.19)	100.01
71	**$^{40}Ar^{14}N^{16}OH_{98.983}$(99.41)**, #ArNO(0.60)	100.01
72	**$^{40}Ar^{32}S_{94.640}$(86.25)**, $^{36}Ar^{36}Ar_{0\ 001}$(9.57), #ArNOH(1.49), $^{40}Ar^{14}N^{18}O_{0\ 198}$(1.06)	98.37
73	**$^{40}Ar^{16}O^{18}OH_{99.113}$(85.15)**, $^{40}Ar^{14}N^{18}OH_{0\ 198}$(7.32), $^{40}Ar^{33}S_{0\ 747}$(7.01), $^{36}Ar^{36}ArH_{0\ 001}$(0.13), #ArNO(0.04)	99.65
74	**$^{74}Se_{0.894}$(72.68)**, $^{40}Ar^{34}S_{4\ 193}$(20.60), #ArOOH(0.04), #ArNOH(0.02)	93.34
75	**$^{75}As_{100}$(100.04)**, $^{40}Ar^{16}O^{18}OH_{0\ 397}$(0.03)	100.07
76	$^{76}Se_{9\ 373}$(2.29), **$^{36}Ar^{40}Ar_{0.677}$(99.35)**	101.64
77	**$^{77}Se_{7.632}$(98.41)**, $^{36}Ar^{40}ArH_{0\ 677}$(6.83)	105.24
78	$^{78}Se_{23\ 773}$(23.69), $^{78}Kr_{0\ 351}$(0.02), **$^{38}Ar^{40}Ar_{0.120}$(73.13)**	96.84
79	**$^{79}Br_{50.697}$(100.16)**, $^{38}Ar^{40}ArH_{0\ 120}$(0.10)	100.26
81	**$^{81}Br_{49.317}$(55.21)**, **$^{40}Ar^{40}ArH_{99.192}$(42.95)**, $^{36}Ar^{45}Sc_{0\ 340}$(1.50)	99.66
82	**$^{82}Se_{8\ 732}$(93.46)**, $^{82}Kr_{11\ 581}$(5.64), $^{40}Ar^{40}Ar^{2}H_{0\ 020}$(0.12)	99.22
83	**$^{83}Kr_{11.496}$(51.94)**, **$^{38}Ar^{45}Sc_{0\ 060}$(48.07)**	100.01

84	**$^{84}Sr_{0.561}$(28.36), $^{84}Kr_{57.004}$(71.63)**	99.99
85	**$^{85}Rb_{72.172}$(70.13)**, $^{69}Ga^{16}O_{59\ 956}$(23.10), $^{40}Ar^{45}Sc_{99\ 600}$(6.77)	100.00
86	**$^{86}Sr_{9.861}$(84.59)**, $^{86}Kr_{17\ 302}$(3.68), $^{36}Ar^{50}Cr_{0\ 015}$(7.13), $^{69}Ga^{17}O_{0\ 024}$(4.65), $^{\#}$ArV(0.09)	100.14
87	**$^{87}Rb_{27.832}$(63.47)**, $^{87}Sr_{7\ 001}$(0.27), **$^{71}Ga^{16}O_{39.804}$(36.10)**, $^{36}Ar^{51}V_{0\ 339}$(0.16)	100.00
88	**$^{88}Sr_{82\ 581}$(83.26)**, $^{\#}$ArCr(16.36), $^{71}Ga^{17}O_{0\ 016}$(0.36)	99.98

Table 3.3H. Possible interference's for mass bias corrected data of NIST 1577b - Bovine Liver

M/Z	Contributing Species	Σ of %
46	$^{46}Ca_{0.004}$(0.02), **$^{\#}$NNO(89.04)**	89.06
47	**$^{14}N^{16}O^{16}OH_{99.142}$(99.88)**, $^{14}N^{15}N^{18}O_{0.002}$(0.13)	100.01
48	$^{48}Ca_{0.187}$(0.25), **$^{31}P^{16}OH_{99.750}$(50.34)**, **$^{32}S^{16}O_{94.792}$(48.79)**, $^{\#}$NOOH(0.52), $^{36}Ar^{12}C_{0.336}$(0.09)	99.99
49	**$^{40}Ar^{9}Be_{99.600}$(40.55)**, **$^{14}N^{16}O^{18}OH_{0.398}$(30.47)**, **$^{\#}$SO(27.09)**, $^{\#}$POH(1.79), $^{36}Ar^{13}C_{0.004}$(0.07)	99.97
50	**$^{50}Cr_{4.345}$(33.35)**, $^{50}V_{0.250}$(0.48), **$^{34}S^{16}O_{4.120}$(58.46)**, $^{36}Ar^{14}N_{0.339}$(4.60), $^{31}P^{18}OH_{0.200}$(2.61), $^{38}Ar^{12}C_{0.059}$(0.45)	99.95
51	**$^{51}V_{99.750}$(99.97)**, $^{\#}$SO(0.02), $^{36}Ar^{15}N_{0.001}$(0.01)	100.00
52	**$^{52}Cr_{83.789}$(47.44)**, **$^{40}Ar^{12}C_{98.504}$(52.46)**, $^{38}Ar^{14}N_{0.060}$(0.06), $^{\#}$SO(0.03)	100.00
53	**$^{53}Cr_{9.501}$(90.22)**, $^{40}Ar^{13}C_{1.096}$(9.79)	100.01
54	**$^{54}Fe_{5.845}$(81.68)**, $^{54}Cr_{2.365}$(0.24), $^{40}Ar^{14}N_{99.231}$(18.09)	100.01
55	**$^{55}Mn_{100}$(99.93)**, $^{40}Ar^{15}N_{0.368}$(0.07)	100.00
56	**$^{56}Fe_{91.754}$(99.85)**	99.85

57	$^{57}Fe_{2.119}$(102.25)	102.25
58	$^{58}Fe_{0.282}$(68.60), $^{58}Ni_{68.077}$(27.25)	95.85
59	$^{59}Co_{100}$(100.00)	100.00
60	$^{60}Ni_{26.223}$(101.19)	101.19
61	$^{61}Ni_{1.140}$(92.17)	92.17
62	$^{62}Ni_{3.634}$(100.70)	100.70
63	$^{63}Cu_{69.173}$(98.57)	98.57
64	$^{64}Zn_{48\ 636}$(100.31), $^{64}Ni_{0\ 926}$(0.02)	100.33
65	$^{65}Cu_{30\ 833}$(101.57)	101.57
66	$^{66}Zn_{27.903}$(101.02)	101.02
67	$^{67}Zn_{4.101}$(97.58), $^{134}Ba^{++}{}_{2\ 420}$(0.02), $^{38}Ar^{14}N^{16}OH_{0\ 338}$(0.01)	97.61
68	$^{68}Zn_{18\ 755}$(101.09), $^{136}Ba^{++}{}_{7\ 850}$(0.01)	101.10
69	$^{138}Ba^{++}{}_{71.700}$(99.97), $^{38}Ar^{14}N^{16}OH_{0\ 060}$(0.22), $^{36}Ar^{16}O^{16}OH_{0\ 338}$(0.03)	100.22

70	**$^{70}Zn_{0.623}$(92.94)**, $^{40}Ar^{14}N^{16}O_{98\ 993}$(7.07)	100.01
71	**$^{40}Ar^{14}N^{16}OH_{98.983}$(99.73)**, $^{\#}$ArNO(0.25)	99.98
72	**$^{40}Ar^{32}S_{94\ 640}$(87.62)**, $^{36}Ar^{36}Ar_{0\ 001}$(9.12), $^{\#}$ArNOH(1.52), $^{40}Ar^{14}N^{18}O_{0\ 198}$(0.45)	98.71
73	**$^{40}Ar^{16}O^{16}OH_{99.113}$(88.95)**, $^{40}Ar^{14}N^{18}OH_{\ 0\ 198}$(7.59), $^{40}Ar^{33}S_{0\ 747}$(7.23), $^{36}Ar^{36}ArH_{0\ 001}$(0.13), $^{\#}$ArNO(0.02)	103.92
74	**$^{74}Se_{0.894}$(70.28)**, $^{40}Ar^{34}S_{4\ 193}$(21.50), $^{\#}$ArOOH(0.04), $^{\#}$ArNOH(0.02)	91.84
75	**$^{75}As_{100}$(99.94)**, $^{40}Ar^{16}O^{18}OH_{0\ 397}$(0.03)	99.97
76	$^{76}Se_{9\ 373}$(2.26), **$^{36}Ar^{40}Ar_{0.677}$(99.12)**	101.38
77	**$^{77}Se_{7.632}$(97.54)**, $^{36}Ar^{40}ArH_{0\ 677}$(6.77)	104.31
78	$^{78}Se_{23\ 773}$(23.60), $^{78}Kr_{0\ 351}$(0.02), **$^{38}Ar^{40}Ar_{0.120}$(73.77)**	97.39
79	**$^{79}Br_{50.697}$(100.09)**, $^{38}Ar^{40}ArH_{0\ 120}$(0.10)	100.19
81	**$^{81}Br_{49.317}$(55.24)**, **$^{40}Ar^{40}ArH_{99.192}$(43.00)**, $^{36}Ar^{45}Sc_{0\ 340}$(1.50)	99.74
82	**$^{82}Se_{8.732}$(93.60)**, $^{82}Kr_{11\ 581}$(5.67), $^{40}Ar^{40}Ar^{2}H_{0\ 020}$(0.12)	99.39
83	**$^{83}Kr_{11.496}$(52.24)**, **$^{38}Ar^{45}Sc_{0\ 060}$(48.02)**	100.26

84	**$^{84}Sr_{0.561}$(28.29), $^{84}Kr_{57.004}$(72.04)**	100.33
85	**$^{85}Rb_{72.172}$(70.83),** $^{69}Ga^{16}O_{59.956}$(22.40), $^{40}Ar^{45}Sc_{99.600}$(6.77)	100.00
86	**$^{86}Sr_{9.861}$(84.44),** $^{86}Kr_{17.302}$(3.71), $^{36}Ar^{50}Cr_{0.015}$(7.07), $^{69}Ga^{17}O_{0.024}$(4.51)	99.73
87	**$^{87}Rb_{27.832}$(64.20),** $^{87}Sr_{7.001}$(0.27), **$^{71}Ga^{16}O_{39.804}$(35.06),** $^{36}Ar^{51}V_{0.339}$(0.47)	100.00
88	**$^{88}Sr_{82.581}$(83.35),** $^{\#}$ArCr(16.27), $^{71}Ga^{17}O_{0.016}$(0.35)	99.97

= Ions with more than one possible combinations of isotopes and with similar abundances.

$^{X}M_{Y}(Z)$

X = The atomic weight for the species M.

Y = The relative abundance for the species M.

Z = The contribution from species M at this mass.

3.4.2. Isotope ratios

Tables 3.4A-D show the % of the error in the isotopic ratio (ISR) for the 100ppb standard solution, TORT 1, NIST 1547 and NIST 1577b which have been corrected for elemental, molecular ions and mass bias contributions.

The MI algorithm makes use of the known isotopic abundances to synthesise the mock spectrum and therefore in its current form it cannot be used to measure unknown isotopic ratios. However, it has been found that re-calculating ratios from the final data is the most powerful method of checking the validity of the predicted spectrum. Where a perfect prediction for all the significant ratios of a particular element has occurred, a calibration based on the total counts for an elemental species works well and provides accurate analytical data. Some elements however were less well determined using this simple procedure. A closer look at the data revealed that in such cases, one or more of the isotope ratios, calculated from the measured counts minus the molecular ion contributions were divergent from the accepted values. These differences can be seen in some minor isotopes, mainly in raw data, e.g. ^{58}Fe and ^{64}Ni in 100ppb standard solution, ^{54}Cr and ^{64}Ni in TORT 1 and NIST 1547 and ^{57}Fe and ^{58}Fe in NIST 1577b. The ISR's for Se in the 100ppb standard solution and biological samples are different from the reported values. These differences might be due to the spectrum not being accurately predicted at these masses or due to not measuring m/z = 80. Of course, gross errors involving very minor isotopes are less important than errors involving major isotopes. Further, elements with many isotopes (e.g. Cr and Zn) are expected to be more affected than those having only one pair of major isotopes. A re-calibration based on the calculated isotopic contribution at one mass (after subtraction of the molecular ion contribution) provided some improvements in analytical data. Examples are Zn, Rb and Sr where calibration based on ^{68}Zn (18.8% abundant), ^{87}Rb (27.8% abundant) and ^{88}Sr (82.6% abundant) reduced the analytical error by more than 7% in

TORT 1, 25% in NIST 1547 and 10% in the NIST 1577b samples respectively. There are a few cases, however, where the analytical error is increased. An example is Zn where calibration based on ^{68}Zn (18.8% abundant) increased the analytical error by less than 5% and 7% in NIST 1547 and NIST 1577b samples respectively.

The reasons for this are that poor prediction of the elemental count at a particular mass propagates into the total count and this carries through into the calibration and analysis procedure. This arises from the use of an incorrect menu of species. However, there will always be uncertainty about the exact molecular ion composition and a robust method should accommodate this.

These observations indicate that a safe mode of applying any multivariate procedure is to synthesise the spectrum and use for analysis only those isotopes for which accurate isotopic ratios are predicted. This is not to imply that the predicted elemental count is discarded as it has already been used to find the most probable spectrum.

Table 3.4A. Isotopic ratio (ISR) calculations for 100ppb standard solution (See end of Table 3.4D for description of column coding)

	ISR 1	ISR 2	% of Error in ISR 2	ISR3	% of Error in ISR 3	ISR 4	% of Error in ISR 4
$^{47}Ti_{7\ 442}/^{46}Ti_{8\ 253}$	0.90	0.66	-27	0.90	0.0	0.89	-1.1
$^{48}Ti_{73\ 723}/^{47}Ti_{7\ 442}$	9.91	10.9	10	10.1	1.9	10.1	1.9
$^{49}Ti_{5\ 412}/^{48}Ti_{73\ 723}$	0.07	0.08	14	0.08	14	0.08	14
$^{50}Ti_{5\ 182}/^{49}Ti_{5\ 412}$	0.96	0.98	2.2	0.98	2.1	0.98	2.1
$^{48}Ti_{73\ 723}/^{46}Ti_{8\ 253}$	8.93	7.23	-19	9.05	1.3	9.05	1.3
$^{49}Ti_{5\ 412}/^{47}Ti_{7\ 442}$	0.73	0.88	21	0.78	6.8	0.76	4.1
$^{50}Ti_{5.182}/^{48}Ti_{73\ 723}$	0.07	0.08	14	0.07	0.0	0.07	0.0
$^{49}Ti_{5\ 412}/^{46}Ti_{8\ 253}$	0.66	0.58	-11	0.68	3.0	0.68	3.0
$^{50}Ti_{5\ 182}/^{47}Ti_{7\ 442}$	0.70	0.86	23	0.74	5.7	0.74	5.7
$^{50}Ti_{5\ 182}/^{46}Ti_{8\ 253}$	0.63	0.57	-10	0.66	4.8	0.66	4.8
$^{51}V_{99\ 750}/^{50}V_{0\ 250}$	399	84.7	-79	413	3.5	429	7.5
$^{53}Cr_{9\ 501}/^{52}Cr_{83\ 789}$	0.11	0.13	18	0.11	0.0	0.11	0.0
$^{54}Cr_{2\ 365}/^{53}Cr_{9\ 501}$	0.25	1.54	516	0.25	0.0	0.25	0.0
$^{52}Cr_{83\ 789}/^{50}Cr_{4\ 345}$	19.3	16.0	-17	19.3	0.0	19.4	0.5
$^{54}Cr_{2\ 365}/^{52}Cr_{83\ 789}$	0.03	0.20	567	0.03	0.0	0.03	0.0
$^{53}Cr_{9\ 501}/^{50}Cr_{4\ 345}$	2.19	2.03	-7.3	2.19	0.0	2.21	0.9

$^{54}Cr_{2\ 365}/^{50}Cr_{4\ 345}$	0.54	3.13	480	0.55	1.8	0.54	0.0
$^{57}Fe_{2.119}/^{56}Fe_{91\ 754}$	0.02	0.01	-50	0.02	0.0	0.02	0.0
$^{58}Fe_{0\ 282}/^{57}Fe_{2\ 119}$	0.13	0.31	138	0.06	-54	0.61	369
$^{56}Fe_{91\ 754}/^{54}Fe_{5\ 845}$	15.7	12.2	-22	15.8	0.6	15.8	0.6
$^{58}Fe_{0\ 282}/^{56}Fe_{91\ 754}$	0.003	0.004	33	0.002	-33	0.01	233
$^{57}Fe_{2\ 119}/^{54}Fe_{5\ 845}$	0.36	0.15	-58	0.38	5.6	0.38	5.6
$^{58}Fe_{0\ 282}/^{54}Fe_{5\ 845}$	0.05	0.05	0.0	0.02	-60	0.23	360
$^{61}Ni_{1\ 140}/^{60}Ni_{26\ 223}$	0.04	0.05	25	0.04	0.0	0.05	25
$^{62}Ni_{3\ 634}/^{61}Ni_{1.140}$	3.19	3.28	2.8	3.18	-0.3	2.96	-7.2
$^{60}Ni_{26\ 223}/^{58}Ni_{68\ 077}$	0.39	0.41	5.1	0.38	-2.6	0.37	-5.1
$^{62}Ni_{3.634}/^{60}Ni_{26\ 223}$	0.14	0.15	7.1	0.14	0.0	0.14	0.0
$^{64}Ni_{0\ 926}/^{62}Ni_{3\ 634}$	0.26	0.17	-35	0.15	-42	0.26	0.0
$^{61}Ni_{1\ 140}/^{58}Ni_{68\ 077}$	0.02	0.02	0.0	0.02	0.0	0.02	0.0
$^{64}Ni_{0\ 926}/^{61}Ni_{1\ 140}$	0.81	0.55	-32	0.47	-42	0.76	-6.2
$^{62}Ni_{3\ 634}/^{58}Ni_{68\ 077}$	0.05	0.06	20	0.05	0.0	0.05	0.0
$^{64}Ni_{0\ 926}/^{60}Ni_{26\ 223}$	0.04	0.03	-25	0.02	-50	0.04	0.0
$^{64}Ni_{0\ 926}/^{58}Ni_{68\ 077}$	0.01	0.01	0.0	0.008	-20	0.01	0.0
$^{65}Cu_{30\ 833}/^{63}Cu_{69\ 173}$	0.45	0.49	9.0	0.45	0.0	0.45	0.0
$^{67}Zn_{4\ 101}/^{66}Zn_{27\ 903}$	0.15	0.20	33	0.15	0.0	0.15	0.0

$^{68}Zn_{18\ 755}/^{67}Zn_{4.101}$	4.57	3.77	-18	4.57	0.0	4.63	1.3
$^{66}Zn_{27\ 903}/^{64}Zn_{48\ 636}$	0.57	0.59	3.5	0.59	3.5	0.57	0.0
$^{68}Zn_{18\ 755}/^{66}Zn_{27\ 903}$	0 67	0.76	13	0.67	0.0	0.68	1.5
$^{70}Zn_{0\ 623}/^{68}Zn_{18\ 755}$	0.03	0.04	33	0.03	0.0	0.03	0.0
$^{67}Zn_{4\ 101}/^{64}Zn_{48\ 636}$	0.08	0.12	50	0.09	12.5	0.08	0.0
$^{70}Zn_{0\ 623}/^{67}Zn_{4\ 101}$	0.15	0.17	13	0.14	-6.7	0.13	-13
$^{68}Zn_{18\ 755}/^{64}Zn_{48\ 636}$	0.39	0.45	15	0.39	0.0	0.39	0.0
$^{70}Zn_{0\ 623}/^{66}Zn_{27\ 903}$	0.02	0.03	50	0.02	0.0	0.02	0.0
$^{70}Zn_{0\ 623}/^{64}Zn_{48\ 636}$	0.01	0.02	100	0.02	100	0.01	0.0
$^{71}Ga_{39\ 892}/^{69}Ga_{60\ 108}$	0.66	0.68	3.0	0.67	1.5	0.67	1.5
$^{73}Ge_{7\ 735}/^{72}Ge_{27\ 543}$	0.28	0.29	3.6	0.28	0.0	0.28	0.0
$^{74}Ge_{36\ 287}/^{73}Ge_{7\ 735}$	4.69	4.82	2.8	4.70	0.2	4.69	0.0
$^{72}Ge_{27\ 543}/^{70}Ge_{21\ 848}$	1.26	1.43	14	1.34	6.4	1.37	8.7
$^{74}Ge_{36\ 287}/^{72}Ge_{27\ 543}$	1.32	1.41	6.8	1.34	1.5	1.33	0.8
$^{76}Ge_{7\ 614}/^{74}Ge_{36\ 287}$	0.21	0.41	95	0.21	0.0	0.21	0.0
$^{73}Ge_{7\ 735}/^{70}Ge_{21\ 848}$	0.35	0.42	20	0.38	8.6	0.39	11
$^{76}Ge_{7\ 614}/^{73}Ge_{7\ 735}$	0.98	1.99	103	1.00	2.0	1.00	2.0
$^{74}Ge_{36\ 287}/^{70}Ge_{21\ 848}$	1.66	2.01	21	1.79	7.8	1.83	10
$^{76}Ge_{7\ 614}/^{72}Ge_{27\ 543}$	0.28	0.58	107	0.28	0.0	0.28	0.0

$^{76}Ge_{7.614}/^{70}Ge_{21.848}$	0.35	0.83	137	0.38	8.6	0.39	11
$^{77}Se_{7.632}/^{76}Se_{9.373}$	0.81	0.10	-88	0.86	6.2	0.85	4.9
$^{78}Se_{23.773}/^{77}Se_{7.632}$	3.12	4.67	50	3.23	3.5	3.20	2.6
$^{76}Se_{9.373}/^{74}Se_{0.894}$	10.5	2.06	-80	4.83	-54	5.89	-44
$^{78}Se_{23.773}/^{76}Se_{9.373}$	2.54	0.46	-82	2.78	9.4	2.72	7.1
$^{77}Se_{7.632}/^{74}Se_{0.894}$	8.54	0.20	-98	4.14	-52	5.01	-41
$^{78}Se_{23.773}/^{74}Se_{0.894}$	26.6	0.94	-96	13.4	-50	16.0	-40
$^{82}Se_{8.732}/^{78}Se_{23.773}$	0.37	0.29	-22	0.41	11	0.42	14
$^{82}Se_{8.732}/^{77}Se_{7.632}$	1.14	1.35	18	1.33	17	1.32	16
$^{82}Se_{8.732}/^{76}Se_{9.373}$	0.93	0.13	-86	1.14	23	1.12	20
$^{82}Se_{8.732}/^{74}Se_{0.894}$	9.77	0.27	-97	1.14	-88	1.12	-88
$^{87}Rb_{27.832}/^{85}Rb_{72.172}$	0.39	0.43	10	0.39	0.0	0.39	0.0
$^{87}Sr_{7.001}/^{86}Sr_{9.861}$	0.71	1.18	66	0.70	-1.4	0.69	-2.8
$^{88}Sr_{82.581}/^{87}Sr_{7.001}$	11.8	7.00	-41	11.8	0.0	11.8	0.0
$^{86}Sr_{9.861}/^{84}Sr_{0.561}$	17.6	17.9	1.7	18.3	4.0	18.3	4.0
$^{88}Sr_{82.581}/^{86}Sr_{9.861}$	8.38	8.24	-1.7	8.18	-2.4	8.15	-2.7
$^{87}Sr_{7.001}/^{84}Sr_{0.561}$	12.5	21.0	68	12.7	1.6	12.7	1.6
$^{88}Sr_{82.581}/^{84}Sr_{0.561}$	147	147	0.0	150	2.0	149	1.4

Table 3.4B. Isotopic ratio (ISR) calculations for TORT 1 - Lobster Hepatopancreas Marine (See end of Table 3.4D for description of column coding)

	ISR 1	ISR 2	% of Error in ISR 2	ISR3	% of Error in ISR 3	ISR 4	% of Error in ISR 4
$^{47}Ti_{7\ 442}/^{46}Ti_{8\ 253}$	0.90	1.85	106	0.88	-2.2	0.91	1.1
$^{48}Ti_{73\ 723}/^{47}Ti_{7\ 442}$	9.91	14.3	44	10.5	6.0	10.2	2.9
$^{49}Ti_{5\ 412}/^{48}Ti_{73\ 723}$	0.07	0.003	-96	0.07	0.0	0.07	0.0
$^{50}Ti_{5\ 182}/^{49}Ti_{5\ 412}$	0.96	1.30	35	0.91	-5.2	0.98	2.1
$^{48}Ti_{73\ 723}/^{46}Ti_{8\ 253}$	8.93	26.4	196	9.21	3.1	9.21	3.1
$^{49}Ti_{5\ 412}/^{47}Ti_{7\ 442}$	0.73	0.05	-93	0.77	5.5	0.75	2.7
$^{50}Ti_{5\ 182}/^{48}Ti_{73\ 723}$	0.07	0.004	-94	0.07	0.0	0.07	0.0
$^{49}Ti_{5\ 412}/^{46}Ti_{8\ 253}$	0.66	0.08	-88	0.68	3.0	0.68	3.0
$^{50}Ti_{5\ 182}/^{47}Ti_{7\ 442}$	0.70	0.06	-91	0.70	0.0	0.74	5.7
$^{50}Ti_{5.182}/^{46}Ti_{8\ 253}$	0.63	0.11	-82	0.62	-1.6	0.67	6.4
$^{51}V_{99\ 750}/^{50}V_{0\ 250}$	399	29.6	-93	3925	884	400	0.2
$^{53}Cr_{9\ 501}/^{52}Cr_{83\ 789}$	0.11	0.11	0.0	0.11	0.0	0.11	0.0
$^{54}Cr_{2\ 365}/^{53}Cr_{9\ 501}$	0.25	0.84	236	0.84	236	0.25	0.0
$^{52}Cr_{83\ 789}/^{50}Cr_{4\ 345}$	19.3	15.2	-21	20.3	5.2	19.3	0.0
$^{54}Cr_{2\ 365}/^{52}Cr_{83\ 789}$	0.03	0.09	200	0.09	200	0.03	0.0
$^{53}Cr_{9\ 501}/^{50}Cr_{4\ 345}$	2.19	1.64	-25	2.21	0.9	2.19	0.0

$^{54}Cr_{2\ 365}/^{50}Cr_{4\ 345}$	0.54	1.38	156	1.86	244	0.54	0.0
$^{57}Fe_{2\ 119}/^{56}Fe_{91\ 754}$	0.02	0.03	50	0.02	0.0	0.02	0.0
$^{58}Fe_{0\ 282}/^{57}Fe_{2\ 119}$	0.13	0.09	-31	0.12	-7.7	0.13	0.0
$^{56}Fe_{91.754}/^{54}Fe_{5\ 845}$	15.7	15.6	-0.6	15.6	-0.6	15.9	1.3
$^{58}Fe_{0\ 282}/^{56}Fe_{91\ 754}$	0.003	0.003	0.0	0.003	0.0	0.003	0.0
$^{57}Fe_{2\ 119}/^{54}Fe_{5\ 845}$	0.36	0.47	31	0.37	2.8	0.38	5.6
$^{58}Fe_{0\ 282}/^{54}Fe_{5\ 845}$	0.05	0.04	-20	0.04	-20	0.05	0.0
$^{61}Ni_{1.140}/^{60}Ni_{26\ 223}$	0.04	0.09	125	0.04	0.0	0.04	0.0
$^{62}Ni_{3\ 634}/^{61}Ni_{1\ 140}$	3.19	2.49	-22	3.49	9.4	3.18	-0.3
$^{60}Ni_{26\ 223}/^{58}Ni_{68\ 077}$	0.39	0.40	2.6	0.40	2.6	0.38	-2.6
$^{62}Ni_{3\ 634}/^{60}Ni_{26\ 223}$	0.14	0.23	64	0.15	7.1	0.14	0.0
$^{64}Ni_{0\ 926}/^{62}Ni_{3\ 634}$	0.26	10.7	4015	20.7	7862	0.76	192
$^{61}Ni_{1\ 140}/^{58}Ni_{68\ 077}$	0.02	0.04	100	0.02	0.0	0.02	0.0
$^{64}Ni_{0\ 926}/^{61}Ni_{1\ 140}$	0.81	26.6	3184	72.3	8826	2.40	196
$^{62}Ni_{3\ 634}/^{58}Ni_{68\ 077}$	0.05	0.09	80	0.06	20	0.05	0.0
$^{64}Ni_{0\ 926}/^{60}Ni_{26\ 223}$	0.04	2.42	5950	3.13	7725	0.11	175
$^{64}Ni_{0\ 926}/^{58}Ni_{68\ 077}$	0.01	0.98	9700	1.26	12500	0.04	300
$^{65}Cu_{30\ 833}/^{63}Cu_{69\ 173}$	0.45	0.47	5.7	0.44	-2.2	0.43	-4.4
$^{67}Zn_{4\ 101}/^{66}Zn_{27\ 903}$	0.15	0.16	6 7	0.14	-6.7	0.15	0.0

$^{68}Zn_{18.755}/^{67}Zn_{4.101}$	4.57	4.53	-0.9	4.96	8.5	4.52	-1.1
$^{66}Zn_{27.903}/^{64}Zn_{48.636}$	0.57	0.61	7.0	0.62	8.8	0.57	0.0
$^{68}Zn_{18.755}/^{66}Zn_{27.903}$	0 67	0.72	7.5	0.72	7.5	0.68	1.5
$^{70}Zn_{0.623}/^{68}Zn_{18.755}$	0.03	0.05	67	0.03	0.0	0.03	0.0
$^{67}Zn_{4.101}/^{64}Zn_{48.636}$	0.08	0.10	25	0.09	12	0.09	12
$^{70}Zn_{0.623}/^{67}Zn_{4.101}$	0.15	0.21	40	0.15	0.0	0.14	-6.7
$^{68}Zn_{18.755}/^{64}Zn_{48.636}$	0.39	0.44	13	0.45	15	0.39	0.0
$^{70}Zn_{0.623}/^{66}Zn_{27.903}$	0.02	0.03	50	0.02	0.0	0.02	0.0
$^{70}Zn_{0.623}/^{64}Zn_{48.636}$	0.01	0.02	100	0.01	0.0	0.01	0.0
$^{77}Se_{7.632}/^{76}Se_{9.373}$	0.81	0.11	-86	0.02	-98	0.81	0.0
$^{78}Se_{23.773}/^{77}Se_{7.632}$	3.12	4.95	59	6.44	106	3.41	9.3
$^{76}Se_{9.373}/^{74}Se_{0.894}$	10.5	54.6	420	334	3081	9.82	-6.5
$^{78}Se_{23.773}/^{76}Se_{9.373}$	2.54	0.52	-80	0.12	-95	2.78	9.4
$^{77}Se_{7.632}/^{74}Se_{0.894}$	8.54	5.77	-32	6.48	-24	8.00	-6.3
$^{78}Se_{23.773}/^{74}Se_{0.894}$	26.6	28.6	7.5	41.8	57	27.3	2.6
$^{82}Se_{8.732}/^{78}Se_{23.773}$	0.37	0.29	-22	0.02	-95	0.41	11
$^{82}Se_{8.732}/^{77}Se_{7.632}$	1.14	1.43	25	0.15	-87	1.41	24
$^{82}Se_{8.732}/^{76}Se_{9.373}$	0.93	0.15	-84	0.003	-100	1.15	24
$^{82}Se_{8.732}/^{74}Se_{0.894}$	9.77	0.15	-98	0.003	-100	11.3	16

$^{87}Sr_{7.001}/^{86}Sr_{9.861}$	0.71	0.73	2.8	0.72	1.4	0.72	1.4
$^{88}Sr_{82.581}/^{87}Sr_{7.001}$	11.8	11.2	-5.1	11.4	-3.4	11.4	-3.4
$^{86}Sr_{9.861}/^{84}Sr_{0.561}$	17.6	17.2	-2.3	17.0	-3.4	17.0	-3.4
$^{88}Sr_{82.581}/^{86}Sr_{9.861}$	8.38	8.20	-2.2	8.17	-2.5	8.15	-2.7
$^{87}Sr_{7.001}/^{84}Sr_{0.561}$	12.5	12.6	0.8	12.2	-2.4	12.2	-2.4
$^{88}Sr_{82.581}/^{84}Sr_{0.561}$	147	141	-4.1	139	-5.4	138	-6.1

Table 3.4C. Isotopic ratio (ISR) calculations for NIST 1547 - Peach Leaves (See end of Table 3.4D for description of column coding)

	ISR 1	ISR 2	% of Error in ISR 2	ISR3	% of Error in ISR 3	ISR 4	% of Error in ISR 4
$^{51}V_{99.750}/^{50}V_{0.250}$	399	1.54	-100	397	-0.5	385	-3.5
$^{53}Cr_{9.501}/^{52}Cr_{83.789}$	0.11	0.10	-9.1	0.11	0.0	0.11	0.0
$^{54}Cr_{2.365}/^{53}Cr_{9.501}$	0.25	0.32	28	0.32	28	0.25	0.0
$^{52}Cr_{83.789}/^{50}Cr_{4.345}$	19.3	3.91	-80	19.3	0.0	19.3	0.0
$^{54}Cr_{2.365}/^{52}Cr_{83.789}$	0.03	0.03	0.0	0.04	33	0.03	0.0
$^{53}Cr_{9.501}/^{50}Cr_{4.345}$	2.19	0.40	-82	2.19	0.0	2.18	-0.5
$^{54}Cr_{2.365}/^{50}Cr_{4.345}$	0.54	0.13	-76	0.71	32	0.54	0.0
$^{57}Fe_{2.119}/^{56}Fe_{91.754}$	0.02	0.03	50	0.02	0.0	0.02	0.0
$^{58}Fe_{0.282}/^{57}Fe_{2.119}$	0.13	0.10	-23	0.14	7.7	0.13	0.0
$^{56}Fe_{91.754}/^{54}Fe_{5.845}$	15.7	16.0	1.9	15.8	0.6	15.8	0.6
$^{58}Fe_{0.282}/^{56}Fe_{91.754}$	0.003	0.003	0.0	0.003	0.0	0.003	0.0
$^{57}Fe_{2.119}/^{54}Fe_{5.845}$	0.36	0.55	53	0.37	2.8	0.38	5.6
$^{58}Fe_{0.282}/^{54}Fe_{5.845}$	0.05	0.05	0.0	0.05	0.0	0.05	0.0
$^{61}Ni_{1.140}/^{60}Ni_{26.223}$	0.04	0.28	600	0.05	25	0.05	25
$^{62}Ni_{3.634}/^{61}Ni_{1.140}$	3.19	0.36	-89	2.55	-20	2.98	-6.6
$^{60}Ni_{26.223}/^{58}Ni_{68.077}$	0.39	0.46	18	0.36	-7.7	0.37	-5.1

$^{62}Ni_{3.634}/^{60}Ni_{26.223}$	0.14	0.10	-29	0.14	0.0	0.14	0.0
$^{64}Ni_{0.926}/^{62}Ni_{3.634}$	0.26	1.72	562	1.95	650	0.26	0.0
$^{61}Ni_{1.140}/^{58}Ni_{68.077}$	0.02	0.13	550	0.02	0.0	0.02	0.0
$^{64}Ni_{0.926}/^{61}Ni_{1.140}$	0.81	0.62	-24	4.96	512	0.77	-4.9
$^{62}Ni_{3.634}/^{58}Ni_{68.077}$	0.05	0.05	0.0	0.05	0.0	0.05	0.0
$^{64}Ni_{0.926}/^{60}Ni_{26.223}$	0.04	0.18	350	0.26	550	0.04	0.0
$^{64}Ni_{0.926}/^{58}Ni_{68.077}$	0.01	0.08	700	0.09	800	0.01	0.0
$^{65}Cu_{30.833}/^{63}Cu_{69.173}$	0.45	0.49	8.9	0.44	-2.2	0.44	-2.2
$^{67}Zn_{4.101}/^{66}Zn_{27.903}$	0.15	0.25	67	0.15	0.0	0.15	0.0
$^{68}Zn_{18.755}/^{67}Zn_{4.101}$	4.57	4.12	-9.9	4.76	4.2	4.44	-2.8
$^{66}Zn_{27.903}/^{64}Zn_{48.636}$	0.57	0.59	3.5	0.59	3.5	0.57	0.0
$^{68}Zn_{18.755}/^{66}Zn_{27.903}$	0.67	1.01	51	0.70	4.5	0.67	0.0
$^{70}Zn_{0.623}/^{68}Zn_{18.755}$	0.03	0.17	467	0.03	0.0	0.03	0.0
$^{67}Zn_{4.101}/^{64}Zn_{48.636}$	0.08	0.14	75	0.09	12	0.08	0.0
$^{70}Zn_{0.623}/^{67}Zn_{4.101}$	0.15	0.70	367	0.14	-6.7	0.15	0.0
$^{68}Zn_{18.755}/^{64}Zn_{48.636}$	0.39	0.60	54	0.41	5.1	0.38	-2.6
$^{70}Zn_{0.623}/^{66}Zn_{27.903}$	0.02	0.17	750	0.02	0.0	0.02	0.0
$^{70}Zn_{0.623}/^{64}Zn_{48.636}$	0.01	0.10	900	0.01	0.0	0.01	0.0
$^{77}Se_{7.632}/^{76}Se_{9.373}$	0.81	0.01	-99	0.69	-15	0.86	6.2

$^{78}Se_{23\ 773}/^{77}Se_{7\ 632}$	3.12	19.4	522	4.83	55	4.62	48
$^{76}Se_{9\ 373}/^{74}Se_{0\ 894}$	10.5	286	2624	11.4	8.6	8.78	-16
$^{78}Se_{23\ 773}/^{76}Se_{9\ 373}$	2.54	0.21	-92	3.32	31	4.00	58
$^{77}Se_{7\ 632}/^{74}Se_{0\ 894}$	8.54	3.13	-63	7.82	-8.4	7.60	-11
$^{78}Se_{23\ 773}/^{74}Se_{0\ 894}$	26.6	60.6	128	37.8	42	35.1	32
$^{82}Se_{8\ 732}/^{78}Se_{23\ 773}$	0.37	0.04	-89	0.23	-38	0.24	-35
$^{82}Se_{8\ 732}/^{77}Se_{7\ 632}$	1.14	0.74	-35	1.09	-4.4	1.12	-1.8
$^{82}Se_{8\ 732}/^{76}Se_{9\ 373}$	0.93	0.01	-99	0.75	-19	0.96	3.2
$^{82}Se_{8\ 732}/^{74}Se_{0\ 894}$	9.77	0.01	-100	0.75	-92	0.96	-90
$^{87}Rb_{27\ 832}/^{85}Rb_{72\ 172}$	0.39	0.42	7.7	0.39	0.0	0.39	0.0
$^{87}Sr_{7\ 001}/^{86}Sr_{9\ 861}$	0.71	0.78	9.9	0.70	-1.4	0.70	-1.4
$^{88}Sr_{82\ 581}/^{87}Sr_{7\ 001}$	11.8	10.1	-14	11.3	-4.2	11.3	-4.2
$^{86}Sr_{9\ 861}/^{84}Sr_{0\ 561}$	17.6	17.7	0.6	18.0	2.3	18.0	2.3
$^{88}Sr_{82.581}/^{86}Sr_{9\ 861}$	8.38	7.89	-5.9	7.90	-5.7	7.88	-6.0
$^{87}Sr_{7\ 001}/^{84}Sr_{0\ 561}$	12.5	13.8	10	12.5	0.0	12.5	0.0
$^{88}Sr_{82\ 581}/^{84}Sr_{0\ 561}$	147	140	-4.8	142	-3.4	141	-4.1

Table 3.4D. Isotopic ratio (ISR) calculations for NIST 1577b - Bovine Liver

	ISR 1	ISR 2	% of Error in ISR 2	ISR3	% of Error in ISR 3	ISR 4	% of Error in ISR 4
$^{51}V_{99.750}/^{50}V_{0.250}$	399	4.20	-99	381	-4.5	399	0.0
$^{57}Fe_{2.119}/^{56}Fe_{91.754}$	0.02	0.03	50	0.03	50	0.02	0.0
$^{58}Fe_{0.282}/^{57}Fe_{2.119}$	0.13	0.14	7.7	0.14	7.7	0.14	7.7
$^{56}Fe_{91.754}/^{54}Fe_{5.845}$	15.7	15.6	-0.6	15.6	-0.6	15.8	0.6
$^{58}Fe_{0.282}/^{56}Fe_{91.754}$	0.003	0.004	33	0.004	33	0.003	0.0
$^{57}Fe_{2.119}/^{54}Fe_{5.845}$	0.36	0.40	11	0.40	11	0.37	2.8
$^{58}Fe_{0.282}/^{54}Fe_{5.845}$	0.05	0.06	20	0.06	20	0.05	0.0
$^{65}Cu_{30.833}/^{63}Cu_{69.173}$	0.45	0.47	4.4	0.47	4.4	0.43	-4.4
$^{67}Zn_{4.101}/^{66}Zn_{27.903}$	0.15	0.16	6.7	0.16	6.7	0.15	0.0
$^{68}Zn_{18.755}/^{67}Zn_{4.101}$	4.57	4.56	-0.2	4.57	0.0	4.43	-3.1
$^{66}Zn_{27.903}/^{64}Zn_{48.636}$	0.57	0.62	8.8	0.62	8.8	0.57	0.0
$^{68}Zn_{18.755}/^{66}Zn_{27.903}$	0.67	0.72	7.5	0.72	7.5	0.67	0.0
$^{70}Zn_{0.623}/^{68}Zn_{18.755}$	0.03	0.04	33	0.03	0.0	0.03	0.0
$^{67}Zn_{4.101}/^{64}Zn_{48.636}$	0.08	0.10	25	0.10	25	0.09	12
$^{70}Zn_{0.623}/^{67}Zn_{4.101}$	0.15	0.17	13	0.14	-6.7	0.14	-6.7
$^{68}Zn_{18.755}/^{64}Zn_{48.636}$	0.39	0.44	13	0.44	13	0.38	-2.6
$^{70}Zn_{0.623}/^{66}Zn_{27.903}$	0.02	0.03	50	0.02	0.0	0.02	0.0

$^{70}Zn_{0.623}/^{64}Zn_{48.636}$	0.01	0.02	100	0.01	0.0	0.01	0.0
$^{77}Se_{7.632}/^{76}Se_{9.373}$	0.81	0.02	-98	2.82	248	2.07	156
$^{78}Se_{23.773}/^{77}Se_{7.632}$	3.12	12.9	314	3.72	19	3.61	16
$^{76}Se_{9.373}/^{74}Se_{0.894}$	10.5	317	2919	3.40	-68	4.57	-56
$^{78}Se_{23.773}/^{76}Se_{9.373}$	2.54	0.25	-90	10.5	313	7.46	194
$^{77}Se_{7.632}/^{74}Se_{0.894}$	8.54	6.24	-27	9.59	12	9.44	10
$^{78}Se_{23.773}/^{74}Se_{0.894}$	26.6	80.4	202	35.6	34	34.1	28
$^{82}Se_{8.732}/^{78}Se_{23.773}$	0.37	0.10	-73	0.35	-5.4	0.35	-5.4
$^{82}Se_{8.732}/^{77}Se_{7.632}$	1.14	1.28	12	1.29	13	1.28	12
$^{82}Se_{8.732}/^{76}Se_{9.373}$	0.93	0.02	-98	3.63	290	2.64	184
$^{82}Se_{8.732}/^{74}Se_{0.894}$	9.77	0.02	-100	3.63	-63	2.64	-73
$^{87}Rb_{27.832}/^{85}Rb_{72.172}$	0.39	0.42	7.7	0.39	0.0	0.39	0.0
$^{87}Sr_{7.001}/^{86}Sr_{9.861}$	0.71	82.3	11492	0.72	1.4	0.70	-1.4
$^{88}Sr_{82.581}/^{87}Sr_{7.001}$	11.8	0.10	-99	11.6	-1.7	11.9	0.8
$^{86}Sr_{9.861}/^{84}Sr_{0.561}$	17.6	5.90	-66	17.6	0.0	17.8	1.1
$^{88}Sr_{82.581}/^{86}Sr_{9.861}$	8.38	8.51	1.6	8.39	0.1	8.38	0.0
$^{87}Sr_{7.001}/^{84}Sr_{0.561}$	12.5	486	3788	12.7	1.6	12.5	0.0
$^{88}Sr_{82.581}/^{84}Sr_{0.561}$	147	50.2	-66	147	0.0	149	1.4

ISR 1= Actual isotopic ratio.

ISR 2= Isotopic ratio derived from mock data with correction for elemental contributions.

ISR 3= Isotopic ratio derived from mock data with correction for elemental and molecular ions contributions.

ISR 4= Isotopic ratio derived from mock data with correction for mass bias, elemental and molecular ions contributions.

$^{X}M_{Y}$

X = The atomic weight for the isotope M.

Y = The relative abundance for the isotope M.

3.4.3. Analytical data

The total predicted count for each component was used to plot calibration curves. The calibration functions were derived according to the method described in Miller and Miller[9] (See Appendix I). The calibration functions were formulated into an EXCEL97 spreadsheet; all the calculations were carried out in EXCEL97. Appendix III shows an example of the calibration spreadsheet results. Table 3.5 shows the calibration functions for the isotopes in the mass range studied.

In order to demonstrate the capabilities of the MI algorithm for quantitative analysis, trace element concentrations were calculated for the chosen reference materials and these are presented in Tables 3.6A-C for the raw data and mass bias corrected data for TORT 1, NIST 1547 and NIST 1577b. The agreement between the determined and certified values is on the whole quite satisfactory and for most elements would meet criteria for simultaneous, multielement, trace determinations (the UK Accreditation Service accepts ± 40 % as a reasonable target for routine work of this kind). Notable exceptions are As and Se in all samples and Sr only in NIST1577b (raw data). However, these elements were at concentrations below the limit of detection and in some case quite close to the detection limit. Se suffers from the fact that mass 80 was not measured and this represents a serious loss of information for an algorithm that infers species contributions from their isotopic patterns. Cu in TORT 1 has a significant error (25.5%), but the actual level of Cu was 25 times higher than the top standard and better calibration would almost certainly improve this result.

The mass bias corrected data are generally superior to that for raw data, showing the benefits of removing instrumental distortion in the isotopic patterns. It would be expected that this improvement should be greater for elements having several isotopes and covering a significant mass range and the data support this hypothesis (e. g. Cr and Fe). Note that all the analytical data was obtained **without blank subtraction** as the spectrum was fully modelled by the algorithm.

Table 3.5. The calibration functions for raw data and mass bias corrected data

Element	Raw Data Calibration Functions				Mass Bias corrected Data Calibration Functions			
	Intercept (a)	Slope (b)	R^2	LOD ng g^{-1}	Intercept (a)	Slope (b)	R^2	LOD ng g^{-1}
^{51}V	7806	5235	0.9998	2.94	3927	2639	0.9998	2.93
^{53}Cr	316	521	0.9999	2.36	159	235	0.9999	1.97
^{55}Mn	-163	6690	0.9999	1.91	-72	2204	0.9999	1.91
^{56}Fe	156848	6133	0.9999	1.62	42357	1678	1	0.56
^{59}Co	-1322	5848	0.9999	2.15	-316	1393	0.9999	2.15
^{60}Ni	-409	1176	1	1.38	-322	270	1	0.86
^{65}Cu	-161	1305	0.9999	2.12	-34	244	0.9998	2.46
^{68}Zn	-5	403	1	0.19	-58	68	1	0.26
^{75}As	-309	782	1	0.65	-47	107	1	0.52
^{76}Se	-335	66	0.9996	3.89	-35	9	0.9997	3.33
^{87}Rb	4671	3306	0.9996	4.14	987	437	0.9980	8.88
^{88}Sr	-22932	11387	0.9973	10.45	-2815	1501	0.9977	9.58

Table 3.6A. Analytical results for TORT 1 - Lobster Hepatopancreas Marine

Element	Certified Value $\mu g\ g^{-1}$	Elemental Signal				Isotope	Isotope Signal			
		Raw Data		Mass Bias Data			Raw Data		Mass Bias Data	
		Found Value $\mu g\ g^{-1}$	% of Error	Found Value $\mu g\ g^{-1}$	% of Error		Found Value $\mu g\ g^{-1}$	% of Error	Found Value $\mu g\ g^{-1}$	% of Error
V	1.4 ± 0.3	1.27 ± 0.13	-9.3	1.27 ± 0.14	-9 3	51	1.26 ± 0.09	-10	1.26 ± 0.08	-10
Cr	2.4 ± 0.6	2.96 ± 0.09	23	2.56 ± 0.12	6.7	53	2.90 ± 0.09	20	2.53 ± 0.11	5.4
Mn	23 4 ± 1.0	20.8 ± 0.44	-11	20.7 ± 0.44	-12	55	20.8 ± 0.45	-11	20.7 ± 0.44	-12
Fe	186 ± 11	170 ± 1.3	-8.6	185 ± 0.4	-0.5	56	168 ± 1.3	-9.7	185 ± 0.5	-0.5
Co	0 42 ± 0.05	0.45 ± 0.13	7.1	0.45 ± 0.13	7.1	59	0.45 ± 0.14	7.1	0.45 ± 0.14	7.1
Ni	2.3 ± 0 3	2.71 ± 0.14	18	2.65 ± 0.13	15	60	2.74 ± 0.14	19	2.74 ± 0.14	19
Cu	439 ± 22	327 ± 3	-26	320 ± 3	-27	65	323 ± 3	-26	311 ± 4	-29
Zn	177 ± 10	153 ± 2	-14	152 ± 1.7	-14	68	165 ± 2	-6.8	151 ± 2.2	-14
As	24.6 ± 2.2	33.8 ± 0.1	37	33.5 ± 0.1	36	75	33.8 ± 0.1	37	33.5 ± 0.12	36
Se	6.88 ± 0.47	9.69 ± 0.13	41	9.74 ± 0.17	42	76	9.36 ± 0.13	36	9.67 ± 0.17	41
Sr	113 ± 5	102 ± 5	-9.7	94 9 ± 4.6	-16	88	98.7 ± 4.9	-13	102 ± 4.6	-9.7

Table 3.6B. Analytical results for NIST 1547- Peach Leaves

Element	Certified Value µg g^{-1}	Elemental Signal				Isotope	Isotope Signal			
		Raw Data		Mass Bias Data			Raw Data		Mass Bias Data	
		Found Value µg g^{-1}	% of Error	Found Value µg g^{-1}	% of Error		Found Value µg g^{-1}	% of Error	Found Value µg g^{-1}	% of Error
V	0.37 ± 0 03	0 29 ± 0.12	-22	0.30 ± 0.13	-19	51	0.29 ± 0.12	-22	0.30 ± 0.13	-19
Cr	1#	1.35 ± 0 09	35	1.16 ± 0.14	16	53	1.35 ± 0.09	35	1.17 ± 0.14	17
Mn	98 ± 3	82.7 ± 6 8	-16	82.7 ± 6.7	-16	55	82.7 ± 6.8	-16	82.7 ± 6.7	-16
Fe	218 ± 14	179 ± 1.4	-18	197 ± 0.4	-9.6	56	179 ± 1.4	-18	197 ± 0.5	-9.6
Co	0.07#	0.08 ± 0.06	14	0.08 ± 0.06	14	59	0.08 ± 0.06	14	0.08 ± 0.06	14
Ni	0.69 ± 0.09	0.74 ± 0 08	7.2	0.67 ± 0.08	-2.9	60	0.75 ± 0.08	8.7	0.72 ± 0 08	4.4
Cu	3.7 ± 0 4	3.61 ± 0.12	-2.4	3.61 ± 0.13	-2.4	65	3.60 ± 0.12	-2.7	3.62 ± 0.13	-2.2
Zn	17 9 ± 0.4	18.3 ± 0.1	2.2	18.3 ± 0.18	2.2	68	19.2 ± 0.1	7.3	17.9 ± 0.1	0.0
As	0.06±0.018	0.15 ± 0.14	150	0.15 ± 0.13	150	75	0.15 ± 0.14	150	0.15 ± 0.13	150
Se	0.12±0.009	0.30 ± 0.12	150	0.26 ± 0.11	117	76	0.29 ± 0.09	142	0.27 ± 0.10	125
Rb	19.7 ± 1.2	19 4 ± 0.27	-1.5	25.7 ± 3.9	30	87	19.4 ± 0.27	-1.5	19.3 ± 0.74	-2.0
Sr	53 ± 4	55.3 ± 2.7	4.3	51.4 ± 0.3	-3.0	88	53.4 ± 2 6	0 8	53.5 ± 2.4	0.9

Table 3.6C. Analytical results for NIST 1577b- Bovine Liver

Element	Certified Value µg g^{-1}	Elemental Signal				Isotope	Isotope Signal			
		Raw Data		Mass Bias Data			Raw Data		Mass Bias Data	
		Found Value µg g^{-1}	% of Error	Found Value µg g^{-1}	% of Error		Found Value µg g^{-1}	% of Error	Found Value µg g^{-1}	% of Error
V	0.123#	0.11 ± 0.11	-11	0.11 ± 0.11	-11	51	0.11 ± 0.11	-11	0.11 ± 0.11	-11
Mn	10.5 ± 1.7	10 5 ± 0.1	0.0	10.5 ± 0.1	0.0	55	10.5 ± 0.1	0.0	10.5 ± 0.1	0.0
Fe	184 ± 15	182 ± 1.4	-1.1	192 ± 0.4	4.4	56	175 ± 1.4	-4.9	193 ± 0.5	4.9
Co	0.25#	0.27 ± 0.14	8 0	0.27 ± 0.13	8.0	59	0.27 ± 0.14	8.0	0.27 ± 0.13	8.0
Cu	160 ± 8	148 ± 1.5	-7.5	142 ± 1.4	-11	65	153 ± 1.6	-4.4	140 ± 1.7	-12
Zn	127 ± 16	133 ± 0.1	4.7	130 ± 1.4	2.4	68	141 ± 0.1	11	128 ± 0.2	0.8
As	0.05#	0.14 ± 0.12	180	0.14 ± 0.12	180	75	0.14 ± 0.12	180	0.14 ± 0.12	180
Se	0.73 ± 0.06	1.34 ± 0.14	84	1.31 ± 0.13	80	76	1.21 ± 0.14	66	1.20 ± 0.13	64
Rb	13.7 ± 1.1	9.70 ± 0.24	-29	13.2 ± 1.97	-3 6	87	9.71 ± 0.24	-29	13.2 ± 0.33	-3.6
Sr	0.136±0.001	0.35 ± 0.39	157	0.18 ± 0.14	32	88	0.32 ± 0.14	135	0.16 ± 0.13	18

= Value not certified.

3.5. Conclusion

The results presented in this chapter demonstrate that Bayesian spectral deconvolution employing the Massive Inference algorithm is a powerful method for the analysis of mass spectra. The algorithm does not claim to provide the true spectrum, but indicates the spectrum that can best be inferred from the data supplied, without recourse to missing or assumed data. The results were encouraging and the unique advantage of not having to subtract an instrumental blank is significant and could be useful in some applications, e.g. solid analysis using laser ablation where no representative blank is available.

References

1. B. L. Sharp, J. Batey, I. S. Begley, D. Gregson, J. Skilling, A. B. Sulaiman and G. Verbogt, *J. Anal. At. Spectrom.*, 1999, **14**, 99.
2. M. A. Vaughan and G. Horlick, *Appl. Spectrosc.*, 1986, **40**, 434.
3. S. H. Tan and G. Horlick, *Appl. Spectrosc.*, 1986, **40**, 445.
4. N. M. Reed, R. O. Cairns and R. C. Hutton, *J. Anal. At. Spectrom.*, 1994, **9**, 881.
5. J. L. M. de Boer, *Spectrochim. Acta, Part B*, 1997, **52**, 389.
6. T. W. May and R. H. Wiedmeyer, *At. Spectrosc.*, 1998, 19, 150.
7. T. Townsend, *J. Anal. At. Spectrom.*, 2000, **15**, 307.
8. The Element ICP-MS, http //www.finnigan.de/products/downld/, September 2002.
9. J. N. Miller and J. C. Miller, *Statistics and Chemometrics for Analytical Chemistry*, 4th edn., Pearson Education Limited, England, 2000, ch. 5, pp.107.

Chapter 4:

The Application of ICP-MS Using a Collision/Reaction Cell

4.1. Introduction

The determination of some important elements is severely compromised by the formation of polyatomic spectral interferences generated by either argon, the solvent, or sample based ionic species. Spectral interferences that obstruct the accurate and sensitive determination of major and minor elements such as $^{40}Ca^{+}$ (interference from $^{40}Ar^{+}$ on the major isotope of Ca) or $^{56}Fe^{+}$ (interference of $^{40}Ar^{16}O^{+}$ on the major isotope of Fe). Other interferences occur on $^{80}Se^{+}$ (interference from $^{80}Ar_2^{+}$ on the major isotope of Se) and $^{75}As^{+}$ (interference from $^{40}Ar^{35}Cl^{+}$ on the mono isotope As). Various means to minimise these interferences such as modification of the sample introduction process[1], use of mixed gas plasmas[2], shield torch and cold plasma techniques[3], use of high resolution sector field mass spectrometers[4] and use of mathematical correction procedures[5], have been developed. Recently, a new approach, collision/reaction cell (CRC) technology, has been introduced to remove many of these harmful species before they enter the mass analyser. Four manufacturers offer collision and/or reaction cells in combination with inductively coupled plasma quadrupole mass spectrometers. The "Platform" (Micromass) and "Excell" (Thermo Elemental) equipped with hexapole collision cells, "ELAN DRC" (Perkin Elmer) provided with a quadrupole dynamic reaction cell and "Agilent 7500c" (Agilent) supplied with an octapole collision cell. The use of collision/reaction cells provides a new dimension to quadrupole ICP-MS instruments. They have enhanced performance and allow the technique to be used in applications that were previously beyond its capabilities.

Collision cells are widely used in organic mass spectrometry to produce fragmentation of molecular ions to aid identification and to provide information on structure[6]. However, it is only recently that reactive transformation has been introduced to ICP-MS as one approach to reduce or remove spectral interferences. A comprehensive review has been published[7] relating to the history, design, operation and application of collision/reaction cells in combination with ICP-MS.

4.2. Basic principles of collision/reaction cells

The layout of a typical CRC instrument is shown in Figure 4.1[8]. In this approach, ions enter the interface region in the normal manner, where they are extracted under vacuum into a CRC that is positioned before the analyser quadrupole. A collision/reaction gas such as hydrogen or/and helium is then bled into the cell, which consists of a multipole (a quadrupole, hexapole or octapole), usually operated in the radio frequency (RF) mode. The RF field does not separate the masses like a traditional quadrupole, but instead has the effect of focusing the ions, which then collide and react with molecules of the collision/reaction gas. By a number of different ion-molecule collision and reaction mechanisms, polyatomic interfering ions will either be converted to harmless non-interfering species, or the analyte will be converted to another ion, which is not interfered with.

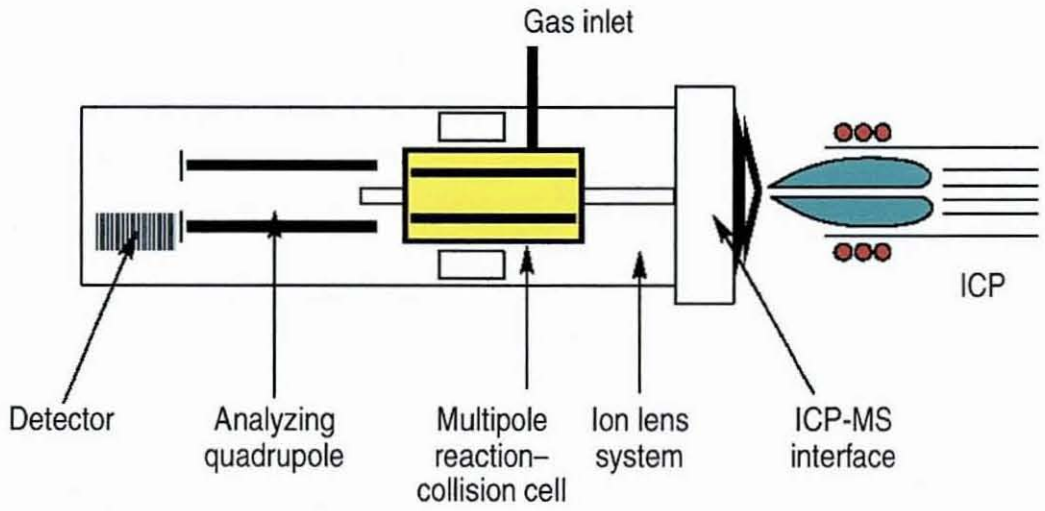

Figure 4.1. Layout of a typical collision/reaction cell instrument. Reproduced from R. Thomas, Spectroscopy, 2002, **17 (2)**, 42.

The reactions that occur within collision/reaction cells can be divided into six different classes. Table 4.1 shows these reactions, with examples, and the change in the m/z ratio of the ions involved in the reactions. Charge

transfer is the preferred reaction for elimination of plasma based interferences[9]. The gas is chosen so that it reacts efficiently with the background ions such as $^{40}Ar^+$ and $^{40}Ar^{16}O^+$ but not, or less efficiently, with the analyte ions ($^{40}Ca^+$ and $^{56}Fe^+$ respectively). The selection is made on the basis of the corresponding energy of ionisation and the rate constant for the reaction.

Table 4.1. Classes of ion molecule reactions[9].

Reaction	Example	m/z change
Hydrogen atom transfer	$Ar^+ + H_2 \rightarrow ArH^+ + H$	$40 \rightarrow 41$
Proton transfer	$ArH^+ + H_2 \rightarrow H_3^+ + Ar$	$41 \rightarrow 3$
Charge transfer	$Ar^+ + H_2 \rightarrow H_2^+ + Ar$	$40 \rightarrow 2$
Condensation	$CeO^+ + O_2 \rightarrow CeO_2^+ + O$	$156 \rightarrow 172$
Association	$Ar^+ + He \rightarrow Ar{\bullet}He^+$	$40 \rightarrow 44$
Collision dissociation	$Ar_2^+ + He \rightarrow Ar + Ar^+ + He$	$80 \rightarrow 40$

For the instrument used in this investigation (Thermo Elemental, VG PQ ExCell), it is recommended to use H_2 as the reaction gas and He as the buffer gas. The reaction chemistry of H_2 involves mainly three different processes and these are hydrogen atom transfer, proton transfer and charge transfer[10]. These reaction processes are extremely selective, and from this point of view can be used to overcome spectral interferences, especially for most of argon based ion species.

4.3. Different collision/reaction cell approaches

There are many complex collisions and reactions that can take place in the CRC, which generate many undesirable interfering species. If these species are not eliminated or rejected, they can potentially lead to additional spectral interferences. Basically two approaches are used to reject the products of these unwanted interactions:

- Discrimination by kinetic energy.

- Discrimination by mass.

The major differences between the two approaches are in the types of multipoles used and their basic mechanism for rejection of the interferences[8].

4.3.1. Discrimination by kinetic energy

The first commercial collision cells for ICP-MS were based on hexapole technology[8], which was originally designed for the study of organic molecules using MS. The more collision induced daughter species that were generated and detected, the better the chance of identifying the structure of the parent molecule. However, this very desirable characteristic for organic analysis was a disadvantage in ICP-MS, where secondary reaction product ions are something to be avoided. There are ways to minimise this problem, but they still limit the type of collision gas that can be used. Unfortunately, highly reactive gases such as ammonia and methane, which are more efficient at interference reduction, could not be used because of the limitations of a non-scanning hexapole (in rf mode) to adequately control the secondary reactions. The fundamental reason is that hexapoles do not provide adequate mass discrimination capabilities to suppress the unwanted secondary reactions, which necessitates the need for kinetic energy discrimination to distinguish the collision product ions from the analyte ions. This is typically achieved by setting the collision cell bias slightly negative with respect to the mass filter bias. This means that the collision product ions, which have the same energy as the cell bias, are discriminated against and rejected, while the analyte ions coming from the ICP, which have a higher energy than the cell bias, are transmitted[8].

The inability to adequately control the secondary reactions meant that low reactivity gases like H_2 and Xe are generally the preferred option. The result was that ion-molecule collisional fragmentation (and not reactions) was thought to be the dominant mechanism of interference reduction. Even though the ion transmission characteristics of a hexapole are

considered to be very good (with respect to the range of energies and masses transmitted), background levels were still relatively high because the interference rejection process was not very efficient. For this reason, its detection capability, particularly for some of the more difficult elements such as Fe, K and Ca, offered little improvement over the cool plasma approach[8].

Modifications to the hexapole design (for example, incorporating software control of the d.c. bias voltage) have significantly improved its collision/reaction characteristics. They now offer good transmission characteristics and the ability to implement kinetic energy discrimination. In addition, they appear to offer basic mass dependent discrimination capabilities, which means that the kinetic energy discrimination barrier can be adjusted with analytical mass[8]. In a recent investigation[11], Sharp and co-workers studied collision cell reactivity and it was found that this is dependent on two processes. The "ion kinetic energy effect" alters the reactivity of the cell (increasing the rate of exothermic reactions and decreasing the rate of endothermic reactions) by slowing down ions from the plasma before they enter the cell. This is achieved by making the hexapole bias potential more positive with respect to the offset potential of the plasma. The conditions required for maximised exothermic reaction rates and removal of argon ion species are similar to those required for maximum analyte transmission. However, these conditions favour the formation of unwanted oxides. At this stage, kinetic energy discrimination, where the difference in bias potentials between the quadrupole mass analyser and the hexapole cell was used to reject slow cell formed ions from reaching the mass analyser, helped to simplify the spectra.

An alternative to a hexapole is to use an octapole (Agilent design) in the CRC. The benefit of using a higher order design is that its transmission characteristics, particularly at the lower mass end, are slightly higher than lower order multipoles. Similar in design to the hexapole, energy discrimination is the predominant mechanism for interference reduction, which means that a lower reactivity gas like H_2 is preferred[12].

The pressurised high-order multipole radio frequency ion guide is superior to the rf-only quadrupole when it is required to slow ions to a desired kinetic energy and radially trap them. It is also advantageous as a chemical reactor for reactivity studies because it can provide efficient collection of products over a wide mass range. The multipole ion guide allows multiple ion–molecule collisions and contains products and un-reacted beam ions up to the point where they drift out of the cell for mass analysis[13].

4.3.2. Discrimination by mass

The other way to reject the products of the secondary reactions is to discriminate them by mass. Unfortunately, higher order multipoles cannot be used for efficient mass discrimination because the stability boundaries are diffuse, and sequential secondary reactions cannot be easily intercepted. The way around this problem is to use a quadrupole (instead of a hexapole or octapole) inside the CRC, and use it as a selective bandpass filter. The benefit of this approach is that highly reactive gases can be used, which tend to be more efficient at interference reduction[8].

The commercial instrument that uses this approach is called the dynamic reaction cell (DRC™, Perkin Elmer)[14]. Similar in appearance to the hexapole and octapole CRC's, the DRC is a pressurised quadrupole positioned before the analyser quadrupole. A highly reactive gas, such as ammonia or methane, is bled into the cell, where ion-molecule chemistry takes place. The gaseous molecules react with the interfering ions to convert them either into an innocuous species different from the analyte mass or a harmless neutral species. The analyte mass then emerges from the dynamic reaction cell free of its interference and is steered into the mass analyser quadrupole for conventional mass separation. The advantage of using a quadrupole in DRC technology is that the stability regions are much better defined than a hexapole or an octapole. So it is relatively straightforward to operate the quadrupole inside the reaction cell

as a mass or bandpass filter, and not just an ion focusing guide[15]. Therefore, by careful optimisation of the quadrupole electrical fields, unwanted reactions between the gas and the sample matrix or solvent (which could potentially lead to new interferences) are prevented.

As a result of using highly reactive gases, the number of ion-molecule reactions taking place is increased and therefore more efficient removal of the interfering species may result. Of course, this also potentially generates more side reactions between the gas and the sample matrix and solvent; however, by dynamically scanning the bandpass of the quadrupole inside the reaction cell, these reactions are rejected before they can react to form new interfering ions[8].

The efficiency of interference rejection (or chemical resolution) can be defined as:

$$\frac{SBR_{with\ gas}}{SBR_{without\ gas}} \qquad (4\text{-}1)$$

Where $SBR_{with\ gas}$ and $SBR_{without\ gas}$ are signal to background ratios with and without the reaction gas in the CRC respectively. The efficiency requires four concomitant conditions: the isobar must react rapidly with the reaction gas, the analyte must be non-reactive with the reaction gas, new isobaric interferences produced within the cell must be avoided, and multiple collisions of the ions with the reaction gas must be provided[16]. For high level isobaric interferences, e.g. $^{40}Ar^{+}$, a nine order of magnitude reduction is required to reduce the background to blank level for $^{40}Ca^{+}$ determination.

4.4. The applications of collision/reaction cells in ICP–MS

The applications of the collision/reaction cell in ICP-MS represent important progress, which is relevant for improving the determination of many key elements in the periodic table. The first application[17] of a collision cell for ICP-MS proposed the collisional fragmentation of

polyatomic ions with an inert gas (N_2, Ar). It was concluded that large gains in metal ion to molecular ion ratios were not possible. Provision of a reactive gas (O_2), however, gave high efficiency of chemical discrimination. It was suggested that ion-molecule chemistry might provide a way around persistent interfrences[17]. Rowan and Houk[18] showed that appropriate selection of the collision gas allowed specific reactive removal of isobaric interference ions. These early works were targeted to remove argon-based interferences. However, Eiden *et al.*[19] took advantage of the specificity of oxidation to resolve atomic isobars of $^{90}Sr^+$ through removal of the interferences from $^{90}Y^+$ and $^{90}Zr^+$ by forming the YO^+ and ZrO^+ and ^{129}I through removal of the ^{129}Xe.

Most applications published so far have focused on the use of the DRC to solve problems specific to particular m/z ratios. Many of these used NH_3 as the reactive gas, e.g. for the determinations of Al[20], K[20], Ca[14, 20], V[20, 21], Cr[20, 22, 23, 24], Mn[20], Fe[14, 20], and Zn[24]. While NH_3 reacts efficiently with the $ArCl^+$ interference ion, it also reacts with As^+, and hence is not preferred for this application. It was found that H_2 is a preferable reaction gas in this instance. The relative reaction rates of $ArCl^+$ and As^+ with H_2 were sufficiently different to allow the interference free determination of trace amounts of As even in the presence of high chloride matrices[20]. H_2 was used also to determine ^{40}Ca[25, 26] and ^{56}Fe[26, 27]. As NH_3 reacts only relatively slowly with Ar_2^+, it is not suitable as a reaction gas for Se determinations and therefore CH_4 has been used[20, 28]. The isobaric interference between Rb and Sr at mass 87 can be eliminated efficiently by conversion of Sr to SrF^+ by reaction with CH_3F; under the same circumstances, Rb will not react[29]. Using O_2 in the DRC was reported to remove interfering oxides in the determination of the Pt group elements[30].

Hexapole collision/reaction cells have been employed using less reactive gases; the majority of reports focussing on H_2 either on its own or mixed with a buffer gas such as He[31, 32]. Sharp and co-workers[31] described the effects of using H_2, He and mixtures of them in a hexapole collision cell and examined the cell performance across a wide range of the mass

spectrum. The use of a hexapole collision cell was also reported[33] for isotopic ratio measurements for Ca, Fe and Se. These are severely affected by either argon ions or argon molecular ion interferences. Feldman *et al.*[10] described the efficiency of H_2 (with He) in reducing molecular ion contributions from species derived from Ar and later reported[34] detection limits for ^{40}Ca, ^{52}Cr, ^{55}Mn, ^{75}As, ^{80}Se. The use of N_2O on its own or with buffer has been investigated for Se determinations[32]. Introducing He or H_2 into the octapole reaction/collision cell was applied for the multielement determination of trace elements and efficiently reduced serious spectral interferences from matrix elements occurring in seawater, particularly those arising from chloride and sodium[35]. It was thought that He could potentially be used as a reaction gas, however, Sharp and co-workers[36] found that He does not react; it is the water in the gas line that is reactive.

4.5. Aims and objectives

This chapter describes the application of ICP-MS using collision/reaction cell technology for the reduction, mainly, of argon based species affecting some analytes at their highest abundance isotopes. The multielement determinations of these elements with other important analytes in biological reference materials were studied.

The hexapole collision cell was employed with a mixture of H_2 and He. For this purpose, analyses were carried out with and without using collision/reaction cell technology to study especially isotopes at trace levels affected by Ar species interferences, together with all other certified and detectable isotopes in the mass range 50-88 amu.

4.6. Experimental

4.6.1. Standard solutions and reference materials

Multielement standard CLMS-2A (Spex, Stanmore, Middlesex, UK) and single element standard for Hg (Perkin-Elmer) and the certified reference

materials BCR 422 – Cod Muscle and NIST 2670 – Human Urine were used in this study. The multielement standard CLMS-2A consists of Ag, Al, As, Ba, Be, Ca, Cd, Co, Cr, Cs, Cu, Fe, Ga, K, Li, Mn, Mg, Na, Ni, Pb, Rb, Se, Sr, Tl, U, V and Zn.

Dilutions were carried out with 'Aristar' grade nitric acid (Fisher Scientific, Loughborough, UK) and 18 MΩ de-ionised water (Barnstead, Dubuque, Iowa, USA). The weight of BCR 422 and NIST 2670 taken were 0.501g and 3.0g respectively. The CRM samples were made up to 10ml with 35% high purity nitric acid ("Aristar", Merk, Poole, Dorset, UK) and then underwent microwave digestion. The microwave conditions were used as detailed in Chapter 2.

All samples were then diluted with 18 MΩ de-ionised water prior to measurement. The final acid concentration was nominally 2 % w/w (based on dilution). Calibration standards were prepared by mixing the multielement standard and Hg single element standard that contained the target elements within this study. Seven standards were prepared with concentrations for all elements of: 0.1, 0.3, 1.0, 3.0, 10, 30 and 100 $\mu g\ l^{-1}$. Standards, blank and a procedural blank were prepared in the same acid concentration. 10 $\mu g\ l^{-1}$ of In was used as the internal standard and 2% w/w nitric acid was used as the wash solution.

4.6.2. Instrumentation and optimisation

All samples were analysed using a Thermo Elemental VG PQ ExCell (Winsford, Cheshire, UK), modified to incorporate stainless-steel gas lines to avoid adventitious ingress of water. The ICP-MS operating conditions are listed in Table 4.2. Nickel sample and skimmer cones were used, with 1.0 mm and 0.7 mm orifices, respectively. The instrument was sited in a general-purpose laboratory, with no specific environmental control measures.

Table 4.2. Operating conditions for the VG PQ ExCell.

Rf power/W	1350
Gases / l min^{-1}	
Plasma	12.6
Auxiliary	0.85
Nebuliser	0.95-1.00
Lenses	tuned for optimum In signal
Hexapole pole bias / V	-1.96 or +3.86*
L3 / V	-80
Focus / V	+20 or +16*
Deflector lens / V	-27
Quadrupole pole bias / V	+2 or -6*
Torch position	tuned for optimum In signal
Acquisition Parameters	
Number of scans	20
Channels per mass	3
Number of replicates	3
Scanning mode	Peak jump
Dwell time per analyte/ms	50

* Denotes lens setting when collision cell mode is enabled.

The instrument was allowed to warm up for at least 30 min. Ion lens settings and nebuliser gas flow rate were optimised on a daily basis to achieve maximum ^{115}In count rate (typically 7×10^7 counts s^{-1} per μg ml^{-1}). A short-term stability test was carried out daily in order to monitor the variation from day to day. After running the short-term stability test in standard mode, the instrument was set to collision cell mode. Hydrogen and helium (both 99.999% purity, BOC Special Gases, Guildford, UK) were introduced to the cell at a high flow rate (6–8 ml min^{-1}) to flush the cell with these gases. Thereafter, the flow rate was set to approximately 3ml min^{-1} and, after around 30 min of equilibration; the instrument was re-

optimised for collision cell mode. This long equilibration time was required due to the length of the gas lines employed and the requirement that the hydrogen cylinder be disconnected from the instrument and stored outside of the laboratory overnight. The critical operating voltages for the hexapole cell bias, associated ion optics and quadrupole bias are given in Table 4.2. These settings were chosen as a compromise for rejecting unwanted species and optimising transmission for analyte ions[31].

4.6.3. Measurement procedure

A previous investigation[31] employed a wide range of He and H_2 flow rates individually and in mixtures. It was found that smaller gas flow rates for both He and H_2 were optimal for a 2% HNO_3 blank and a multielement standard in 2% HNO_3. Subsequently, in the presence of a constant 1.0 ml min^{-1} He flow, the H_2 flow was increased mainly in 0.2 ml min^{-1} steps between 1.3 and 2.3 ml min^{-1}. For each flow rate, data were acquired from 2% HNO_3 blank solution, BCR 422 and NIST 2670 in 2% HNO_3 for the target analyte ions with particular attention being given to the masses 50-88 amu where almost all the argon species exist. The experiments were randomised in order to minimise any problems with drift. Using the optimum condition for collision gases, the experiments were carried out with and without using the collision cell.

4.7. Results and discussion

4.7.1. Removal of spectral interferences

To investigate the efficiency of attenuation of the interfering ions, their intensities were measured as a function of hydrogen gas flow rates (with a constant flow rate for helium at 1 ml min^{-1}) in a 2% nitric acid blank, BCR 422 and NIST 2670 in 2% nitric acid solutions. Figures 4.2A-D shows that application of the collision/reaction cell in ICP–MS enabled reduction of the intensity of argon ions at mass 36 and argon molecular ions mainly at masses 37(ArH), 52(ArC), 54(ArN), 56(ArO), 76(Ar_2), 78(Ar_2), and 80(Ar_2) amu by several orders of magnitude (mass 40 was omitted). Another

observation was the reduction of the intensities at masses 24, 25 and 26 amu, as shown in Figure 4.2E, this might be due to collisional scattering of the Mg ions.

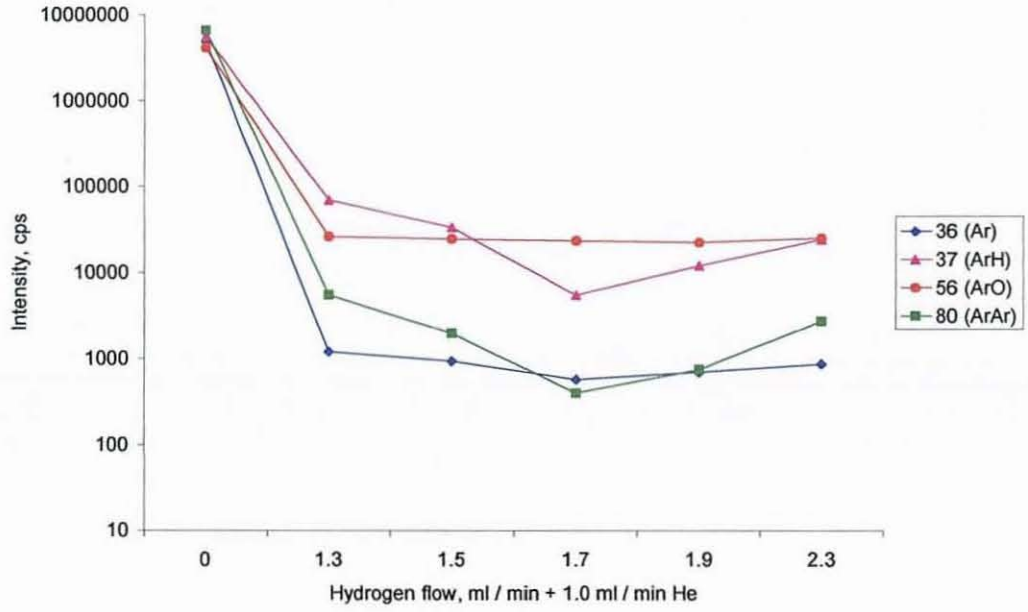

Figure 4.2A. Dependence on hydrogen flow rates of the intensities (with constant 1.0 ml / min helium) of argon ions and of molecular argon based ions, measured at masses 36, 37, 56 and 80 amu, in 2% HNO_3 blank solution.

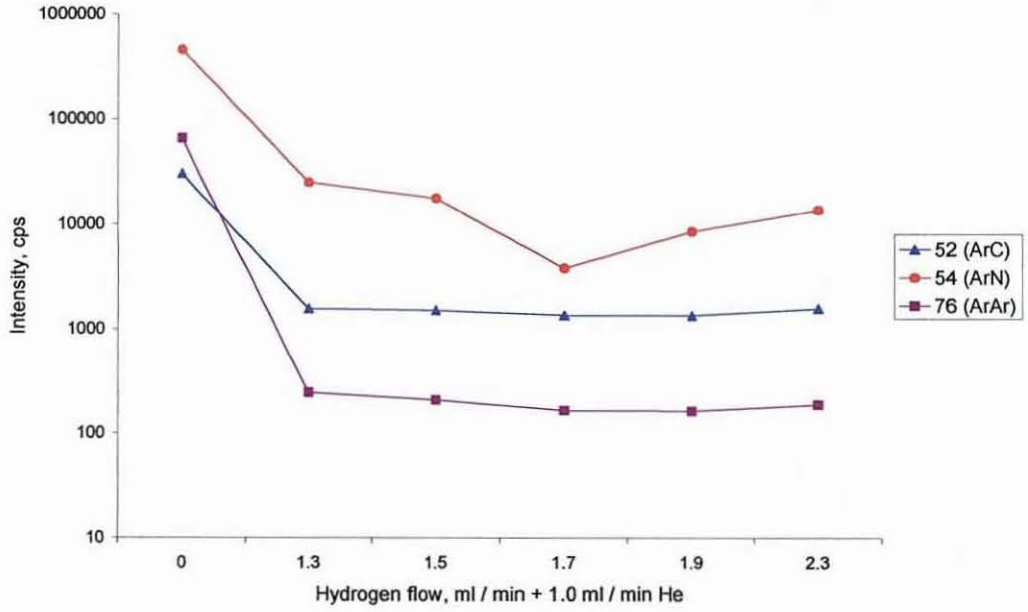

Figure 4.2B. Dependence on hydrogen flow rates of the intensities (with constant 1.0 ml / min helium) of molecular argon based ions, measured at masses 52, 54 and 76 amu, in 2% HNO_3 blank solution.

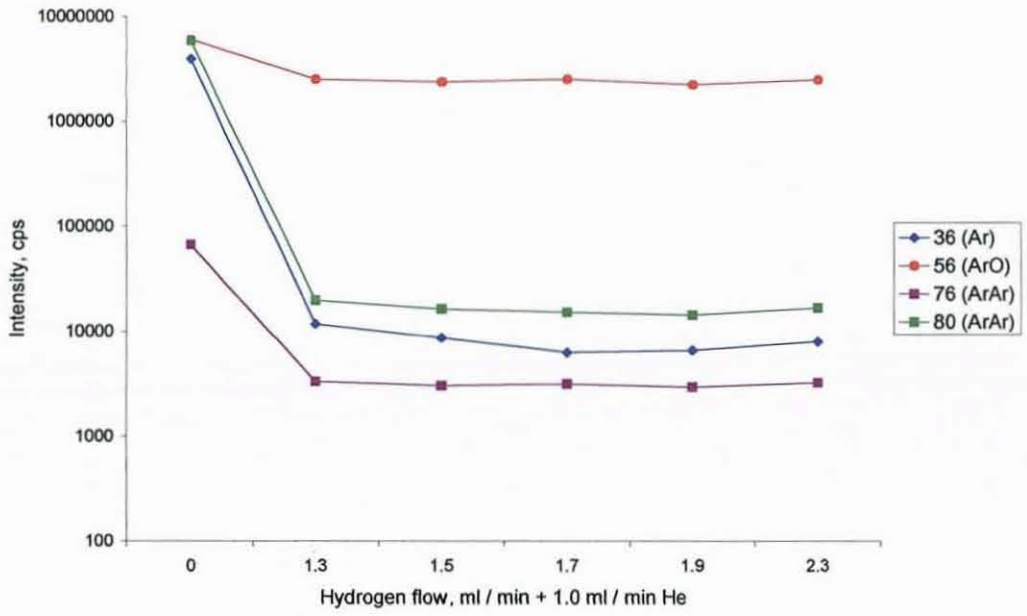

Figure 4.2C. Dependence on hydrogen flow rates of the intensities (with constant 1.0 ml / min helium) measured at masses 36, 56, 76 and 80 amu, for BCR 422 in 2% HNO_3 solution.

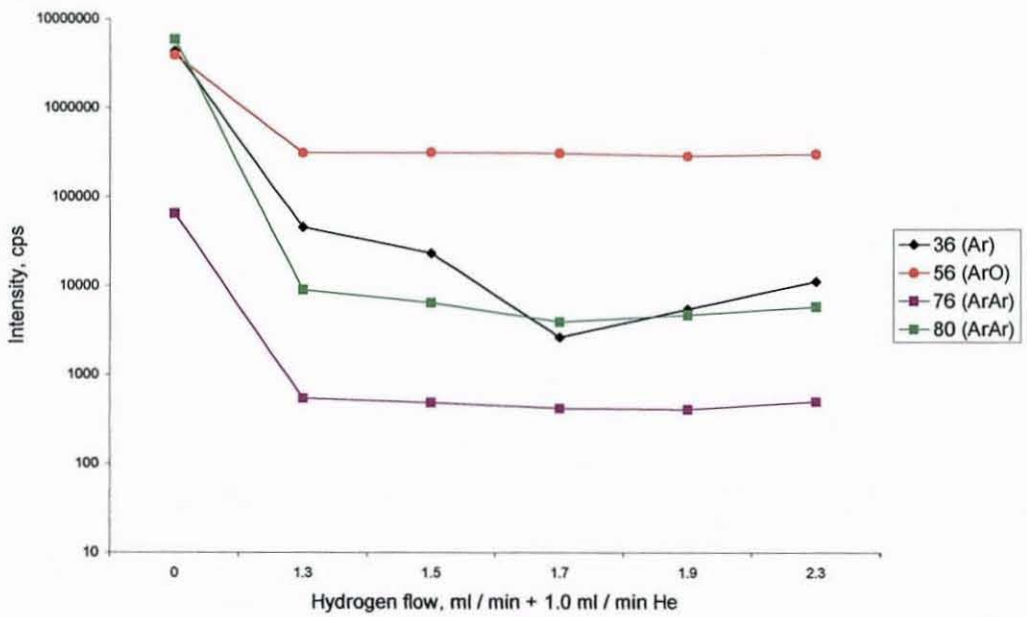

Figure 4.2D. Dependence on hydrogen flow rates of the intensities (with constant 1.0 ml / min helium) measured at masses 36, 56, 76 and 80 amu, for NIST2670 in 2% HNO_3 solution.

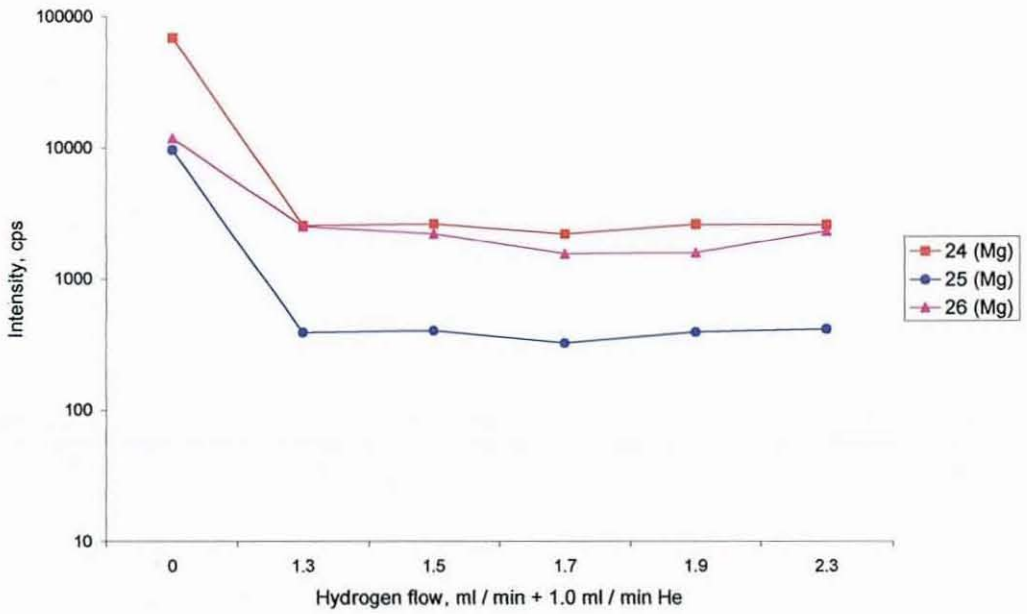

Figure 4.2E. Dependence on hydrogen flow rates of the intensities (with constant 1.0 ml / min helium) measured at masses 24, 25 and 26 amu, in 2% HNO_3 blank solution.

It should be mentioned that the selection of hydrogen gas flow rates was based on a previous investigation carried out by Sharp[31] and co-workers. A lower flow rate of H_2 was selected as an optimum condition for this type of analysis for two reasons. Firstly, to avoid degradation of the analyte signals due to scattering and secondly, to avoid the formation of hydrides that might take place with high concentrations of H_2 gas.

As shown in Figures 4.2A-E, the ion signal is not a linear function of gas flow rate. The initial reduction in signal is due to the onset of the chemical reaction (plus a contribution due to scattering for lighter elements < m/z = 40). The rate is exponentially dependent on the pressure and so if plotted on a log scale a linear decrease is observed. The signal from the interferent should eventually approach zero, but often a plateau is reached due to residual analyte in the solution blank[16]. Figure 4.3 shows this phenomena for 100ppt Ca standard solution and for deionised water blank at m/z=40.

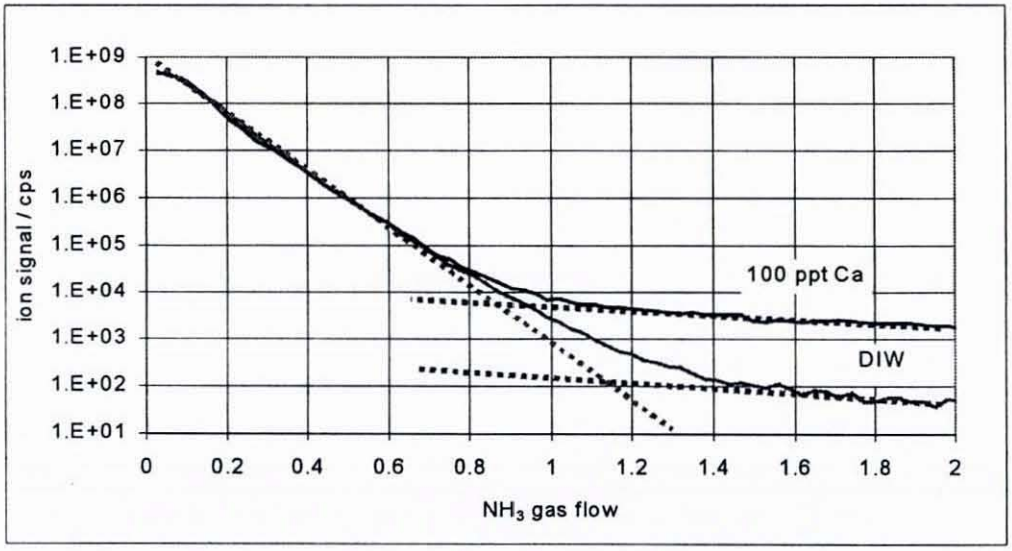

Figure 4.3. Experimental reaction profiles for m/z=40 for 100 ppt Ca and for deionised water blank. The dashed lines approximate the linear portion of signal slope, and are proportional to the rate constants. Reproduced from S. D. Tanner, V. I. Baranov, and D. R. Bandura, *Reaction Chemistry and Collisional Processes in Multipole Devices*, in Plasma Source Mass Spectrometry: The New Millennium, eds. G. Holland and S. Tanner, Royal Society of Chemistry, UK, 2001, pp 99.

For the certified elements in either BCR 422 or NIST 2670, m/z values from 50 to 88 at a gas flow of 1.7 ml min^{-1} H_2 + 1.0 ml min^{-1} He were studied. Signals were suppressed over this mass range for many m/z values and the magnitude of suppression was up to 4 orders of magnitude - compared with enhancements of less than 1 order of magnitude. This suppression of ion signals (interferences) relative to their response under conventional ICP-MS condition is shown in Figures 4.4A-D for 2% nitric acid blank, 100 $\mu g\ l^{-1}$ multielement standard, BCR 422 and NIST 2670 in 2% nitric acid solutions respectively.

The data observed, in Figures 4.4A-D, show that the suppression of signal at m/z = 80 was higher than at other masses, e.g. m/z=52, 54 and 56. This is because the analyte signal to background signals at this mass is much higher than that for m/z=56 (because Se concentration is low compared with Fe level in the samples).

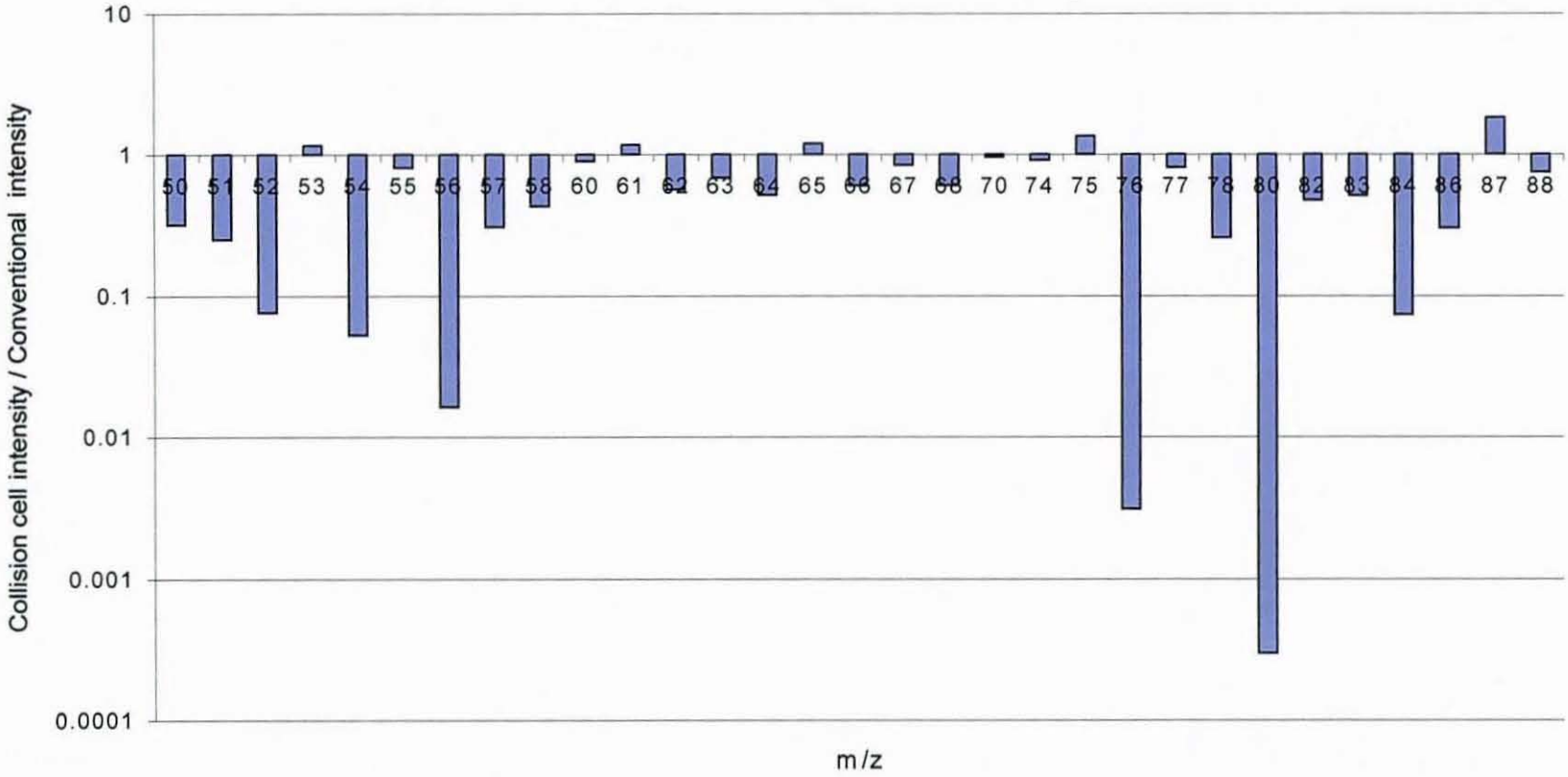

Figure 4.4A. Suppression and enhancement of the 2% nitric acid blank solution in the mass range 50-88.

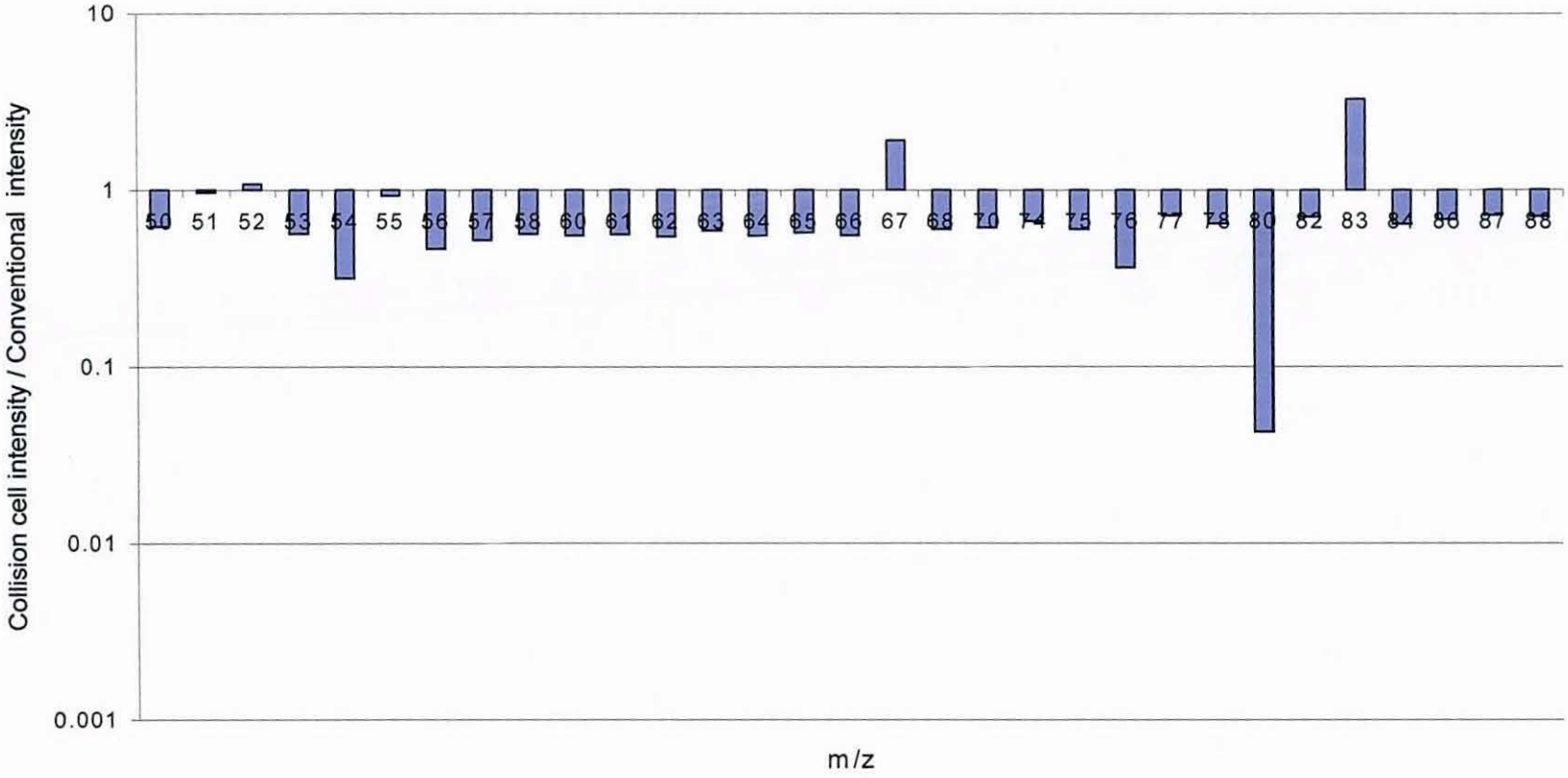

Figure 4.4B. Suppression and enhancement of the 100ppb standard solution in 2% nitric acid in the mass range 50-88.

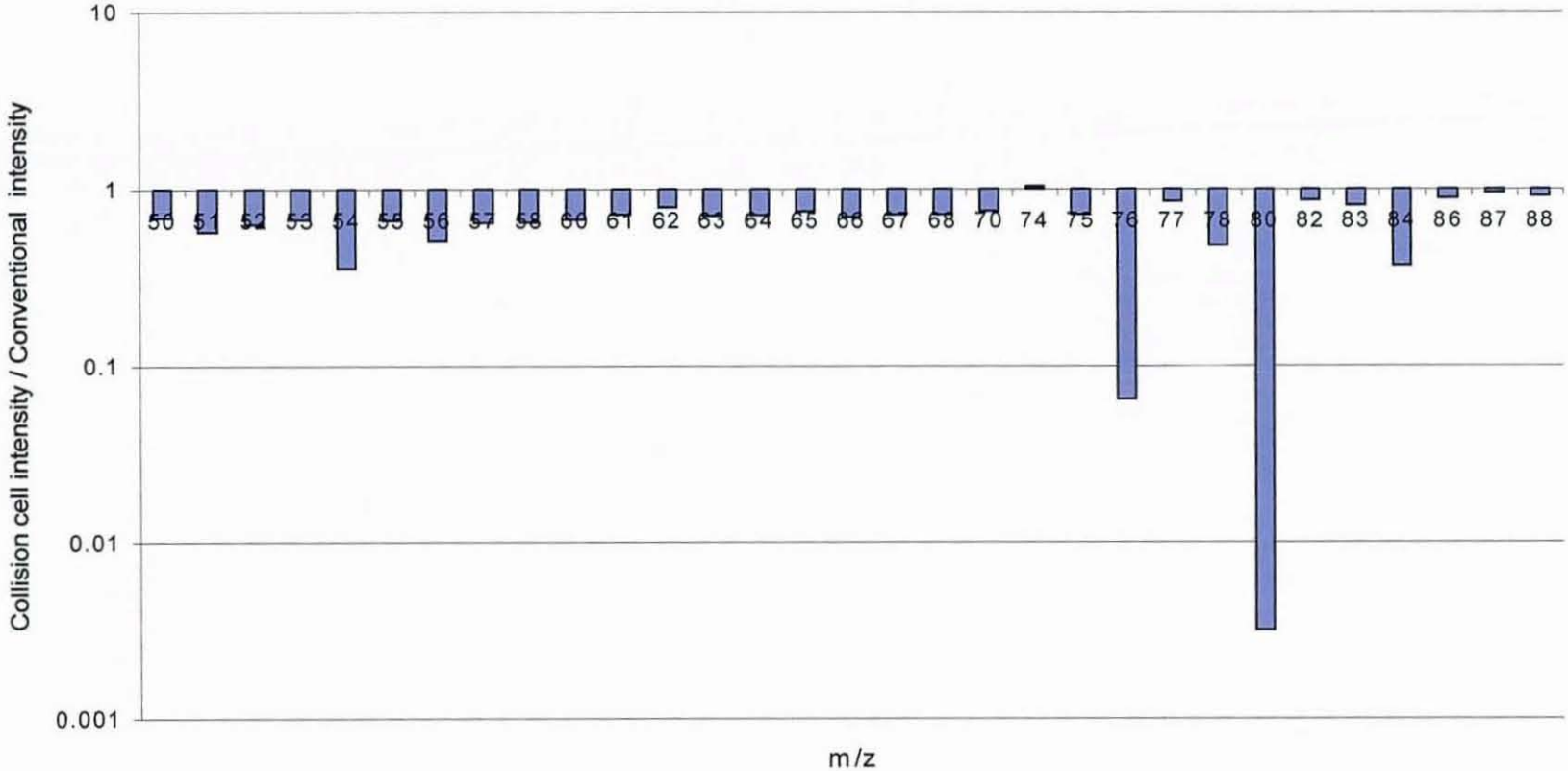

Figure 4.4C. Suppression and enhancement of the BCR 422 – Cod Muscle in 2% nitric acid in the mass range 50-88.

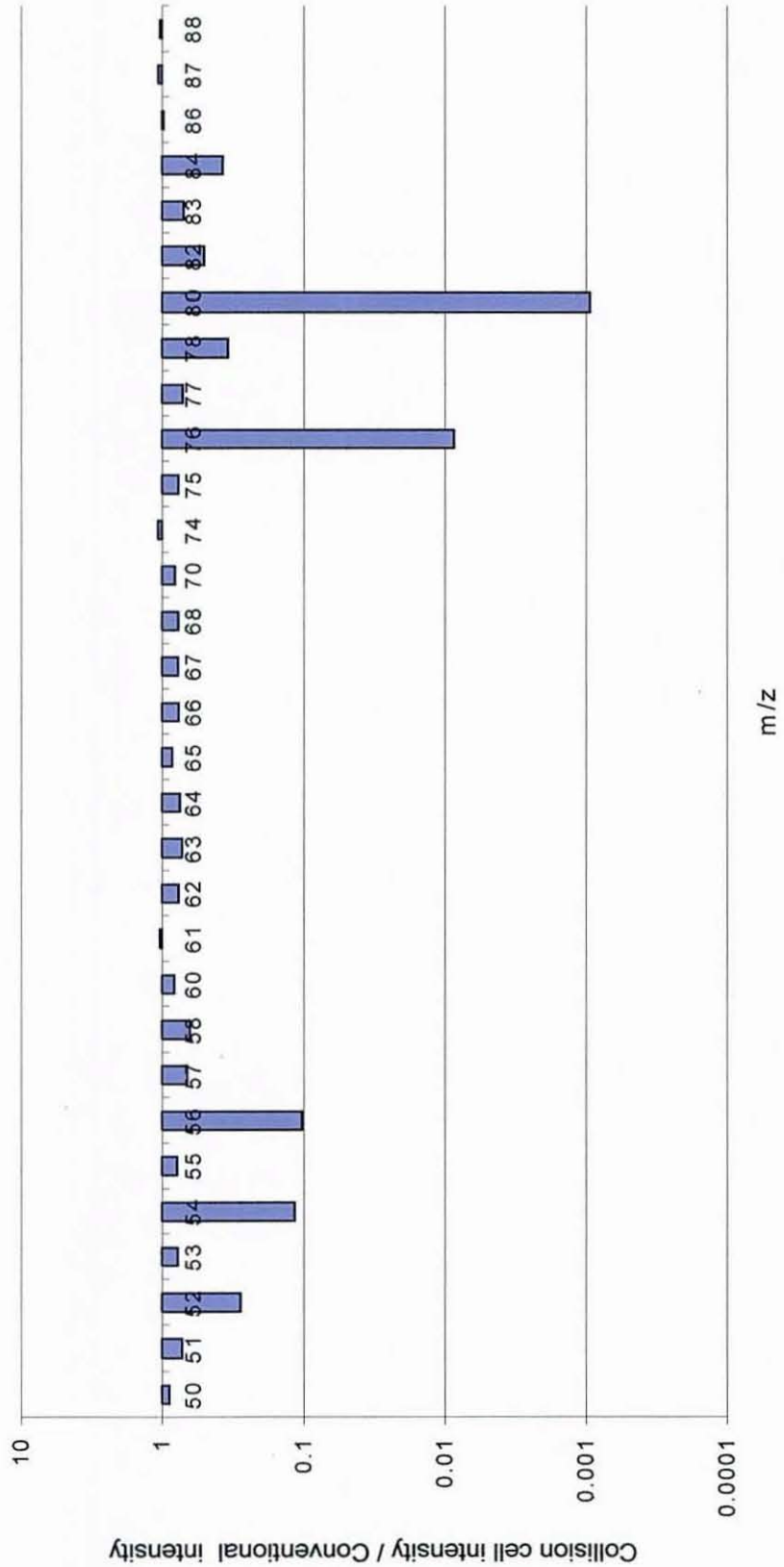

Figure 4.4D. Suppression and enhancement of the NIST 2670 – Human Urine in 2% nitric acid in the mass range 50-88.

4.7.2. Analytical data

The calibration functions (as shown in Appendix I) were formulated into an EXCEL97 spreadsheet, all the calculations were carried out in EXCEL97. The blank solution was treated as a point on the calibration curve.

In order to demonstrate the capabilities of the collision cell for quantitative analysis, trace element concentrations were calculated for the chosen reference materials and these are presented in Tables 4.3A and 4.3B for conventional and collision cell modes respectively for BCR 422 and NIST 2670. The ± figures quoted were derived directly from the calibration functions according to the method described in Miller and Miller[37]. The agreement between the determined and certified values is demonstrated and for many elements would meet criteria for simultaneous, multielement, trace determinations (the UK Accreditation Service accepts ± 40 % as a reasonable target for routine work of this kind).

Improvements in analyte determinations by using the collision cell were achieved for Ni, Zn, As in both samples and Cu in the NIST 2670. Arsenic determinations suffer from ArCl interferences and, by using CRC, the effect of ArCl can be minimised. ArNa interfered with Cu and using CRC did reduce this interferences. Improvements in Ni and Zn determinations were achieved, but the interfering species affected have not been identified.

Cr and Mn in NIST 2670 and Se in BCR 422 were better determined by conventional mode. This might be due the formation of new interferences in collision cell mode. For example, for Cr (ClOH), Mn (ArNH) and Se (BrH). The found concentrations of Mn and Cu in cod muscle sample were higher than the documented values in both modes and no explanation has been found. The concentration of Fe in both samples was too high and contamination was the likely explanation. The Se concentration in human urine sample was below the limit of detection and is best determined by other methods, e.g. hydride generation.

The use of a collision cell was expected to be superior to that for the conventional mode as this takes advantage of removing argon based molecular ion interferences. However, the analytical results show that this expectation was not met for all elements as a result of the complexes of the matrix that play a significant factor and introduce un-expected interferences. Furthermore, the analysis was carried in a laboratory for general-purpose experiments with no special conditions for trace analysis and this can introduce significant contamination. This observation was shown in the blank reading for some analytes such as Fe.

4.8. Conclusion

The application of collision/reaction cells in ICP-MS using H_2 as a reaction gas and He as a buffer is an effective means for reduction of argon ions and argon polyatomic ion interferences as has been shown in this Chapter. In addition, this technique does not affect the sensitivity (at least for elements above m/z ~ 40) compared with high resolution instruments or by reduced robustness of the plasma as it is the case with the cool plasma technique. When hydrogen is introduced as a collision gas, the rate of hydride formation must be taken into consideration, because it affects the measurement accuracy of ions of mass m + 1. Hydride formation did not affect the analytes under investigations (except for ^{52}Cr, ^{55}Mn and ^{80}Se) with the lower flow rate of hydrogen used in these experiments. Hydride formation can cause serious problems and can introduce unexpected new interferences (e.g. ^{239}UH on ^{239}Pa).

The use of this technology should enable ICP-MS to carry out multielement determinations for some analytes that are not possible using conventional ICP-MS conditions. The blank, however, must be free from contamination. For example for Fe, if the real extent of $^{40}Ar^{16}O^{+}$ reduction is to be apparent, the blank must be free from contamination.

Table 4.3A. Analytical results for biological samples in conventional mode.

Isotope	Calibration functions				BCR 422 – Cod Muscle			NIST 2670 – Human Urine		
	Intercept (a)	Slope (b)	R^2	LOD (ng g^{-1})	Certified Value µg g^{-1}	Found Value µg g^{-1}	% of Error	Certified Value µg g^{-1}	Found Value µg g^{-1}	% of Error
^{52}Cr	29689	49106	0.9995	0.11		5.30 ± 0.34		0.013#	0.014 ± 0.01	7.69
^{55}Mn	-16108	88657	0.9971	0.90	0 543 ± 0.03	0.815 ± 0 35	50.09	0.03#	0.031 ± 0.06	3.33
^{54}Fe	322885	4015	0.9991	5.02	5.46 ± 0.30	11.48 ± 1.93	110		3.22 ± 0.33	
^{60}Ni	11362	14385	0.9994	2.85		2.49 ± 0.98		0.07#	0.026 ± 0.17	-62 86
^{63}Cu	-5944	44253	0.9964	1.00	1.05 ± 0.07	1.86 ± 0.40	77.14	0.13 ± 0.02	0.11 ± 0.07	-15.38
^{68}Zn	21724	6923	1	0.15	19.6 ± 0.5	17.10 ±0.62	-12.76	1.5#	1.2 ± 0 01	-20.00
^{75}As	12415	7593	0.9992	4.60	21.1 ± 0.5	18.3 ± 1.84	-13.27	0.06#	0.020 ± 0.04	-66 67
^{78}Se	17631	2128	0.9958	0.32	1.63 ± 0.07	1.58 ± 0 27	-3.07	0.030 ± 0.008	0.081 ± 0.02	170

 # Value not certified.

Table 4.3B. Analytical results for biological samples in collision cell mode.

Isotope	Calibration functions				BCR 422 – Cod Muscle			NIST 2670 – Human Urine		
	Intercept (a)	Slope (b)	R^2	LOD (ng g^{-1})	Certified Value µg g^{-1}	Found Value µg g^{-1}	% of Error	Certified Value µg g^{-1}	Found Value µg g^{-1}	% of Error
^{52}Cr	2681	30190	0 9999	0.05		5 62 ± 0.18		0.013#	0.017 ± 0 01	30.77
^{55}Mn	-4692	46216	0.9982	0.70	0.543 ± 0 03	1.018 ± 0 27	87.48	0 03#	0.035 ± 0.05	16.67
^{56}Fe	116750	31542	0.9990	5.13	5.46 ± 0.30	12.18 ± 2.77	123		3.18 ± 0.36	
^{60}Ni	8232	7924	0.9994	2.76		3.01 ± 0.95		0.07#	0 047 ± 0.16	-32 86
^{63}Cu	-610	24473	0.9981	0.72	1.05 ± 0.07	2.33 ± 0.31	122	0.13 ± 0.02	0.138 ± 0.05	6.15
^{68}Zn	10216	4159	1	0.91	19.6 ± 0.5	18.94 ±0.38	-3.37	1.5#	1.35 ± 0.07	-10.00
^{75}As	309	4819	0.9999	0.04	21.1 ± 0.5	21 3 ± 0.51	0.95	0.06#	0.077 ± 0.01	28.33
^{80}Se	1872	3105	0.9998	0.09	1.63 ± 0.07	1.72 ± 0.22	5.52	0.030 ± 0.008	0.068 ± 0.01	127

 # Value not certified.

References

1. C. J. Park and S. A. Yim, *J. Anal. At. Spectrom.*, 1999, **14**, 1061.
2. C. J. Amarasiriwardena, N. Lupoli,V. Potula, S. Korrick and H. Hu, *Analyst*, 1998, **123**, 441.
3. C. J. Park and J. K. Suh, *J. Anal. At. Spectrom.*, 1997, **12**, 573.
4. T. Townsend, *J. Anal. At. Spectrom.*, 2000, **15**, 307.
5. J. Goossens, L. Moens and R. Dams, *Talanta*, 1994, **41**, 187.
6. E. De Hoffman, J. Charette and V. Stroobant, *Mass spectrometry: principles and applications*, John Wiley & Sons, Chichester, 1996.
7. S. D. Tanner, V. I. Baranov and D. R. Bandura, *Spectrochim. Acta, Part B*, 2002, **57**, 1361.
8. R Thomas, *Spectroscopy*, 2002, **17 (2)**, 42.
9. D. R. Bandura, S. D. Tanner, V. I. Baranov, G. K. Koyanagi, V. V. Lavrov and D. K. Bohme, *Ion-Molecule Chemistry Solutions to the ICP-MS Analytical Challenges*, in Plasma Source Mass Spectrometry: The New Millennium, eds. G. Holland and S. Tanner, Royal Society of Chemistry, UK, 2001, pp 130.
10. I Feldmann, N. Jakubowski and D Stuewer, *Fresenius J. Anal. Chem.*, 1999, **365**, 415.
11. M. A. Dexter, H. J. Reid and B. L. Sharp, *J. Anal. At. Spectrom.*, 2002, **17**, 676.
12. E. McCurdy and D. Potter, *Agilent Technologies ICP-MS Journal*, 2001, **10**, 2.
13. V. I. Baranov and S D. Tanner, *J. Anal. At. Spectrom.*, 1999, **14**, 1133.
14. S. D. Tanner and V. I. Baranov, *At. Spectr*, **20 (2)**, 1999, 45.
15. U. Voellkopf, K. Klemm and M. Pfluger, *At. Spectr*, **20 (2)**, 1999, 53.
16. S. D. Tanner, V. I. Baranov, and D. R. Bandura, *Reaction Chemistry and Collisional Processes in Multipole Devices*, in Plasma Source Mass Spectrometry: The New Millennium, eds. G. Holland and S. Tanner, Royal Society of Chemistry, UK, 2001, pp 99.
17. D. J. Douglas, *Can. J. Spectroscopy*, 1989, **34**, 38.

18. J. T. Rowan and R. S. Houk, *Appl. Spectrosc.*, 1989, **43**, 976.
19. G. C. Eiden, C. J. Barinaga and D. W. Koppenaal, *Rapid Commun. Mass Spectrom.*, 1997, **11**, 37.
20. S. D. Tanner, V. I. Baranov and U. Vollkopf, *J. Anal. At. Spectrom.*, 2000, **15**, 1261.
21. H. Liu and S. Jiang, *J. Anal. At. Spectrom.*, 2002, **17**, 556.
22. H. Liu and S. Jiang, *J. Anal. At. Spectrom.*, 2001, **16**, 858.
23. Y. Chang and S. Jiang, *J. Anal. At. Spectrom.*, 2001, **16**, 1434.
24. C. Ho and S. Jiang, *J. Anal. At. Spectrom.*, 2002, **17**, 688.
25. B. Hattendorf and D. Gunther, *J. Anal. At. Spectrom.*, 2000, **15**, 1125.
26. D. Gunther, B. Hattendorf and A. Audetat, *J. Anal. At. Spectrom.*, 2001, **16**, 1085.
27. D. R. Bandura, V. I. Baranov and S. D. Tanner, *J. Anal. At. Spectrom.*, 2000, **15**, 921.
28. J. J. Sloth and E. H. Larsen, *J. Anal. At. Spectrom.*, 2000, **15**, 669.
29. L. J. Moens, F. F. Vanhaecke, D. R. Bandura, V. I. Baranov and S. D. Tanner, *J. Anal. At. Spectrom.*, 2001, **16**, 991.
30. L. A. Simpson, M. Thomsen, B. J. Alloway and A. Parker, *J. Anal. At. Spectrom.*, 2001, **16**, 1375.
31. C. P. Ingle, P. K. Appelblad, M. A. Dexter, H. J. Reid and B. L. Sharp, *J. Anal. At. Spectrom.*, 2001, **16**, 1076.
32. S. Mazan, N. Gilon, G. Cretier, J. L. Rocca and J. M. Mermet, *J. Anal. At. Spectrom.*, 2002, **17**, 366.
33. S. F. Boulyga and J. S. Becker, *Fresenius J. Anal. Chem.*, 2001, **370**, 618.
34. Feldmann, N. Jakubowski and D. Stuewer, *Fresenius' J. Anal. Chem.*, 1999, **365**, 422.
35. P. Leonhard, R. Pepelnik, A. Prange, N. Yamada and T. Yamada, *J. Anal. At. Spectrom.*, 2002, **17**, 189.
36. M. A. Dexter, P. K. Appelblad, C. P. Ingle, J. H. Batey, H. J. Reid and B. L. Sharp, *J. Anal. At. Spectrom.*, 2002, **17**, 183.

37. J. N. Miller and J. C. Miller, *Statistics and Chemometics for Analytical Chemistry*, 4th edn., Pearson Education Limited, England, 2000, ch. 5, pp.107.

Chapter 5:

A Sample Preparation Method for Iodine Determination in Milk by ICP-MS

5.1. Introduction

The aim of this chapter was to develop a method for the determination of ^{129}I in milk samples by ICP-MS. This requires the use of the collision/reaction cell technology to reduce the Xe spectral interference at this mass by using O_2 as a reaction gas. However, there was insufficient time to achieve this objective, but the work described in this chapter is the first stage in the analysis (sample preparation).

Milk is recognised as the most complete food in the human diet because it contains all macronutrients such as proteins, lipids and carbohydrates and all micronutrients such as elements, vitamins and enzymes. This fact is particularly important in the case of the early childhood because milk is the only source of nutrients during the first months of a baby's life. A lot of information has been accumulated concerning the composition of milk in terms of fat, protein and vitamins[1]. However, less attention has been paid to the elemental composition of milk in spite of the great importance of essential elements for nutritional purposes[2, 3].

5.2. Milk composition

In dairy technology, the term milk refers exclusively to cow's milk that is collected as unaltered mixed milk from a large number of (usually several hundred) healthy cows. Milk from other sources must be labelled according to the species of the animal (e.g., goat's milk). Whole milk is a colloidal system composed of a continuous aqueous phase in which its species are dissolved. Whole cow's milk contains typically 110 g kg^{-1} of non-fat solids and between 35 and 80 g kg^{-1} of fat. Removal of the milk fat by centrifugation or spontaneous creaming leads to skimmed milk on the one hand and to cream on the other[4].

All milks contain specific proteins, fats, carbohydrates, minerals, vitamins and other components, which may have important roles. These are organised as follows: proteins in colloidal dispersion as micelles, and most

minerals and carbohydrates in true solution[5]. Most of the micelle particles are casein micelles, which exist as complexes of protein and salts, in a colloid, making about 80% in bovine milk[1]. The principal carbohydrate in most milk is lactose with small amounts of glucose and galactose, the biosynthetic precursors of lactose. Table 5.1 shows the proximate analyses of bovine, human, goat and sheep milks[1].

Table 5.1. Proximate composition (wt %) of bovine, human, goat and sheep milks. Reproduced from R. G. Jensen, Handbook of Milk Composition, Academic Press, USA, 1995.

Composition	Bovine	Human	Goat	Sheep
Protein	3.4	1.0	2.9	5.5
Casein	2.8	0.4	2.5	4.6
Fat	3.7	3.8	4.5	7.4
Lactose	4.6	7.0	4.1	4.8
Ash	0.7	0.2	0 8	1.0

The major ionic constituents of milk consist of sodium, potassium, chloride, calcium, magnesium and phosphate ions and Table 5.2 shows the mean concentrations of these minerals in mature human and cow milk[6]. The high calcium content is a biological requirement for the newborn mammal to enable build-up of bone mass. Like other biological materials, milk contains a large number of trace and ultra-trace components. These components can be categorised into two groups:

- The essential trace minerals those are required in the diet of humans such as iodine.
- Heavy metals such as (e.g. Pb) and nuclear weapon pollution (e.g. ^{90}Sr).

5.3. Iodine

Iodine is one of the essential trace minerals that are required in the diet of humans. There are over 30 different isotopes of iodine, with ^{127}I being the only stable isotope[7]. Iodine is one of the most important trace elements in

human nutrition. It has only one physiological function namely as a constituent of thyroxine, the hormone secreted by the thyroid gland. A deficiency of iodine causes an enlargement of the thyroid, the enlarged gland being known as a goiter[1]. Iodine deficiency can also result in a wide range of mental, psychomotor and growth abnormalities as well as increased infant mortality. To protect against deficiency, the recommended daily intake for adults ranges from 150 μg to 200 μg, this is seldom achieved[8].

Table 5.2. Mean concentrations (mg l^{-1}) of some of the major minerals in mature human and cow milk. Reproduced from P.F. Fox, Development in Diary Chemistry-3, Elsevier, 1985.

	Mature Human milk	**Cow milk**
Sodium	150	500
Potassium	600	1500
Chloride	430	950
Calcium	350	1200
Magnesium	28	120
Phosphorous	145	950

There are also health concerns associated with high levels of iodine in the diet. Excessive exposure to iodine can inhibit the function of the thyroid gland and produce symptoms of iodine deficiency (e.g. goitre, impaired brain function). To help protect against the toxic effects of excessive iodine exposure, it has a recommended maximum daily intake of 17 μg kg^{-1} bodyweight per day[9] (equivalent to 1020 μg/day for a 60-kg person).

However, the most hazardous iodine species are the radioactive isotopes such as ^{129}I and ^{131}I and these might be present in biological samples as a result of nuclear power generation, reprocessing and accidents in nuclear plants.

5.3.1. Iodine in milk

Milk is the major contributor to dietary exposure to iodine. Iodine is present naturally in cow's milk, but concentrations can be influenced by its presence in animal feed and/or from hygiene products used in the dairy industry. The iodine content of milk varies seasonally with higher concentrations present in winter milks[10]. This seasonal variation may reflect the greater use of compound feeding stuffs during the winter months. Iodine may be naturally present in the ingredients used in animal feeding stuffs or may be added via supplements. Iodine is included in compound feeding stuffs to protect animal health as well as providing a source of iodine in human diets.

Most iodine in milk is said to be covalently bound, but Bratter *et al.*[3] reported that about 80% of iodine was present in breast milk in the form of iodide, in addition to various organic compounds. In another investigation[11], iodine was found to be principally present as iodide in milk samples of different animals (cow, goat) and humans, whereas the infant formulas from different manufacturers had more than half of the iodine bound to high molecular weight species.

5.3.2. General considerations for iodine sample preparation

Most analytical procedures require some degree of dissolution/digestion of the sample. This enables the analyte of interest to be released from the matrix into the surrounding solution. The characteristics of the analyte need to be controlled when developing dissolution schemes. Dissolution also simplifies the subsequent calibration step, ensuring that both the sample and the calibration solutions are in essentially the same chemical and physical state. However, the way the analyte is chemically released from the bulk matrix will differ not only for different analytes, but also for the same analytes in different matrices. Consequently, methods are adopted that are not only dependent on the analyte but the sample matrix as well. The extent to which matrix constituents interfere in the

determination process is significantly reduced by dissolution, leading to a lower limit of detection for the determination.

Iodine is a "tricky" element in analytical chemistry. While the sensitivity of ICP-MS for iodine is excellent, its background level, its tendency to adsorb onto glass, and its chemistry all have to be controlled for successful quantitative analysis in complex matrices. The element iodine normally exists as iodide in nature; however other common forms include iodate and molecular iodine. Iodide, in the presence of acid and atmospheric oxygen, will form molecular iodine. Molecular iodine will cause memory affects and background problems due to its adsorption onto glass. Consequently, total iodine by ICP-MS is best performed in dilute base such as ammonium hydroxide. Dissolution is best performed in basic solution such as ammonium hydroxide or tetramethyl ammonium hydroxide (TMAH).

5.3.3. Iodine determination in biological materials

The determination of iodine in biological materials has been a difficult analytical problem. For precise and accurate analytical determination at low levels of concentration (μg g^{-1} and ng g^{-1} levels), sensitive analytical methods with a low risk of contamination are necessary. So far, X-ray fluorescence (XRF) analysis[12], neutron activation analysis (NAA)[13], the catalytic method[14], ion chromatography[15], ICP-AES[16] and ICP-MS[17-20] are the techniques that have been most employed for the determination of iodine in biological materials. XRF and NAA are time consuming and need relatively extensive sample preparation. The catalytic method, developed by Sandell and Kolthoff[14], was the most used, reliable and common technique for many years. This method is based on the catalytic effect of iodine on the oxidation-reduction reaction between Ce^{IV} and As^{III}. Biological samples are first dry-ashed and then dissolved in water or acids, and the reaction started by addition of Ce^{IV} and As^{III} reagents. The rate of reaction varies with the iodine concentration. The Sandell and Kolthoff method has been used to determine iodine concentrations in

human milk, cow's milk and infant formula. Nowadays, ICP-MS is the usual analytical technique applied and has replaced the classical Sandell and Kolthoff method.

ICP-MS is a popular technique for trace element determinations because of its excellent sensitivity, element specificity and high sample throughput without the need for extensive sample preparation. The determination of iodine by ICP-MS, however, poses some significant challenges. The ICP-MS detection limit for iodine is higher than for most elements because of iodine's higher ionization energy (10.45 eV) and it is therefore only ionised to about 25%[21]. In addition to this decreased sensitivity, a signal memory effect is a major consideration for iodine analysis by ICP-MS. The selective evaporation of iodine as HI or I_2 from droplets present in the spray chamber is a possible cause of the memory effect but it does not occur from iodide or iodate[22]. The iodide and iodate would behave like other ions in terms of memory effect. At low pH, iodide is easily oxidised to molecular iodine by dissolved oxygen as is shown in the following equations[23]:

$$I_{2\,(aq)} + 2e^- \rightarrow 2I^- \qquad E^\circ = 0\,62V$$

$$O_{2\,(g)} + 4H^+ + 4e^- \rightarrow 2H_2O \qquad E^\circ = 1.23V$$

The overall equation for the reaction:

$$4I^- + O_{2\,(g)} + 4H^+ \rightarrow 2H_2O + 2I_{2\,(aq)} \qquad E^\circ = +0.61V$$

At high pH, iodide and iodate exist without forming the molecular iodine. Regardless of the source, this memory effect produces an elevated background signal and necessitates long rinse times between samples to return the background counts to acceptable levels. However, metals are precipitated at high pH, and therefore a simultaneous analysis of iodine with other metals is not possible unless a chelating agent such as EDTA is used. The chelating agent serves as a stabiliser for the metal ions at high pH[24].

Several strategies have been utilised to minimise the memory effect associated with iodine analysis by ICP-MS. Larsen and Ludwigsen[17] prepared plant and animal materials for analysis by wet ashing to mineralise organic matter and to convert volatile iodine to nonvolatile species. Another strategy is to prepare the sample in alkaline media to prevent the oxidation of I^- to I_2 or the formation of HI. Milk and milk powder[17, 19, 20], serum[20], urine[25], and soil samples[26] have been analysed by ICP-MS in alkaline solution. This method is useful in cases where samples are easily made alkaline. Rinsing the sample introduction system for 3 min with a 0.5% v/v ammonia solution has also been used to overcome memory effects[22]. Flow injection analysis (FIA) has been used previously for the analysis of iodine using ICP-MS detection. Sturup and Buchert[20] analysed alkaline solutions of milk and milk powders using FIA, as did Kerl *et al.*[27] who analysed plant and tissue materials using an acid-hydrogen peroxide digestion process. The principle advantage of FIA is that the amount of analyte entering the spray chamber is reduced, which helps to minimise memory effects. In addition, high sample throughput is possible because long rinse times to reduce background signal are avoided[28].

The development of a simple and direct procedure for milk analysis is attractive, because of speed (i.e., samples can be automatically diluted using an autosampler) and the potential avoidance of contamination resulting from reduced sample manipulation. Durrant and Ward[29] carried out a multielement analysis of human milk, including the determination of iodine. The samples were diluted to 2% v/v in aqueous solution. Allain *et al.*[18] described the simultaneous determination of iodine and bromine in plasma and urine after a ten-fold dilution of the samples with 1% nitric acid. Baumann[19] reported the rapid and sensitive determination of iodine in fresh milk and milk powder. The sample preparation involved a 20-fold dilution with 0.5% v/v ammonia solution.

Because these methods retain the organic matrix, they require a considerable dilution of the analyte. Destruction of the organic matrix leads

to a reduction of spectral interferences from carbon species and cone blockage in the quadrupole ICP-MS instrument. Decomposition techniques such as dry ashing, hot-plate digestion, high-pressure ashing and microwave digestion have been employed prior to the detection step which often requires that iodine has been converted to and isolated in a particular chemical or physical form amenable to the final detection. Wet ashing with HNO_3 needs a strong oxidising agent such as perchloric acid ($HClO_4$) in order to avoid losses. Although such a combination is very effective with respect to quantitative oxidation of iodide to iodate, the use of large amounts of perchloric acid[17] poses a safety risk during handling in combination with organic materials. Oxygen combustion was found to be very effective during subsequent determination of halides. This combustion was successfully applied to determine trace amounts of iodine in organic matter[25]. This method, however, is limited by the small amount of samples (10-30 mg) that can be combusted in a flask and also by possible iodine contamination in the filtration step. Another analytical approach employing ICP-MS was based on an alkaline extraction with ammonia[19, 22], because, under such conditions, both iodide and iodate are stabilised. A combination of alkalis employing potassium hydroxide and tetramethylammonium hydroxide (TMAH) was used to determine iodine in milk by FI-ICP-MS[20]. Another digestion method based on an alkaline extraction procedure using only TMAH at elevated temperature has been employed[8]. These procedures lead to the conversion of iodine into iodide or iodate, which is then determined by ICP-MS without any concern for the speciation of the iodine in the original sample.

5.4. Aims and objectives

This chapter describes a sample preparation procedure for the determination of iodine in milk that could also be used for multielement determinations. This method is based on solubilisation, alkaline hydrolysis and oxidation. Thus milk sample was digested with 25% TMAH and 5% Triton X-100, then oxidised with 20 volume H_2O_2 for 2 hours at 70 °C and finally the metals were dissolved and stabilised with EDTA. The final

solution is both clear and stable and is capable of efficient nebulisation. The accuracy and precision of the method was evaluated by the analysis of milk reference materials (whole milk powder NIST 8435 and skimmed milk powder BCR 063R).

5.5. Experimental

5.5.1. Methodology

The investigation was carried out in two phases:

1. Development of a sample preparation procedure for the determination of iodine in milk samples. To achieve this target, several options were explored to find a suitable method and this was subdivided into three stages:
    - UV digestion.
    - Acid digestion.
    - Alkaline digestion.
2. Determination of iodine by ICP-MS using the successful sample preparation method from the previous step.

5.5.2. Reagents, standard solutions and reference materials

A number of reagents were used in this study; these were of analytical reagent grade. Titanium oxide fine powder (Degussa P25) and TMAH (25 wt. % in water) ordered from Aldrich, ammonium persulphate, sodium dodecyl sulphate (SDS), nitric acid (70 %), hydrogen peroxide (>6 % w/v or 20 volume) and ammonium hydroxide (30 wt. % in water) supplied by Fisher, Triton X-100 and Tween 80 purchased from Sigma and $(NH_4)_2H_2EDTA$ obtained from Avacado. A 1000 mg l^{-1} stock standard solution of potassium iodide was prepared from the salt (supplied by Fisher). This primary standard was used to prepare a 10 $\mu g\ g^{-1}$ secondary standard. The secondary standard solution was prepared daily in TMAH to reduce the possibility of iodine losses. The final concentration of TMAH in

the secondary standard was 2% (w/w). Dilution was carried out with 18 MΩ de-ionised water (Barnstead, Dubuque, Iowa, USA).

The initial reagents were not pure enough and ultra-pure reagents were ordered. TMAH supplied by Apollo Scientific Ltd. (Bredbury, Stockport Cheshire) and Triton X-100 and hydrogen peroxide (>30 % w/v) purchased from Romil Ltd. (Waterbeach, Cambridge). A 1000 mg l^{-1} iodide stock standard solution was purchased from Spex (Stanmore, Middlesex). This primary standard was used to prepare a 10 μg g^{-1} secondary standard in the same media (See above).

Six standards were prepared from the secondary standard solution for linearity studies with concentrations for iodide of: 1, 5, 10, 30, 50 and 100 ng g^{-1}. Standards, blank and a procedural blank were prepared in TMAH and Triton X-100 matrix. The final concentrations of TMAH and Triton X-100 were 6.7% and 1.3% w/w respectively. 200 ng g^{-1} of Sb was used as the internal standard and 1% w/w TMAH was used as the wash solution.

Two certified reference materials were obtained from the National Institute of Standards and Technology (NIST 8435 - whole milk powder) and the European Community Bureau of Reference (BCR 063R - skimmed milk powder). The certified reference materials were purchased from the Laboratory of the Government Chemist (Salford Quays, Salford). Several milk samples were purchased from local stores. The weights of the solid and liquid milk were about 0.5 and 3 g respectively. The final concentrations for TMAH and Triton X-100 in the digested samples were nominally 6.7% and 1.3% w/w respectively (based on dilution).

5.5.3. Milk sample preparation

The majority of the current effort in analytical chemistry has been focussed on the lowering of detection limits and widening linear dynamic ranges. Current technology allows very low levels to be determined in almost any matrix. Attention is returning to making improvements in the methods of

sample preparation because many existing sample preparation procedures limit the analytical process[30]. A simple, fast, reproducible sample preparation procedure is the ultimate target. While using microwave digestion for biological samples is well known[31], the number of samples that can be prepared at the same time is small and safety aspects are a consideration with some matrices. An inexpensive method readily capable of automation would be of inestimable value for routine analysis.

5.5.3.1. UV digestion

Liquids or slurries of solids may be decomposed by UV radiation in the presence of oxidative reagents such as TiO_2 and H_2O_2. The corresponding digestion cell should be placed in the closest possible proximity to the UV lamp to ensure a high light yield. Using UV irradiation at 254 nm enhances the oxidation power of H_2O_2, by generation OH radicals, but has a limited application because this wavelength needs an expensive digestion cell and Hg lamp and there are safety considerations. Digestion with solid oxidants has growing applications and mainly uses TiO_2 in the oxidation process. The use of aqueous TiO_2 suspensions has been reported and the wavelength required is ≥340 nm. The digestion mechanism involves the formation of OH radicals from TiO_2 and the solvent molecules that is initialised with the aid of the UV radiation. This reactive radical is able to oxidise the organic matrix. Effective cooling of the sample is essential, since losses might otherwise be incurred for highly volatile elements[32].

An investigation of using TiO_2 with UV light to digest milk matrix was carried out. The irradiation source was a 100 W Xenon arc lamp (Light Support). The photochemical reactor was cylindrical (20 mm diameter) with a 50 mm path length. The temperature was kept constant at 25 °C by water circulation. Approximately 3.0g TiO_2 powder was added to an aqueous solution of the milk sample (3 ml of milk diluted to 50 ml with H_2O) and stirred magnetically in oxygen equilibrated solution for 24 hours. Sample solution was withdrawn from the digest for analysis and

centrifuged to separate TiO_2 particles. At the end of the experiment, the digested sample looked like a white suspension mixture with colloidal particles spread throughout the aqueous layer.

The performance of the digest was studied by looking at the degradation of tryptophan, an aromatic amino acid that should be resistant to oxidation and is part of the milk protein. The fluorescence measurements were carried out using a Spex FluoroMax spectrofluorophotometer. The excitation and emission wavelengths for tryptophan are 280 nm and 340 nm respectively[33]. Figure 5.1 shows the changing tryptophan fluorescence intensity as a function of time. This observation led to the conclusion that using TiO_2 under these conditions did not produce an efficient decomposition of the organic components in milk sample.

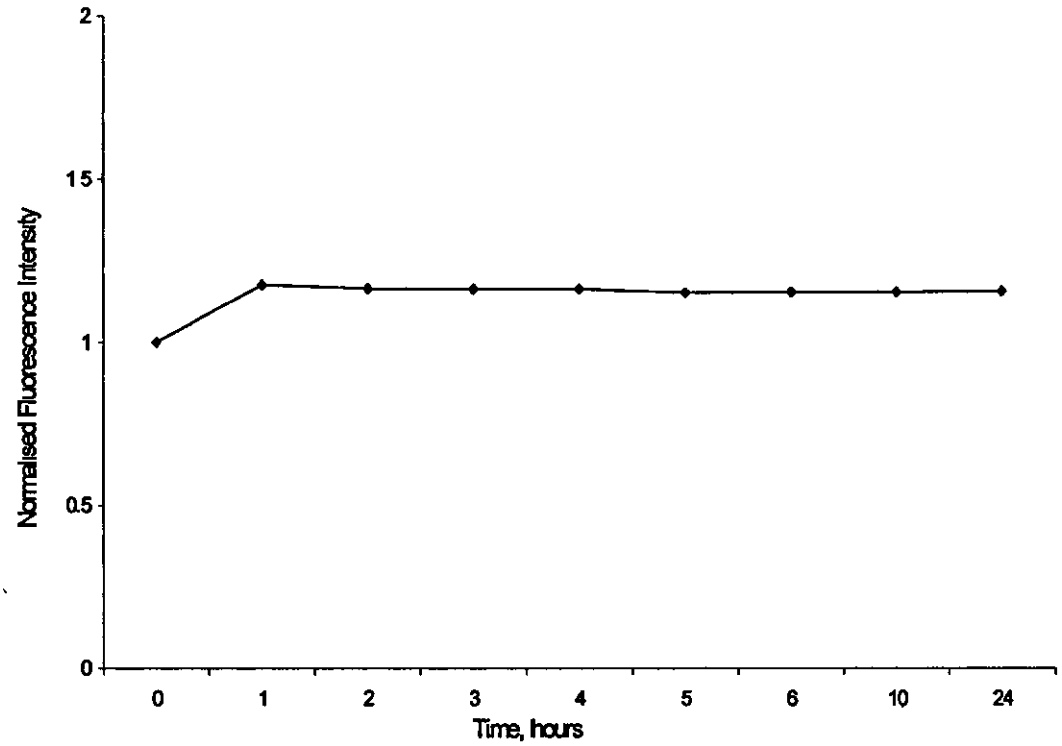

Figure 5.1. The change of the normalised fluorescence intensity as a function of time for tryptophan.

5.5.3.2. Acid digestion

Digestion with oxidising acids is the most common sample preparation procedure. The acid used has two roles. The primary function of the acid is to break down the matrix. The second function is to oxidise all oxidisable species that are in solution. Heat will increase the rate of matrix breakdown. Since it is matrix breakdown that is being investigated, digestion studies were carried out in vessels open to the atmosphere.

Nitric acid is an almost universal digestion reagent, since it does not interfere with most determinations in ICP-MS and is available commercially in sufficient purity. However, its oxidising power is often insufficient under atmospheric pressure conditions[34]. Hydrogen peroxide, $(NH_4)_2S_2O_8$ and sodium dodecyl sulphate (SDS) can usefully be employed in conjunction with nitric acid as a way of improving the quality of a digestion. Because the concentration of fat in milk is relatively high, it was thought that using a surfactant might help the dissolution process. Metal based oxidising reagents such as $KMnO_4$, that might introduce spectral interferences or contamination were avoided.

To test tubes 3ml of milk and about 2ml of (70%) HNO_3 was added. To each tube, an oxidising reagent was added with or without the surfactant. The samples were then heated between 70-80 °C and shaken regularly for 1 hour. After that, the samples were removed from the water bath and then allowed to cool. The appearance and transparency of the samples were then viewed. The observations are shown in Table 5.3.

It can be seen from the observations in Table 5.3 that none of the oxidising reagents used successfully destroyed the organic components in milk sample.

5.5.3.3. Alkaline digestion

Alkaline digestion is attractive because it is an appropriate medium for the determination of iodine by ICP-MS. As said previously, use of metal based reagents such as NaOH was avoided. Therefore, NH_4OH and tetramethylammonium hydroxide (TMAH) were used. TMAH is a clear organic base that is strongly alkaline and is increasingly used in biological applications. The oxidising reagents that can be used in basic solution are limited but H_2O_2 can be used safely under these conditions.

Table 5.3. Observations of the acid digestion procedures.

Reagents	Observation
HNO_3 (70%) + H_2O_2 (20 volume)	Aqueous solution with colloidal particles and precipitate
HNO_3 (70%) + H_2O_2 (20 volume) + Triton X-100 (5% w/v)	Aqueous solution with colloidal particles and precipitate
HNO_3 (70%) + H_2O_2 (20 volume) + Tween 80 (5% w/v)	Aqueous solution with colloidal particles and precipitate
HNO_3 (70%) + $(NH_4)_2S_2O_8$ (s)	Aqueous solution with colloidal particles
HNO_3 (70%) + $(NH_4)_2S_2O_8$ (s) + Triton X-100 (5% w/v)	Yellow solution with yellow precipitate
HNO_3 (70%) + $(NH_4)_2S_2O_8$ (s) + Tween 80 (5% w/v)	Aqueous solution with colloidal particles
HNO_3 (70%) + SDS (s)	Dark solution with brown precipitate
HNO_3 (70%) + SDS (s) + Triton X-100 (5% w/v)	Dark solution with brown precipitate
HNO_3 (70%) + SDS (s) + Tween 80 (5% w/v)	Dark solution with brown precipitate

To test tubes 3ml of milk and about 2ml of the alkaline reagent were added. To each tube, H_2O_2 was added with or without the surfactant. The

samples were then heated between 70-80 °C and shaken regularly for 1 hour. After that, the samples were removed from the water bath and then allowed to cool. The appearance and transparency of the samples were then viewed. The observations are shown in Table 5.4.

From Table 5.4, it can be seen that using NH_4OH did not successfully digest the milk matrix whereas the TMAH seems to be more efficient for performing the digestion. TMAH digestion shows a browning color that indicates a reaction, called the Maillard reaction, might have occurred. When a free NH_2 group in an amino acid reacts with any reducing sugar such as lactose, this reaction takes place[35]. From the analytical point of view, it is not important to know the products of this reaction, however, it is important that these products are degraded and that the analyte is retained.

The probable mechanism for the function of TMAH is by denaturing/hydrolysis of the protein molecules. Denaturation means unravelling the 3-dimensional shape of the protein molecule and it seems that changing the shape of the protein could make the NH_2 group available to react with the reducing sugar. Triton X-100 almost certainly helps to dissolve the milk fat. Further experiments were carried out to find a reliable mechanism to degrade the remaining organic components in the milk. The initial decomposition with TMAH and Triton X-100 rendered the matrix more susceptible to oxidation. Both acid and alkaline oxidation can be used at this point, bearing in mind that I^- or IO_3^- and not I_2 are the desired species for analysis.

Table 5.4. Observations of the alkaline digestion procedures.

Reagents	Observation
NH_4OH (1M)	White solution
NH_4OH (1M) + H_2O_2 (20 volume)	White solution
NH_4OH (1M) + H_2O_2 (20 volume) + Triton X-100 (5% w/v)	White solution
NH_4OH (1M) + H_2O_2 (20 volume) + Tween 80 (5% w/v)	White solution
TMAH (25 wt. %)	Brown solution and precipitate with a solid layer in the top
TMAH (25 wt. %) + H_2O_2 (20 volume)	Brown clearer solution and precipitate with a solid layer in the top
TMAH (25 wt. %) + H_2O_2 (20 volume) + Triton X-100 (5% w/v)	Clear solution and white precipitate
TMAH (25 wt. %) + H_2O_2 (20 volume) + Tween 80 (5% w/v)	Brown clearer solution and precipitate with a solid layer in the top

To test tubes 3ml of milk and an excess volume of TMAH and Triton X-100 were added. Tubes were placed into a water bath between 70-80 °C and shaken regularly for 1 hour. Then an excess amount of the oxidising reagent was added gently to the tube and the tubes returned to the water bath for 2 hours. After that, the samples were removed from the water bath and allowed to cool. The appearance and transparency of the samples were then viewed. The observations are shown in Table 5.5.

From Table 5.5, it can be seen that the use of oxidising reagents in acidic solution did not offer successful digestion of the brown components. The alkaline digestion using H_2O_2 did. It was thought that the white participate was metal (Ca) hydroxide or the salts of resistant organic acids. These components can be dissolved using a chelating reagent and therefore,

EDTA was added and the white solid disappeared which supported the previous hypothesis. The digested sample solution was clear, homogeneous and stable for at least 24 hours. Further investigations were carried out to explore the optimum weight and concentration of TMAH, Triton X-100, H_2O_2 and EDTA and the time and temperature. The ideal procedure for milk sample digestion depends on the analyte of interest. If only iodine needs to be determined, it is not necessary to add EDTA whereas sample preparation for multielement determinations in milk samples requires the addition of the EDTA.

Table 5.5. Observations of the digestion of Maillard reaction products.

Oxidising reagents	Observation
HNO_3 (70%) + H_2O_2 (20 volume)	Brown solution and precipitate
HNO_3 (70%) + $(NH_4)_2S_2O_8$ (s)	Brown solution and precipitate
HNO_3 (70%) + SDS (s)	Brown solution and precipitate
H_2O_2 (20 volume)	Clear aqueous solution with white precipitate

The following is the analytical procedure that has been used for iodine determinations in solid or liquid milk. To a centrifuge tube, add 3g of deionised water, then add about 0.5g of dried sample and mix them well, or about 3g of the liquid sample. Add 4g of TMAH (25 wt. % in water), 4g of Triton X-100 (5% w/v), 4g of H_2O_2 (20 volume) gently and place the tube into a water bath at 70 °C. Shake regularly for 2 hours. Centrifuge the tube at about 5000-rpm for 5 minutes.

5.5.4. Instrumentation and optimisation

The ICP-MS used was a Thermo Elemental VG PQ ExCell (Winsford, Cheshire, UK) equipped with concentric polyamide nebuliser, glass impact bead spray chamber and nickel sample and skimmer cones with 1.0 mm

and 0.7 mm orifices respectively. Typical instrument operating conditions are summarised in Table 5.6. The instrument was sited in a general-purpose laboratory, with no specific environmental control measures. The optimisation procedure for the ICP-MS was as described in Chapter 4.

Table 5.6. Operating conditions for the VG PQ ExCell

Rf power/W	1350
Gases / l min^{-1}	
Plasma	12.6
Auxiliary	0.85
Nebuliser	0.95-1.05
Acquisition Parameters	
Number of scans	100
Channels per mass	1
Number of replicates	5
Scanning mode	Peak jump
Dwell time per analyte/ms	10

5.6. Results and discussion

In order to demonstrate the capabilities of the sample preparation procedure for quantitative analysis, iodine concentrations were determined for the chosen reference materials and commercial samples. The blank solution was treated as a point on the calibration curve. The calibration curve for iodine using the analytical grade reagents is given in Figure 5.2. The regression equation was derived directly from the calibration functions according to the method described in Miller and Miller[36]. Table 5.7 presents the found concentration for iodine in the certified reference materials.

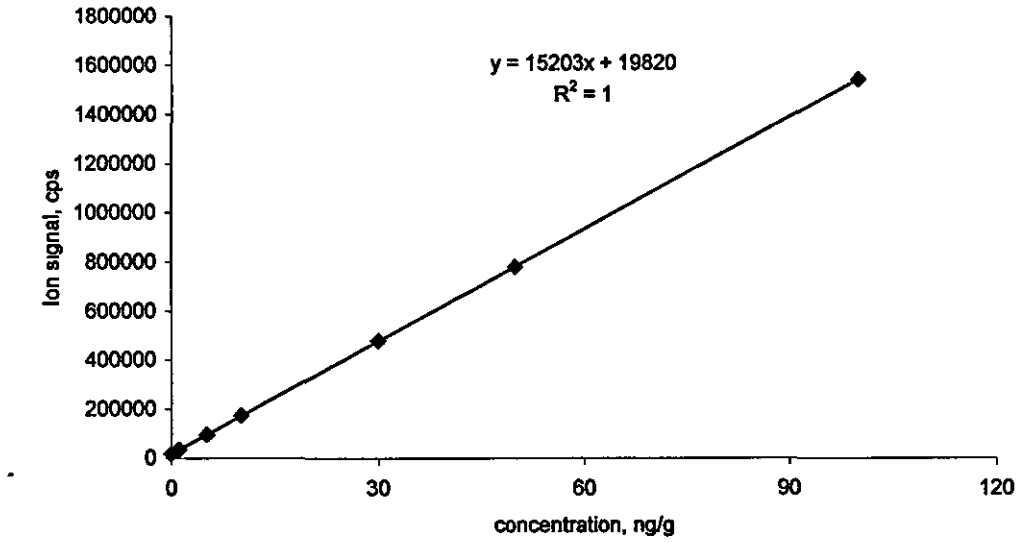

Figure 5.2. Calibration curve for iodine using analytical grade reagents (standards prepared from potassium iodide salt).

Table 5.7. Quantitative results for iodine in certified reference materials using analytical grade reagents.

	Iodine concentration μg g^{-1}		
	certified value	Found value	% of error
NIST 8435 (n=3)	2.3 ± 0.4	3 34 ± 0.16	45.22
BCR 063R (n=3)	0.81 ± 0 05	0 89 ± 0.18	9.88

The bias in the analytical data for these samples was probably due to the contamination in the reagents used in the sample preparation step, contamination in the reference material (NIST 8435) or contamination in potassium iodide salt used to prepare the standards.

The reagents used to prepare the samples and standards were checked for purity. Matching concentrations for each reagent similar to those used

in the sample preparation step were used and it was found that all these reagents (water, TMAH and Triton X-100) do not introduce any significant contamination to the samples for ^{127}I determination. The levels of iodine in these reagents were less than 0.4 ng g^{-1} individually. The ultimate target was the determination of ^{129}I (See Section 5.1.) and therefore the highest purity for the reagents was essential as the sensitivity for ^{129}I is much lower than ^{127}I (after the reduction of ^{129}Xe spectral interferences) and for this reason ultra-pure reagents were used. However, if ^{127}I is determined, the analytical grade reagents can be employed safely.

Because the analysis was carried out in a solution that contained a small amount of precipitate, this could block either the sample introduction system or the interface region in the ICP-MS. Adding EDTA (to remove the precipitate) during the sample preparation procedure did not affect the results.

As a result of the high temperature used in the sample preparation step, there is a possibility of the solution decreasing in volume, which might have an affect the iodine determination. The correction for evaporation was less than 5% and did not offer any real benefit.

Memory effect has been reported to be one of the problems limiting the determination of iodine. To avoid this effect, all steps were carried out in alkaline media. It can be noted here that the preparation of secondary standard solution in deionised water or alkaline media did not make any difference as this solution was prepared daily. The washing time between the samples used 1% TMAH and the background signal was less than 0.4 ng g^{-1} which indicated an absence of any memory effect.

Another investigation employed another sample of NIST 8435 (supplied by CSL Food Science Laboratory, Sand Hutton, York) to check for any possible contamination in the sample. Analysis of this sample, using the same sample preparation method, did not remove the analytical bias.

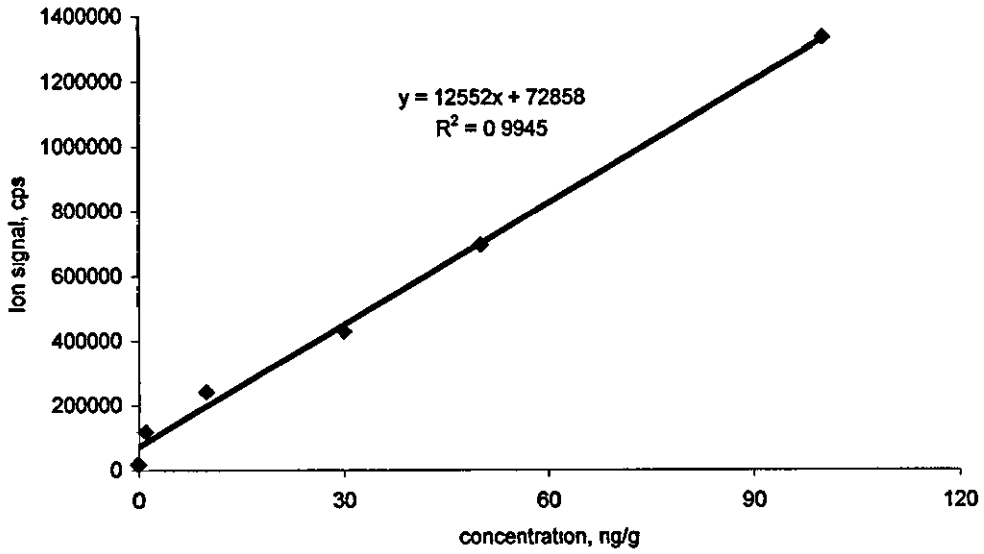

Figure 5.3. Calibration curve for iodine using ultra-pure reagents (standards prepared from iodide stock standard solution).

The analysis was repeated using iodide stock standard solution purchased from Spex, Stanmore, Middlesex, UK. The calibration curve for iodine using this standard is given in Figure 5.3. Table 5.8 presents the found concentration for iodine in the certified reference materials using high purity reagents. The agreement between the determined and certified values is on the whole quite satisfactory and would meet criteria for single trace determinations (the UK Accreditation Service accepts ± 25 % as a reasonable target for routine work of this kind). The problem therefore appeared to derive from the purity of the KI solid used to prepare the original standards.

Table 5.8. Quantitative results for iodine in certified reference materials and commercial samples using high purity reagents

	Iodine concentration μg g^{-1}		
	certified value	Found value	% of error
NIST 8435 (n=6)	2.3 ± 0 4	2.17 ± 0 21	-5.65
BCR 063R (n=4)	0.81 ± 0.05	0.66 ± 0.26	-18.52
Whole liquid milk S1	NA	0.48 ± 0.14	—
Whole liquid milk S2	NA	0.46 ± 0.15	—
Semi-skimmed liquid milk S1	NA	0.38 ± 0.18	—
Semi-skimmed liquid milk S2	NA	0.36 ± 0.14	—
Skimmed liquid milk S1	NA	0.37 ± 0.17	—
Skimmed liquid milk S2	NA	0.36 ± 0.18	—

S1 and *S2* = samples purchased from local stores 1 and 2 resistively.

5.7. Conclusion

ICP-MS has good sensitivity for the determination of iodine in milk. The developed sample preparation procedure led to a reduction of the organic contents of the samples and produced an aqueous solution that could be introduced to the ICP-MS instrument without concern for blockage in the sample introduction system or MS interface. The determination of iodine in alkaline solution suppresses the formation of volatile species. In addition, this method of sample preparation is rapid and easy to automate so that it would be appropriate for high sample throughput. Furthermore, the quantities of samples and reagents consumed in the preparations are small which means that it is an inexpensive method. In principle, this sample preparation procedure can also be applied to the determination of other elements. The metals were stabilised using EDTA which keeps the ions in solution at high pH.

References

1. *Handbook of Milk Composition*, eds. R. G. Jensen, Academic Press, USA, 1995.
2. F. A. R. Martine, M. L. F. Sanchez and A. S. Medel, *J. Anal. At. Spectrom.*, 2000, **15**, 163.
3. P. Bratter, I. Navarro Blasco, V. E. Negretti de Bratter and A. Raab, *Analyst*, 1998, **123**, 821.
4. R. Jost, *Milk and Dairy Products*, in Ullmann's Encyclopaedia of Industrial Chemistry, 6th edn, Wiley-VCH, Germany, 2002.
5. R. G. Jensen, A. M. Ferris and C. J. Lammi-Keefe, *J. Dairy Sci.* , 1991, **74**, 3228.
6. A. Flynn and P. Power, *Nutritional Aspects of Minerals in Bovine and Human Milks*, in Development in Diary Chemistry-3, eds. P.F. Fox, Elsevier, 1985, pp183.
7. *CRC Handbook of Chemistry and Physics*, eds. D. R. Lide, CRC Press, 72nd edn., 1992.
8. P. A. Fecher, I. Goldmann and A. Nagengast, *J. Anal. At. Spectrom.*, 1998, **13**, 977.
9. Iodine in milk, http://archive.food.gov.uk/maff/archive/food/infsheet/2000/no198/198milk.htm, September 2002.
10. N. J. Langford, J. Lewis and H. M. Crews, 10th Biennial National Atomic Spectroscopy Symposium, Sheffield, UK, July 17-20, 2000.
11. L. F. Sanchez and J. Szpunar, *J. Anal. At. Spectrom.*, 1999, **14**, 1697.
12. E. A. Crecelius, *Anal. Chem.*, 1975, **47**, 2034.
13. X. Hou, C. Chai, Q. Li and K. Wang, *Fresenius' J. Anal.Chem.*, 1997, **357**, 1106.
14. G. Knapp, B. Maichin, P. Fecher, S. Hasse and P. Schramel, *Fresenius' J. Anal.Chem.*, 1998, **362**, 508.
15. H. L. Tucker and R. W. Flack, *J. Chromatogr. A*, 1998, **804**, 131.
16. S. P. Dolan, S. A. Sinex and S. G. Capar, *Anal. Chem.*, 1991, **63**, 2539.

17. E. H. Larsen and M. B. Ludwigsen, *J. Anal. At. Spectrom.*, 1997, **12**, 435.
18. P. Allain, Y. Mauras, C. Douge, L. Jaunault, T. Delaporte and C. Beaugrand, *Analyst,* 1990, **115**, 813.
19. H. Baumann, *Fresenius' J. Anal.Chem.*, 1990, **338**, 809.
20. S. Sturup and A. Buchert, *Fresenius' J. Anal.Chem.*, 1996, **354**, 323.
21. G. Horlick, S. H. Tan, M. A. Vaughan and Y. Shao, *Inductively Coupled Plasmas-Mass Spectrometry,* in Inductively Coupled Plasmas in Analytical Atomic Spectrometry, eds. A. Montaser and D. W. Golightly, VCH, New York, 1987, pp. 361.
22. H. Vanhoe, F. V. Allemeersch, J. Versieck and R. Dams, *Analyst,* 1993, **118**, 1015.
23. D. A. Skoog, D. M. West and F. J. Holler, *Fundamental of Analytical Chemistry*, 5th edn., Snunders College Publishing, 1988.
24. T. Delves, *VAM Bulletin*, 20, spring 1999, 16.
25. P. Schramel and S. Hasse, *Microchim. Acta,* 1994, **116**, 205.
26. H. Yamada, T. Kiriyama and K. Yonebayashi, *Soil Sci. Plant Nutr.,* 1996, **42**, 859.
27. W. Kerl, J. S. Becker, H. J. Dietz and W. Dannecker, *J. Anal. At. Spectrom.*, 1996, **11**, 723.
28. F. Camuna, J. E. Sanchez-Uria and A. S. Medel, *Spectrochim. Acta*, 1993, **48B**, 1115.
29. S. F. Durrant and N. I. Ward, *J. Micronutr. Anal.*, 1989, **5**, 111.
30. K. S. Subramanian, *Spectrochim. Acta*, 1996, **51B**, 291.
31. K. J. Lamble and S. J. Hill, *Analyst*, 1998, **123**, 103R.
32. O. Legrini, E. Oliveros and A. M. Braun, *Chem. Rev.*, 1993, **93**, 671.
33. S. Determann, J. M. Lobbes, R. Reuter and J. Rullkotter, *Mar. Chem.,* 1998, **62**, 137.
34. C. Vandecasteele and C. B. Block, *Modern Methods for Trace Element Determination*, John Wiley & Sons Ltd, England, 1993, ch. 2, pp.9.
35. J. W. Baynes, *The Role of Oxidation in the Maillard Reaction in vivo*, in Maillard Reaction: Consequences for the Chemical and Life

Sciences, eds. R. Ikan, John Wiley & Sons Ltd, England, 1996, ch. 3, pp.56.

36. J. N. Miller and J. C. Miller, *Statistics and Chemometics for Analytical Chemistry*, 4th edn., Pearson Education Limited, England, 2000, ch. 5, pp.107.

Chapter 6:

Conclusions and Future Work

6.1. Introduction

This project set out to investigate robust and efficient approaches to reduce the effect of spectral interferences in ICP-MS. Bayesian spectral deconvolution employing the Massive Inference algorithm and the collision/reaction cell (CRC) have been used. The development of a sample preparation procedure for the determination of iodine in milk samples has also been studied.

6.2. Bayesian spectral deconvolution of ICP-MS

The MI programme offers fast searching time, flexibility in changing the menu and good estimation for most of the elements investigated. The use of the MI programme has been focused on the development of a standard procedure to be set with current data analysis approaches used in ICP-MS. The performance of the algorithm is determined by the selection of appropriate components in the species menu. Establishing an efficient and robust method for determining the component menu is a prerequisite before MI could be used routinely for ICP-MS analysis. This is because there is a need to change the menu each time to suit the sample matrix. Prior to this work, no guidance was available for establishing a good component menu, however, the strategy that has been followed in this thesis can be used (See Chapter 3).

The Bayesian method takes account of acquired knowledge to improve the quality of prediction and this is manifested in defining/refining the menu of components to be included in the modeling process. From this work and general observation of data published in the literature, it appears that in the vast majority of cases the residual background count (even under the cleanest of conditions) occurs as a result of combinations of minor elemental and molecular ion contributions that have insufficient S/N to allow identification. In practice, the instrumental background is observed at a very few spectral positions where no ions exist. The true and complete menu is therefore not normally known and it will be the case that

on some occasions combinations of surrogate species will provide a good estimate of the background from false premises.

A further consideration is that the data is distorted by the instrument response function, however, attempts to correct for this showed only a small benefit. This was because of the limited S/N that is of the same order as the bias (a few percent per amu).

Notwithstanding uncertainty about the true menu, the method does provide good analytical data and appears to be robust providing the appropriate tests are applied. Here the Evidence (overall goodness of spectral fit), the spectral fit at individual masses, the isotope ratios and the quality of data provided for reference materials have been employed. For analytical purposes, given that a reasonable synthesis of the spectrum has been achieved, the isotope ratios are the best guide to the ultimate quality of the data. Thus achieving satisfactory results for a reference material and then obtaining good isotope ratios for an unknown sample of similar composition indicates the likelyhood of an accurate analytical result.

The MI algorithm may not be the best approach in all circumstances because if single isotopes, free from interferences, are available then they will yield equally good (if not better) results. However, the MI algorithm is still very valuable in helping to find the best isotopes to use and to identify what interferences there might be. In simple cases, it could even be used to guide the setting up of a conventional correction equation. This is certainly against the spirit of the multivariate approach, but if the mathematics indicates that a simpler method is appropriate, then why not use it. Other than the setting up time, nothing is lost through the use of the MI algorithm and unforeseen errors might be avoided.

A major benefit of this form of spectral deconvolution is that it removes the necessity for blank subtraction because the counts at any mass are fully predicted from the molecular ions in the species menu. This is so for mass spectrometry, where the non-specific instrumental background is very low

and lost in the noise; it would not be the case in optical spectrometry where the background is often the major part of the signal in a measurement channel. The technique could have particular value in the direct analysis of solids, e.g., by laser ablation sampling, where sample blanks are rarely available. Use of a procedural blank to monitor contamination remains vital, but if the isotope ratios determined for such a blank are correct, then it can be subtracted with the knowledge that there is a genuine additional elemental contribution to the sample that has to be allowed for.

Further investigation is essential for using the MI algorithm in ICP-MS data analysis. The following suggestions might be helpful to provide additional information:

- Incorporate the MI algorithm as a sub-routine in a windows based programme that would incorporate the tests outlined in this thesis. This would enable the automatic creation of the menu for obtaining calibration and analytical data. The results so obtained could be compared with these obtained by conventional means. Correction for mass bias could also be incorporated into this software.
- There is a need to develop a programme that generates all possible species with abundances for 1, 2, ..., n atom combinations for a given mass (or even fractional mass). There are some commercial programmes that do this in part, but none comprehensively.

6.3. Collision/reaction cell ICP-MS

A collision/reaction cell using H_2 as a reaction gas and He as a buffer gas was shown to be an effective means for reduction or even elimination of argon-based polyatomic ion interferences. This technique does not incur the loss of sensitivity as in the application of high resolution or the reduced robustness of the plasma as is the case with the cold plasma technique.

The function of the collision cell is to reduce/remove spectral interferences from the ion beam by controlled ion-molecule reactions at near-thermal

conditions. Background ion intensities caused by argon based molecular ions were reduced by several orders of magnitude by collision induced reaction with hydrogen and helium as cell gases. These led to improved accuracy and precision for difficult to analyse elements under conventional plasma conditions.

Unfortunately the lab environment was not sufficiently well controlled to enable the potential gains in performance to be realised. Many of the low mass elements e. g. Ca, Cr and Fe that have spectral interferences that can be reduced using collision/reaction cell technology are ubiquitous in the environment and very clean conditions are required to reduce the analytical blank.

The experience of carrying out this work suggests that there is a need to investigate:

- The robustness of collision/reaction cells with high matrix samples.
- Means of reducing oxides that are formed or elevated when the cell is used.

6.4. The determination of iodine in milk samples

An analytical sample preparation method based on ICP-MS has been developed for the accurate determination of iodine in solid and liquid milk samples. The key to a successful analysis was to reduce the organic contents of the sample and ensure that the iodine was retained. This was achieved by using tetramethyl ammonium hydroxide (TMAH), Triton X-100 and hydrogen peroxide at about 70 C in an open vessel digestion for 2 hours. By using EDTA as chelating reagent, the method can be used for multielement determinations of trace and ultra-trace elements. The purities of the regents used in the preparation step were critical to avoid the introduction of un-expected spectral interferences.

The time allocation of this project did not allow for detailed study on the use of the sample preparation method for the determination of ^{129}I. The

digestion procedure, however, can be used for the determination of ^{129}I. This requires the removal of the spectral interference from ^{129}Xe which can be done by using a collision/reaction cell. In this case, O_2 can be used as a reaction gas as its reactivity with Xe is faster than with ^{129}I. The possibility of forming metal oxides and metal dioxides are likely and much care must be paid to optimise and control the chemistry and the collision cell conditions. Other types of milk products such as cream and other biological samples such as yeast might be digested using the method studied here. In these cases, the procedure might need to be re-optimised.

Finally it can be concluded that the Bayesian approach, as implemented in the MI algorithm, and collision cell technology are powerful and useful additions to the range of methods that can be used to deal with the problem of spectral interferences in ICP-MS.

Appendices

Regression calculations[1]

- If the individual points are denoted by (x_1,y_1), (x_2,y_2), (x_3,y_3), ..., (x_i,y_i), ..., (x_n,y_n), where n is number of points. The slope (b) and the intercept (a) of the regression line are then given by:

$$b = \frac{\sum_i \{(x_i - \bar{x})(y_i - \bar{y})\}}{\sum_i (x_i - \bar{x})^2} \qquad \& \qquad a = \bar{y} - b\bar{x}$$

  Where $\bar{x}$ and $\bar{y}$ represent the mean of the x and y values respectively.

- The random errors in the y-direction ($S_{y/x}$) can be estimated by:

$$S_{y/x} = \sqrt{\frac{\sum_i (y_i - \hat{y}_i)^2}{n-2}}$$

  Where $\hat{y}_i$-values are the points on the calculated regression line corresponding to the individual x-values.

- The standard deviation of the intercept (S_a) can be given:

$$S_a = S_{y/x}\sqrt{\frac{\sum_i x_i^2}{n\sum_i (x_i - \bar{x})^2}}$$

- The estimated standard deviation (S_{x_o}) of the concentration value x_o is:

$$S_{x_o} = \frac{S_{y/x}}{b}\sqrt{\frac{1}{m} + \frac{1}{n} + \frac{(y_o - \bar{y})^2}{b^2\sum_i (x_i - \bar{x})^2}}$$

  Where y_o is the experimental value from which concentration value x_o is to be determined and m is the number of readings.

- Limit of detection (*LOD*) is given by:

$$LOD = y_B + 3s_B$$

  Where y_B is the blank signal and s_B is the standard deviation of the blank. The value of the intercept (a) and ($S_{y/x}$) can be used as an estimation of y_B and s_B respectively.

1. J. N. Miller and J. C. Miller, *Statistics and Chemometics for Analytical Chemistry*, 4th edn., Pearson Education Limited, England, 2000, ch. 5, pp.107.

Operating procedure for Massive Inference programme

- The data file should be compiled and saved as an MS-DOS text file, with the following format:
- First column is the mass range studied, e.g. 51-88.
- Second column is the average raw count at that mass.
- Third column is the standard deviation at that mass.

46	1000	90
47	1000	90
48	1000	90
49	1000	90
.	.	.
.	.	.
.	.	.
.	.	.
etc		

- The component menu is the list of potential components in the sample matrix, it is compiled and saved as an MS-DOS text file, all the components should be keyed in one column.

Ti
V
ArN
Ar2
Ba++
.
.
.
etc

Ar_2 should be keyed in as Ar2, subscripts are not recognised.

Ba^{++} should be keyed in as Ba++, superscripts are not recognised.

The syntax of using Testmass is as follows:

Testmass [data file] [component file] > [output file]

Examples:

Testmass 100ppb.txt menu.txt > output.res

The above instruction means: input the data file: 100ppb.txt and the component menu file: menu.txt to Testmass; the estimated results are directed to the output file: output.

The output from the programme contains the following information:

- The relative abundances of all species in the menu at each mass.
- The evidence (E).
- The total predicted count for each component with the error in this count and the probability that the species has been detected by the algorithm.
- The spectral fit at each mass in the region studied.
- Correlation matrix for the selected species.

MASS	46	47	48	49	50	51
Ti	8	7.3	73.8	5.5	5.4	---
V	---	---	---	---	0.25	99.75
ArN	---	---	---	---	0.3358	0.0012
ClO	---	---	---	---	---	75.5897
SiO	3.2789	0.0105	0.0062	---	---	---
Evidence	=	-814.462				
Elem	%(+)	Counts	+-	Correlation		
Ti	100	476687	2299	1	0	0
V	100	511942	2541	1	8	0
ArN	88	68488	2546	1	0	0
ClO	100	26214	1443	0	1	0
SiO	81	310883	17715	7	1	0
Mass	Data	Mock	(Data-Mock)/Noise			
46	52456	51988	0.1728			
47	34873	34850	0.1363			
48	379388	380074	-0.3902			
49	30658	30419	1.0984			
50	55261	55345	-0.5362			
51	530983	530977	0.0024			

Regression calculations

For example: ^{55}Mn (raw data)

	x_i ($\mu g\ l^{-1}$)	y_i (cps)	x_i^2	$(x_i-\bar{x})(y_i-\bar{y})$	$(x_i-\bar{x})^2$	$(y_i-\hat{y}_i)^2$
	0.1	1159	0.01	2813098	421 4222	32359 27
	0 3	2454	0 09	2759365	413 2508	19067 43
	1	7235	1	2570504	385 2808	57733 52
	3	20392	9	2076651	310 7665	856 0545
	10	64148	100	786985	112.9665	9016869
	30	203858	900	615381 6	87 82367	9162692
	100	668100	10000	42059532	6299 824	374166 9
Sum	144.4	967346	11010 1	53681517	8031.334	18663744
Means	20 63	138192.3				
n	7					
R^2	0 9999					
Slope (b)	6684 0098					
Intercept (a)	310 7122					
$S_{y/x}$	1932.0323					
S_a	855 0020					
m	3					
Limit of detection ($\mu g\ l^{-1}$)	0 86716					

TORT 1	y_o (cps)	1365547
	Solution Concentration ($\mu g\ l^{-1}$)	204 25
	Solid Concentration ($mg\ l^{-1}$)	20 59
	The 95% confidence limits (t_{n-2} = 2 57) ($mg\ l^{-1}$)	0.16
	Certified value ($mg\ l^{-1}$)	23 4
	% Error	-12.01
NIST 1547	y_o (cps)	5440824
	Solution Concentration ($\mu g\ l^{-1}$)	813 96
	Solid Concentration ($mg\ l^{-1}$)	73 86
	The 95% confidence limits (t_{n-2} = 2.57) ($mg\ l^{-1}$)	0.60
	Certified value ($mg\ l^{-1}$)	98
	% Error	-24 63
NIST 1577-b	y_o (cps)	770967
	Solution Concentration ($\mu g\ l^{-1}$)	115.30
	Solid Concentration ($mg\ l^{-1}$)	11 72
	The 95% confidence limits (t_{n-2} = 2.57) ($mg\ l^{-1}$)	0.1
	Certified value ($mg\ l^{-1}$)	10.5
	% Error	11 59